Breakage Probability of Repeated Stressing of Granules by Configuring the Stressing Points

Dissertation
zur Erlangung des akademischen Grades

Doktoringenieur
(Dr.-Ing.)

von: Salman
geb. am: 11th. October 1973 in Soppeng, Indonesia

genehmigt durch die Fakultät für Verfahrens- und Systemtechnik
der Otto-von-Guericke-Universität Magdeburg

Gutachter:
Prof. Dr.-Ing. Evangelos Tsotsas (Vorsitz)
Prof. Dr.-Ing. habil. Jürgen Tomas (Gutachter)
Jun.-Prof. Dr.-Ing. Andreas Bück (Gutachter)
Jun.-Prof. Dr.-Ing. Sergiy Antonyuk (Gutachter)

Eingereicht am:

Promotionskolloquium am: 27.06.2014

Acknowledgement

It gives me a great pleasure to express my humble gratitude to **Prof.-Dr.-Ing. habil. Jürgen Tomas** for his approval, time, and suggestion during the research period.
I am deeply and sincerely thankful for **Dr. rer. nat. Sergej Aman** for his invaluable guidance, constant encouragement, numerous progressive suggestions and keen interest throughout the research period. I hardly say the best grateful for him.
My special admiration for **Prof Ulrich Hauptmanns.** As a DAAD's head for Sachsen Anhalt, he nicely accepted my application to get a scholarship for master program in Quality Safety and Environment (QSE).
My tribute to **Dr. Patrick Bussian** from Sasol Germany GmbH for his free 2.5 mm Al_2O_3 spheres. The sincere thank to **Dr. Baldur Unger**, General Manager of Business Unit Molecular Sieves of Chemiewerk Bad Köstritz GmbH, for his free Zeolite 4AK.
Very grateful I present to my colleagues and office staff in the department:
Dr. rer. nat. Werner Hintz, Nicolle Degen, Dr.-Ing. Peter Müller, Dr.-Ing. Andreas Schlinkert, Dipl.-Ing. Bernd Ebenau, Dipl.-Ing. Sebastian Kleinschmidt, M.Sc. Olatunji Olakunle Nosiru, Dipl.-Ing. Katja Mader-Arndt, Dipl.-Ing. Martin Pieper, M.Sc. Alexander Russell, M.Sc. Christian Schwenke, M.Sc. Hannes Glöckner, M.Sc. Sarah Kockentiedt, M.Sc. Zheni Radeva, M.Sc. Zinaida Kutelova, Dipl.-Ing. Alexander Pisarevsky, Dipl.-Ing. Alexander Aman, M.Sc. Sören Stein, Dipl.-Ing. (FH) Antje Keitel, Dipl.-Ing. (FH) Peter Siebert, and **Madeleine Seekircher.**
I always remember the moments I had with my colleagues during my research and staying in Germany. Specially the moment: monthly meeting, grilling, excursion to castles, industries and Germany jungles.
I am thankful to laboratory staff: **-Ing. Sabine Schlusselburg** in Gb. 15 what a nice and helpful woman, and also to machine room staff: **Herr Gehrke, Herr Kürschner,** and **Herr Ritzmann** and friends (they are very warm), and they provide me technical support. Along with them I am equally grateful to my family and friends: **Arizal, Suherman, Sabariman, Wang, Ihsan Maulana**, for providing a good environment for my personal and personal development.
The important thank also to the *Directorate General of Higher Education*, *Ministry* of National Education, *Indonesia (Dikti)* for the financial support. My respect to **Ibu Iin Budiarsih** the Indonesian staff/lecturer who keeps conveying the financial support every semester.
I am thankful to those people who always wish me success, good wishes and provide cooperation in every step of my life.

Salman

Abstract

Cyclic stressing of granules in industrial processes reduces the quality of particulate materials. The aim of the present work is investigating the breakage probability of granules by taking into account the orientation of contact point of stressing by repeated stressing. Eventually, this thesis is a contribution of the understanding of the behavior of particles in industrial praxis.

The research develops the model as a fitting of breakage probability of granules by repeated stressing. The breakage probability depends on the number of fractures, stress and force distribution, number of stressing and contact point of stressing.

The model afterward is validated experimentally by drop weight, pendulum impact, compression and air cannon impact tests. The used material tests are gamma Aluminum oxide (γ-Al_2O_3), Zeolite 4AK, and Zirconium (ZrO_2) with varied particle sizes.

The presented results in this thesis are applicable to inhomogeneous spherical specimens either to study the breakage mechanisms or to apply the model in planning and analyzing in the scope of testing units.

Kurzreferat

Bei industriellen Prozessen kann durch zyklische Beanspruchung die Qualität granularer Medien verringert werden. Die vorliegende Arbeit untersucht hierzu die Bruchwahrscheinlichkeit von Granulaten unter Berücksichtigung der Orientierung der Kontaktpunkte bei zyklischer Beanspruchung. Die Arbeit liefert damit einen Beitrag zum Verständnis von verhalten der beanspruchter Partikel in der industriellen Praxis. Die Arbeit beschreibt die Entwicklung eines model für die Bruchwahrscheinlichkeit, um experimentelle Ergebnisse ausgewertet nach der Monte-Carlo-Methode anzupassen. Die Bruchwahrscheinlichkeit korreliert mit der Anzahl der Bruchvorgänge, der Spannungs- und Kraftverteilung und mit der Anzahl der Spannungs- und Kontaktpunkte während der Beanspruchung.

Das erhaltene Modell wird anschließend experimentell mittels Prallversuchen validiert. Als Versuchsmaterialien wurden γ-Aluminiumoxid (γ-Al_2O_3), Zeolith 4AK und Zirconium (ZrO_2) unterschiedlicher Partikelgrößen genutzt. Mit Druck- und Prallversuchen werden die Untersuchungen ergänzt.

Die Ergebnisse der Arbeit können auf inhomogene, kugelförmige Partikel angewendet werden, womit entweder die Bruchmechanismen analysiert oder das Modell bei der Auswertung im Rahmen zyklischer Experimente eingesetzt werden kann.

TABLE OF CONTENTS

Nomenclature

Symbol	Description	Unit
A_{ij}	Cross sectional area of the solid bridge bond	mm^2
A	Fitted value for experimental data	-
b'	Fitted value for experimental data	-
c	Constants in breakage probability distribution	-
c_p	Correlation parameters	-
d	Granule size	mm
$d_{r,i}$	Particle size of asperity	mm
e	Weibull exponent.	-
E	Potential energy	J
E_p	Elastic strain energy stored per unit volume	J/mm^3
$E_{m,G}$	Granule mass-related breakage energy	J/kg
$E_{m,min}$	Minimum energy	J
$E_{m,kin}$	Mass-specific impact energy	J/kg
E_n	Specific particle fracture energies	J/kg
$E_{k,n}$	Stiffness energy	J
E_i	Input energy	J
E_{imp}	Impact energy	J
E_v	Energy stored per unit volume	J/mm^3
e_n	Coefficient of restitution	-
F_j	Distributed stressing forces	N
$f_{Mat.}$	Integrated parameter of particle property	-
$F^*_{b,i}$	Magnitude of breakage force after application of force F_j	N
F_b	Breakage forces	N
$F_{b,\mathrm{mean}}$	Mean breakage force	N
F_{m+1}	Further breakage force number	N
$F_{b,s}$	Shear bond forces	N
$F_{b,n}$	New set of breakage force	N
h_0	Drop height	mm
h_1	Striker distance of pendulum	mm
$i_{1,2}$	Empirical parameter	-
i	Stressing number	-
i_t	Distribution parameter	-
j_p	Distribution parameter	-
j_1	Empirical parameters	-
j_2	Empirical parameters	-
J	Set of random distributed stressing forces	-
k	Degradation rate constant	-
k_e	Exponential distribution	-
k_s	Shape parameter	-
L	Element chain length	mm

L_0	Initial length of element at the chain	mm
L_s	Distributed length in the chain	mm
m_p	Correlation parameters.	-
M_B	Cross sectional moment	Nm
m_G	Mass of granule	kg
N_p	Empirical parameters	-
N_b	Number of broken granules	-
N_i	Number of stressing	-
N_{nb}	Number of nonbroken granules	-
N	Number of tested granules	-
N_0	Number of granules	-
n^{th}	Loading event	-
$p_{i,b}$	Breakage probability increments	-
P	Breakage probability	-
P_n	Percentage of broken granules	%
q	Degradation parameter	-
R^2	Coefficient of correlation	-
R_B	Radius of the solid bridge bond	mm
S_f	Fraction of broken granules	-
S	Standard deviation	-
s_n	Stressing series are applied along the same axis or stress direction.	-
t	Time of stressing events	s
v_{50}	Empirical correlation parameters	-
v	Impact velocity	m/s
v_o	Velocity of the striker	m/s
v_r	Variance	-
w_0	The breakage probability by the first stressing	-
w	Breakage probability at the certain event	-
X	Variable of regression relationship	-
x_{63}	Quantile of 63%	-
Y	Variable of regression relationship	-
z	The weak element of chain	-

Greek symbols

α	Statistical dimensionless constant	-
μ	Mean	-
σ	Tensile stress	Pa
σ_0	Initial tensile stress	Pa
σ_s	Standard deviation	-
σ_t	Distributed tensile stress	Pa
γ_d	Damage accumulation coefficient	-
γ	Fitting parameter	-

CHAPTER 1
INTRODUCTION

1.1 Mechanical problems of granules in industries

Granular materials are widely used in many industrial applications such as sludge granules, adsorbents, ceramics, catalysts, pesticides, fertilizers, tablets, etc [1]. Economic importance equates to approximately 10^{10} t/a of granule products which are manufactured in Germany alone every year [2].

Powders are often granulated to avoid technological problems such as time consolidation and segregation. However, deformation or breakage may occur during transportation, handling and storage of granules. It can alter the particle size distribution and depreciate the product quality, and on occasions may form harmful toxic dust.

Granules in industrial process are subjected to diverse stressing circumstances. For example interparticle collisions and particle-wall collisions that occurs during pneumatic conveying or during processing in a reactor. As a result, the product quality is reduced due to particle attrition and breakage [3].

The transportation of granules is a highly energy intensive process, due to this fact, granule breakage can occur. The maximum stressing conditions during these operations define the lower limit of the strength which all granules should have in order to be able to resist the stressing. On the other hand, they should be soft enough in order to retain solvability, dispensability and moisturization, properties, and to avoid complications during further processing [3]. For example, in the production of high performance ceramics, powders are granulated first, so that they do not break during transport, but eventually fail during further stressing [4].

During handling or processing, undesirable breakage of granules occurs as the granules experience multiple stressing events with concurrently occurring several dissipatory mechanisms. These may lead to damage during this cyclic stressing; this phenomenon is known as fatigue.

This thesis deals with heterogeneous materials such as most ores that are encountered in practice. The breakage probability will be predicted using the present developed and validated model.

1.2 Repeated stressing of solid particles

The breakage behavior of solid particles under cyclic stressing has been determined in a variety of disciplines. Several investigators have studied the behavior of particulate materials using fatigue tests such as air-gun [5], drop tests [6], compression [1][7] and within integrated industrial units [8].

Pitchumany et al. [9] introduced a nonlinear mechanism to study the stressing of a single particle until fracture. The breakage behavior with the formation and propagation of damages was proposed. The intensity of stressing, the particle size and the microstructure influence on material resistance against cyclic loading was explained. This result was confirmed by Beekman et al. by characterizing solid particles by their attrition resistance, fatigue lifetime and breaking mechanism under impact loads [10].

An advanced test based on continuum fracture mechanics has been examined by King et al. [11] to describe solid particle breakage by repeated low-energy stressing. He observed a link between fracture accumulation and progressive weakening that ultimately results in particle breakage. According to the author, the repeated impact tests provide information about the breakage behavior of particles based on their history.

A model for describing the progeny size distribution in repeated impacts has been also validated using data from drop weight testing by Tavares et al. [12]. Only one fitting parameter was used to describe the progressive growth of damage. The increasing of this parameter ultimately leads to fracture of a particle under stresses significantly lower than those required for breakage in a first event. At that test the damage accumulation coefficient was described that is not influenced by particle shape, but is marginally affected by particle size [12-13]. This coefficient is not significantly influenced by stressing model. However it can be used to determine fracture probability by repeated single and double impacts tests.

In different to the damage accumulation result, Petukov et al. [14] carried out the fatigue test that was accomplished at low stressing velocity. The authors described the strength of tested solid particles and observed it to increase with the stressing number. In this test the weaker particles were breaking at first and only the stronger particles survived to be tested later at the advanced stressing treatments. In terms of the proposed model, the strength of the survived particles would increase due to removing of weaker particles by repeated stressing.

For comminution systems, the surviving particles by repeated stressing were examined integratedly by Kalman [15]. The strength distribution by repeated stressing is related to the breakage ratio (selection function) to evaluate the performance of comminution systems. The breakage ratio is a function of the impact velocity and the number of impacts. By measuring the crush strength of the survived particles after each impact, the physical examination for the function of breakage ratio was provided. However the function is limited only to the certain apparatus application.

Another study that described the probability of fracture in multiple impacts was proposed by Vogel and Peukert [16]. The probability model of fracture was determined as a function of parameters such as stressing number, particle size, material-specific consideration, and stiffness energy (threshold energy). However the model to be valid only for predicting breakage in a small number of impacts (2 or 3) on polymer spheres. The model assumes that the Weibull distribution by larger impact number is capable of describing the fracture probability distribution of the material [17]. However, this assumption is valid only for highly heterogeneous materials [18]. A review of these models is given in **Table 1.1.**

The model can be applied but is also limited to describe breakage by repeated impacts of constant magnitude, although this limitation was overcome in a modified version of the model described recently by Morrison et al. [18].

The solid particles that were described above are assumed as homogenous particles. This means the strength at the every contact point of a tiny surface of particle is considered to be uniformly distributed. It clearly performs different result if the method or model is applied to the particles with distributed properties such as strength, modulus of elasticity, or yield point.

Table 1.Models of breakage probability by repeated stressing of particles.

No.	Authors	Breakage model	Index, remarks	
1.	Rumpf [19]	$E_v . d = const.$	E_v d	energy stored per unit volume of particle in J particle size in mm
2.	Weibull [17]	$P(x_t, k_s, x_{63}) = 1 - exp\left[-\left(\frac{x_t}{x_{63}}\right)^{k_s}\right]$	$P(x_t,k_s,x_{63})$ x_t k_s x_{63}	breakage probability as a function of x_t, k_y and x_{63} quantity "time-to-failure" shape parameter 63% quantile
3.	Weichert, R. [20]	$P(d, E_m) = 1 - exp[-cd^2 E_m^e]$	$P(d,E_m)$ c E_m e	breakage probability as a function of d and E_m constant value mass-related breakage energy in J/kg Weibull exponent
4.	Salman, A.D. [21]	$P(v, n) = 1 - exp\left[-\left(\frac{v}{c_p}\right)^{u}\right]$	$P(v,n)$ v c_p, u	percentage of broken particles number impact velocity in m/s correlation parameters
5.	Tavares et. al [6]	$P_{10}(E_k) = A\left[1 - exp\left(-\frac{b'E_k}{E_{50b}}\right)\right]$	$P_{10}(E_k)$ A, b' E_k E_{50b}	breakage probability as a function of proportion passing in 1/10th of the original particle size in a sample (%) fitted values for experimental data stressing energy used in each impact in J median particle fracture energy in J
6.	Peukert, W. and Vogel, L [16]	$P(d,i,E_m) = 1 - \exp(-f_{mat.} \cdot d \cdot i \cdot (E_{m,kin} - E_{m,\min}))$	$P(d,i,E_m)$ $f_{Mat.}$ d i $E_{m,kin}$ $E_{m,min}$	breakage probability as function of fraction of broken particles particle shape parameter particle size in mm number of impacts mass-specific impact energy in J/kg minimumenergy in J/kg
7.	Petukhov, Y. and Kalman, H. [14]	$P(v, w_i, w_f) = w_f + \frac{w_i - w_f}{1 + \left(\frac{v}{v_{50}}\right)^{i_t}}$ where $i_t = i_1 - i_2 e^{-i/N_p}$	$P(v,w_i,w_f)$ w_i w_f v v_{50} i_t i_1, i_2, N_p i	breakage probability as a function of v, w_i *and* w_f initial breakage probability final breakage probability impact velocity in m/s median velocity in m/s distribution parameter empirical parameters number of impacts
8.	Aman, S. and Tomas, J. [22]	$P(E_k, d) = \frac{1}{i}\sum_{j=1}^{i}\left[1 - exp\left(-\left(0.9\frac{E_k . d^3}{E_{mean} .\ d_{r,i}^3}\right)^{e}\right)\right]$	$P(E_k,d)$ E_k E_{mean} i $d_{r,i}$ e	breakage probability as a function of E_k and d kinetic energy in J arithmetic mean of kinetic energy in J number of stressing events particle size of asperity in mm Weibull exponent

1.3 The breakage probability of inhomogeneous granules

In general, granules have to be considered by taken into account their inhomogeneous properties. The deformation and breakage behavior of granules were considered as hemispherical asperities [22]. Many authors have examined inhomogeneous granules or particles, to understand the breakage behavior of different materials. Aman et al. [23] represented irregular shaped particles as combination of hemispherical asperities with size lower than the considered particle size itself. Schreier et al. [24] analyzed the liberation of aggregate particles during impaction of comparatively large concrete spheres at velocities up to 75 m/s. By using a large-scale pneumatic cannon, liberation grades were obtained.

With additional devices, Schubert et al. [25] described the breakage behavior of very inhomogeneous compounds and concrete by using impact, double impact and compression stressing. The experiment was validated by using Finite and Discrete Element Method (FEM and DEM) simulations and to study the cracking phenomena of particle-particle compounds at different velocities.

This is also confirmed by Salman et al. [26] where particle failure under normal and oblique impact was examined by using soda lime glass spheres, with diameters ranged between 0.4 and 12.7 mm.

To investigate sophisticatedly the fracture behavior of the complicated materials like particle compounds, Khanal et.al [27] described stress distribution of different particle breakages regard to mechanical properties and shape by using DEM. The Two-Dimensional discrete element analysis was carried out. The new surface generation and particle size distributions are also analyzed to study the efficiency of the crushing system. Concrete spheres of 150 mm diameter with properties of B35 (35 N/mm^2 compressive strength) were chosen to represent particle compounds.

Regarding the fatigue of inhomogeneous particles by repeated stressing, by modifying Griffith's theory, Rozenblat et al. [7] developed a theoretical fatigue model of particles to describe how the fatigue strength of individual particles changes by repeated compression cycles. The predictions of the model were validated by experimental results for two kinds of crystal particles: NaCl and MgO. The results show, that as the compression stresses acting on the particles and the number of compressions increase, the fatigue compression strength decreases. In addition, fatigue trend is observing the various particles that demonstrate dependence on the material's properties.

Considering of shaped particles as well, breakage probability as a distribution function is not yet precisely defined due to its sensitivity to particle shape. Therefore testing irregular particles may determine the breakage behaviour of stressed particles. Hemispherical asperity at particles is responsible for crack generation and particle breakage [22]. The breakage probability distribution of particles is calculated as a superposition of the breakage probabilities of asperities. Based on geometrical similarity it is assumed the irregularly shaped particles have same normalized log-normal size distribution of asperities [23].

Breakage of particles is affected by the size distribution of asperity caps surrounding particle surface [3, 24]. Therefore examination of breakage behaviour of inhomogeneous particles has to take into account the shape that is represented by hemispherical asperities consideration.

A whole description of physical phenomena occurring during the inhomogeneous particle breakage includes a very large number of parameters, and it is not yet available [6-9]. Furthermore, the problem is more complex by the fact that breakage can be dependent on some parameters that are very difficult to take into account. For example, breakage is often history-dependent, i.e. the number of micro-cracks and dislocations responsible for breakage increases due to previous loadings [6], [15], [26-28].

1.4 Breakage behavior of granules

In general, the previous research focused on the solid particle breakage either by single or cyclic stressing (loading). In another part, several studies also examined the breakage behavior by taking into account, particles as homogeneous granules. Breakage of granules has been studied to a limited extent in order to improve the understanding of ensemble breakage in particulate processing applications.

Antonyuk et al. [29] described the deformation and breakage behavior of granules by compression tests. Three industrial spherical granules γ-Al_2O_3, the synthetic zeolite Köstrolith® and sodium benzoate (C_6H_5COONa) were used as model materials to study the mechanical behavior from elastic to plastic range. Under repeated loading–unloading conditions deformation and breakage behavior were investigated. The breakage force and contact stiffness during elastic and elastic–plastic contact were examined. Breakage probability as a function of mass-related breakage energy was described by using Weibull statistics. It was shown that more mass-related breakage energy is needed to break smaller granules than bigger ones. The energy dissipation and microcrack formation during cyclic loading in granules lead to the reduction of the breakage force [29]. By using the Wöhler curve, the number of the cycles up to the fracture decreases with increasing stress amplitude as defined by Simmchen et al. [30].

Antonyuk et al. [29] also established single impacts to study the breakage behavior of granules. The deformation behavior was explained with the help of the contact model. The Breakage probability was approximated by the use of Weichert's approach [20]. The results conform to two dimensional discrete element simulations of the granules deformation by impact.

With same method and materials, Müller et al. [31] found that elastic, elastic-plastic are dominant. Additionally Russel et al. [32] confirmed it by repeated stressing of zeolite 4A granules regarding to moisture content by compression test. The reduction of fracture strength occurs due to the formation and propagation and microcracks in each stress cycle.

A complete description of physical phenomena that occurs during granules breakage is not yet available. Especially difficult in predicting breakage parameters of granules by repeated stressing particularly considering several parameters. The stressing accumulation at the contact area also has a large influence on the probability breakage. It is important to focus study on the contact point of stressing related to the granules surface orientation by stressing that may generate another behavior of breakage.

1.5 Focus of the research

In describing the influence of granule orientation on the breakage probability, one can clearly see that granules must be considered inhomogeneous. In this term properties particularly the strength surround the surface of spherical shape is not uniform. Hence it needs to take into account inhomogeneous granules by repeated stressing and later on developing parameter models that can be applied in industrial practice –that is based on Monte-Carlo.

For achieving the better breakage probability results, it is very important to understand the rotation of granules by repeated stressing.

The previous researches considered the granule surface is homogeneous namely the strength surround granule is uniform. Hypothetically by considering the granule as inhomogeneous shape, it may perform different behavior depending on the contact point.

The configuration of contact point by repeated stressing is a new research that is proposed in this work. Most of research carried out experiments by stressing of solid particles and granules regardless contact point configuration during stressing. This research develops breakage probability model that is validated by experiments with taking into account the configuration of granules by cyclic stressing.

1.3 Outline of contents

This research mainly include three parts, the first part is explanation of the breakage probability model by repeated stressing. The second part develops a breakage probability model, and the third part, model is validated by experiments. The outline of the proposed research is organized as follows.

In total, there are eight chapters. Chapter 1 introduces the application of granules in industries, repeated stressing of solid particles, breakage probability of inhomogeneous particles and breakage behavior of granules. Various studies behind interaction of particles or granules with stressing, wall collisions and interparticle collision itself, are reviewed in Chapter 2. This chapter also explains the characteristic of materials testing that are used in the experiments and their breakage characteristics. The used materials are gamma Aluminum oxide (γ-Al_2O_3), Zeolite Köstrolith® 4AK, and Zirconium oxide (ZrO_2).

Chapter 3 deals with the developed model of breakage probability of repeated stressing of granules. It particularly focuses on the mathematical model and its integration into the previous model that has been used for characterizing the repeated stressing of granules.

Chapter 4 describes deformation behavior of granules by compression test. The stressed granules is evaluated in a very low stressing velocity by uniaxial stressing. Chapter 5, the report goes to the experimental validation by using double impact testing by taking into account the stressing contact point.

Chapter 6 also investigates the breakage probability by using another equipment — pendulum impact. Chapter 7 concerns to another experiment i.e. single impact test by air canon. The breakage probability is described by regarding the pretreated and nontreated granules. Finally, some future developments for improving the granules processing are pointed out.

CHAPTER 2
BREAKAGE PROBABILITY MODELS

2.1 Weibull based models of particle breakage

It is difficult to take into account all parameters that can influence the breakage behavior especially for inhomogeneous granules. By a given granules size, the fracture force and energy are statistically distributed variables, even by the single stressing [27].

The mechanical characteristics of the primary particles and the bonding agents are randomly distributed within granules. Still with the identical production process, the strength of the individual granules differs depending on its microstructure. The microstructure of granules can be affected by the distribution and orientation of bonds, defects and pore size distribution. Besides bond strength and orientation the size distribution of inhomogeneous pores are responsible for the breakage behavior. As a result, the mechanical properties and breakage parameters vary by testing the geometrically similar granules of the same size [20].

By experiments, breakage probability of granules depends on the granule properties, process system units, and stressing parameters like stressing intensity (force, stress, and frequency stressing number per unit time). To fit the experimental data most of breakage probability studies are related to Weibull distribution. This approach is commonly applied to obtain the breakage probability as a percentage of the number of broken particles [21][33-39].

Breakage probability function can be defined as a cumulative probability, that its complementary cumulative distribution function is a stretched exponential function [39]. The Weibull distribution at Eq. (2.1) is related to a number of other probability distributions $P\ (x_t,k_s,x_{63})$, in particular, it interpolates between the exponential distribution and the Rayleigh distribution [40].

$$P\left(x_t, k_{s,}, x_{63}\right) = 1 - exp\left[-\left(\frac{x_t}{x_{63}}\right)^{k_s}\right] \qquad (2.1)$$

Where x_t the quantity "time-to-failure", k_s is the shape parameter and x_{63} is a quantile 63%.

The Weibull statistic is based on the principle of the weakest element in a chain. It gives the probability for the fracture of tensile stressing of a chain [17]. The chain consists of z elements with individual length L_0. The tensile stress σ is applied along the chain with total length L as shown in **Figure. 2.1**. It is assumed that the breakage probability of one element is $w(\sigma,L_0)=w_0$.

Hence, the probability of survival is 1-w_0. Consequently, the probability of survival for the chain consisting of two elements with common length $2L_0$

$$1 - w(\sigma, 2L_0) = (1 - w_0)^2 \tag{2.2}$$

For the chain with length L the Eq. (2.2) can be extended

$$w(\sigma, L) = 1 - (1 - w_0)^{L/L_0} \tag{2.3}$$

By the introducing a new function

$$f\left(\frac{\sigma}{\sigma_t}\right) = \ln[1/(1 - w_0)] \tag{2.4}$$

Where σ_t is tensile stress at a single element, one obtains

$$w(\sigma, L) = 1 - \exp\left(-\frac{L}{L_0} \cdot f\left(\frac{\sigma}{\sigma_t}\right)\right). \tag{2.5}$$

Weibull found that for most of the materials that he investigated

$$f\left(\frac{\sigma}{\sigma_0}\right) = \left(\frac{\sigma}{\sigma_t}\right)^e \tag{2.6}$$

Where e is Weibull parameter. In terms of Weibull model the breakage probability can be described as a function of σ_t. It should be pointed out σ does not necessarily denote a stress but rather a load in general.

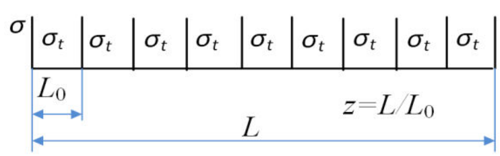

Figure 2.1. The fracture of a stretched chain which consists of z elements with distributed strength σ_t under applied tensile stress σ.

Therefore

$$w = 1 - exp\left[-z\left(\frac{\sigma}{\sigma_t}\right)^e\right] \tag{2.7}$$

Where z is the number of elements.

2.2 Rumpf similarity principle

Concerning the physical parameters of particles or granules, breakage probability can be described base on the breakage of geometrically similar and physically identical particles. In terms of a dimensional analysis, Rumpf [19] considered the breakage pattern depending on elastic strain energy stored per unit volume E_v of particle and particle size *d.* According to Rumpf the breakage pattern are similar when

$$E_v \cdot \ d = const. \tag{2.8}$$

A similar breakage pattern corresponds to the same breakage probability by given product $E_v \cdot d$. Rumpf's principle, considers a similar breakage pattern. That means the form of cracks is similar. Therefore, the crack pattern can be described by a single characteristic length. The ratio of characteristic crack length and initial particle size has to remain constant to fulfill similarity.
Based on Rumpf's similarity principle, Weichert [20] introduced the Weibull statistic to the field of comminution to describe the breakage probability of elastic-brittle spheres. It was assumed that the cracks appear at the circumference of contact circle. The length of chain L is the circumference of contact circle. Consequently, length of chain is proportional to particle size *d*. As results the breakage probability distribution $P(d,E_m)$ includes the particle size and mass-related breakage energy E_m.

$$P(d, E_m) = 1 - \exp(-c \cdot d^2 \cdot E_m^e) \tag{2.9}$$

Where c is a constant and e is the Weibull exponent. For the glass spheres, for instance, with diameter $d = 4$ mm, $e = 2.8$ and $c = 5.57*10^4$ (kg/J)$^{2.8}$ m^{-2} are obtained [20].
A similar equation was used by Salman et al. [41] by experimentally studied the impact of single particles. A relationship between the percentage of broken particles number $P(v,n)$ and the impact velocity was derived by a two-parameters cumulative Weibull distributions, Eq. (2.10).

$$P(v, n) = 100 \ exp\left[-\left(\frac{v}{c_p}\right)^u\right] \tag{2.10}$$

Where v is the impact velocity, and c_p and u are correlation parameters. Salman et al. [41] reported that $c_p = 19.5$ and $u = 7.4$, for example, aluminum oxide particles. **Figure 2.2** illustrates a typical relation between normal impacts velocity and number of broken particles for fertilizer [41].

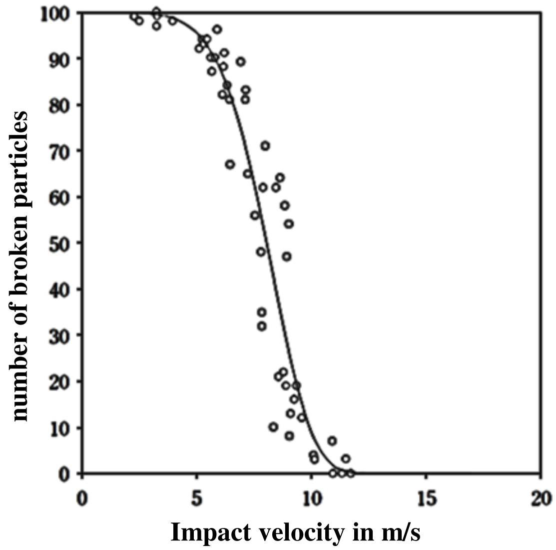

Figure 2.2 Typical relationship between particle impact velocity and number (percentage) of broken particles (7mm diameter spherical fertilizer particles under normal impact) [41].

2.3 The breakage probability by repeated stressing

In terms of the Weibull statistics also, Vogel et al. [42] developed a model to describe breakage probability by repeated impact of particles. The fraction of broken particles was calculated based on particle size d, number of impacts i and the mass-specific impact energy $E_{m,kin}$. Vogel et al [42] defined the model of breakage probability $P(d,i,E_m)$ as an approach based on the both - Weichert and Rumpf models. The breakage probability is derived as;

$$P(d,i,E_m) = 1 - \exp(-f_{mat.} \cdot d \cdot i \cdot (E_{m,kin} - E_{m,\min})) \tag{2.11}$$

The new integrated parameter $f_{Mat.}$ takes into account differences arising from particle shape and mechanical properties. The $E_{m,\mathrm{kin}}=1/2v^2$ (or the volume-specific energy $\rho/2v^2$) and a significant minimum energy $E_{m,min}$ has to be provided to take into account the elastic energy. Below this energy threshold, $E_{m,\mathrm{min}}$ either breakage does not occur or only a few debris are produced which can be attributed rather to attrition than to particle fracture (a mass loss $\geq$ 10% is necessary to be accounted as fracture) [42]. In terms of this model the breakage probability by repeated impact was found as a function of total amount of energy stored into particle by sequence of repeated impacts [42].

To validate the model Vogel et al. [42] conducted single-particle comminution experiments to determine the unknown material parameters. By grinding tests, particles of different materials (polymers, limestone, glass) were used and the size varies from 95 µm to 8 mm [42].

As result the breakage probability was determined as a function of the specific impact energy (single impacts). Smaller particles exhibit a smaller breakage probability because of the circumference of the contact area is smaller, and therefore, less flaws are affected by the critical tensile stress [42].

The results of the multiple impacts follow the Weibull distribution as a function of the total net energy. The results of the first impact of the particles and the second or successive impacts are defined as function of the total net energy. It is concluded that the energy provided by impacts which did not lead to particle breakage was not wasted. It led to an increase in the number of internal flaws and an extension of existing cracks which weaken the material and are of benefit for the following stress event [42].

The same assumption was used to take into account the influence of the impact number on the parameter $f_{Mat.}$, the energy threshold corresponds to the kinetic energy of the first impacts.

This parameter has a great merit because it is constant for each material and is not depending on the particle size and the number of impacts. However, it would be much more useful if it can be measured or calculated independently.

Petukov et al. [14] introduced model of the breakage probability $P(v,w_i,w_f)$ as a function of the impact velocity v and number of impact by using impact machine.

$$P(v, w_i, w_f) = w_f + \frac{w_i - w_f}{1 + \left(\frac{v}{v_{50}}\right)^{i_t}} \tag{2.12}$$

Where w_i is the initial breakage probability, and w_f is the final breakage probability. The distribution parameter i_t is a function of the impact number for all tested materials (GNP and potash—granules; and salt—crystals). The v_{50} is the median velocity (the velocity that causes 50% of the population to break). The effect of the number of impacts is pronounced in the empirical correlation parameters v_{50} and i_t. Therefore, the breakage probability in this term is defined as a function of the impact velocity for up to certain number of impacts.

A first order exponential decay function can be determined for the distribution parameter:

$$i_t = i_1 - i_2 e^{-i/N_p} \quad (2.13)$$

Where i_1, i_2, and N_p are the empirical parameters and i is impact number. The author obtained that the strength of tested solid particles increases with the increasing of impact number [14]. By repeated stressing the weaker particles were breaking at first and only the stronger particles are survived to the next test. In difference to model of damage accumulation the strength of the survived particles increases due to removing of weaker particles by repeated stressing.

More comprehensively Kalman et al. [43] evaluated particle damage by repeated stressing in the level of multiple system units. The author integrated comminution units namely ball-mill, pin-mill or jet-mill, pneumatic conveying pipelines and chutes. Potash particles were impacted repeatedly inside comminution units with varied impact velocities and number of impacts. These parameters are evaluated on their influence to the particles damage.

It was obtained that by cyclic impact in a low velocity only the weakest particles were broken. This experiment considered the damage by taking into account the particles-walls collision only, with neglecting the collision of particles against each other [43].

The advanced validation of breakage probability by a different way was described by Tavares et al. [44]. In examining the probability of fracture, Tavares et al. [44] examined quantitatively the size distribution of the progeny in order to simulate breakage due to repeated stressing by impact tests. A convenient description of the fineness of the progeny from breakage of single narrow-sized particles is given by the parameter P_{10} (E_k), which corresponds to the percent in weight of the original material which will pass through a sieve with aperture of 1/10th of the initial size of the particles tested. Therefore the relationship between size distribution and the stressing energy used in each impact E_k is

$$P_{10}(E_k) = A\left[1 - exp\left(-\frac{b'E_k}{E_{50b}}\right)\right] \quad (2.14)$$

Where A and b' are model parameters which should be fitted to experimental data and E_{50b} is the median particle fracture energy of broken particles.

By investigating the repeated loading either in compression or in double impact test, Tavares et al. [44] also described fracture during loading and the deformations regarding to the stiffness of spherical particles. The damage model introduced a new parameter the damage accumulation coefficient γ. It was found that the model requires only one parameter γ to fit the breakage probability by repeated loading. One important assumption in the model is the stiffness of the particle progressively degrades with repeated impacting see **Figure 2.3**. The increasing of γ parameter ultimately leads to fracture of a particle by a stress that is significantly lower than those required for breakage by single stressing.

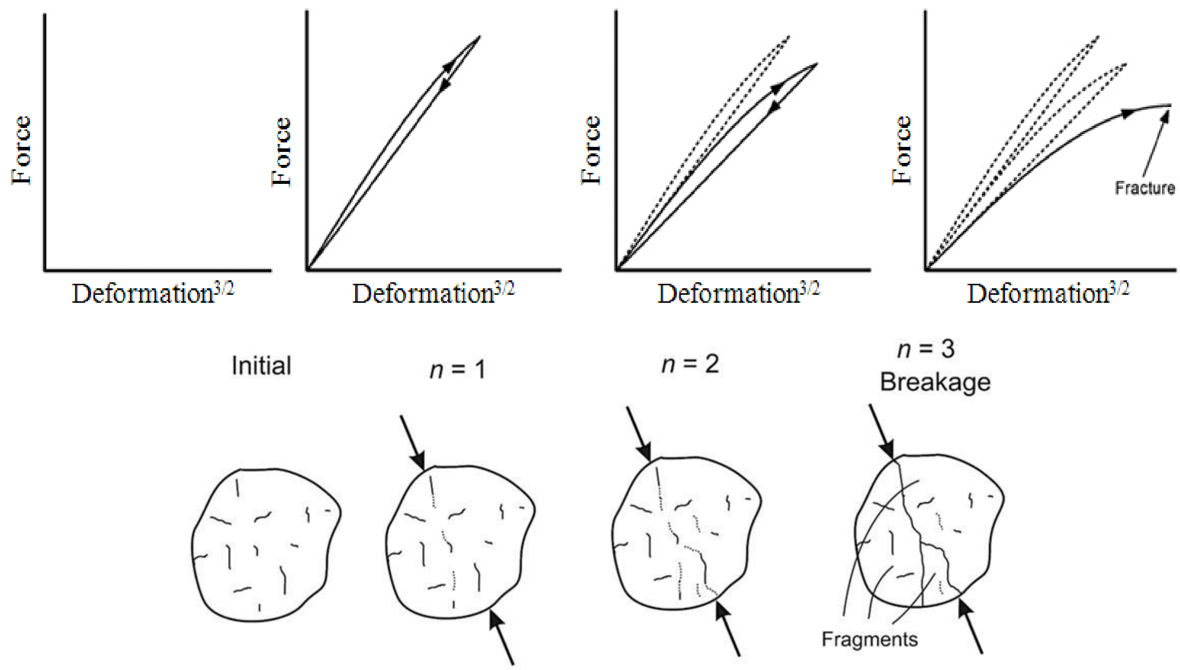

Figure 2.3 Illustration of the effect of weakening due to accumulation of damage in repeated loading events [44].

Tavares et al. [44] needs large number of particles to precisely determine the breakage probability. The smaller the number of particles the larger are the uncertainties involved in the estimates of the cumulative amount of broken particles in the n^{th} loading event.

Furthermore, the damage accumulation and its coefficient were also validated by using impact load cell or slow compression tester. The distribution of breakage probability as a function of energies of the particular size fraction of the original material $P_0(E)$. It was calculated to describe the data appropriately is the upper-truncated lognormal, given by

$$P_0(E) = \frac{1}{2}\left[1 + erf\left(\frac{lnE^* - lnE_{50}}{\sqrt{2£^2}}\right)\right] \tag{2.15}$$

With

$$E^* = \frac{E_{max}E}{E_{max} - E} \tag{2.16}$$

where E_{max}, E_{50} and £ are model parameters. The relationship between the specific particle fracture energies E_n at successive loading events is given by

$$E_n = E_{n-1}(1 - D^*_n) \tag{2.17}$$

which is solved by considering that the amount of damage sustained in the n^{th} loading cycle was estimated by

$$D_n^* = \left[\frac{2\gamma E_{k,n}}{\left(2\gamma - 5D_n^* + 5\right)E_{n-1}}\right]^{\frac{2\gamma}{5}} \tag{2.18}$$

Where D_n^* is damage accumulation at the n^{th} loading events.

In another way, to improve the development model, an alternative method had been proposed by Austin et al. [45] by calculating the number of stressing events that are required to break a material with a given strength. The smaller number of particles, the larger the uncertainties involved in the estimates $P_n(S)$. An estimate of this experimental error due to sampling may be obtained from the confidence interval of the proportion of broken particles, determined using the binomial distribution [45],

$$P_n \pm Z(\alpha/2)\sqrt{\frac{P_n(1-P_n)}{N}} \tag{2.19}$$

where P_n is the cumulative proportion broken in the n^{th} loading event and N is the number of particles tested in the experiment. The α is the statistical significance of the confidence interval (taken in the present work as 0.1 or 10%), and Z is the tabulated normal scores [45]. Eq. (2.19) is actually the approximation to the binomial distribution using the Gaussian distribution. However, this may only be used for stressing events of equal magnitude.

2.4 The breakage and deformation behavior of inhomogeneous particles and granules

Regarding to breakage and deformation behaviour of inhomogeneous particles, the researches consolidated models and experiments in some ways.

Schreier et al. [25] accomplished a test rig large-scale pneumatic cannon to study the impact crushing of concrete for liberation and recycling. The apparatus allows the adjustment of intensive stressing conditions, e.g., impact and double impact, single and multiple stressing. The crushing fragments were described as subcollectives of truncated logarithmic normal distributions of a multimodal distribution function. The result of multiple stressing experiments result exhibited normalized frequency distribution after 1 to 6 stressing events, see **Figure 2.4**.

In extended computation, Schubert et al. [45], described the liberation of concrete aggregates by impact crushing in the same large scale pneumatic cannon. Both experiments, Finite Element Method (FEM) and Discrete Element Method (DEM) were adopted to study the cracking phenomena of aggregates. The increasing of liberation degrees showed that the simulation results in a good agreement with the experimental data.

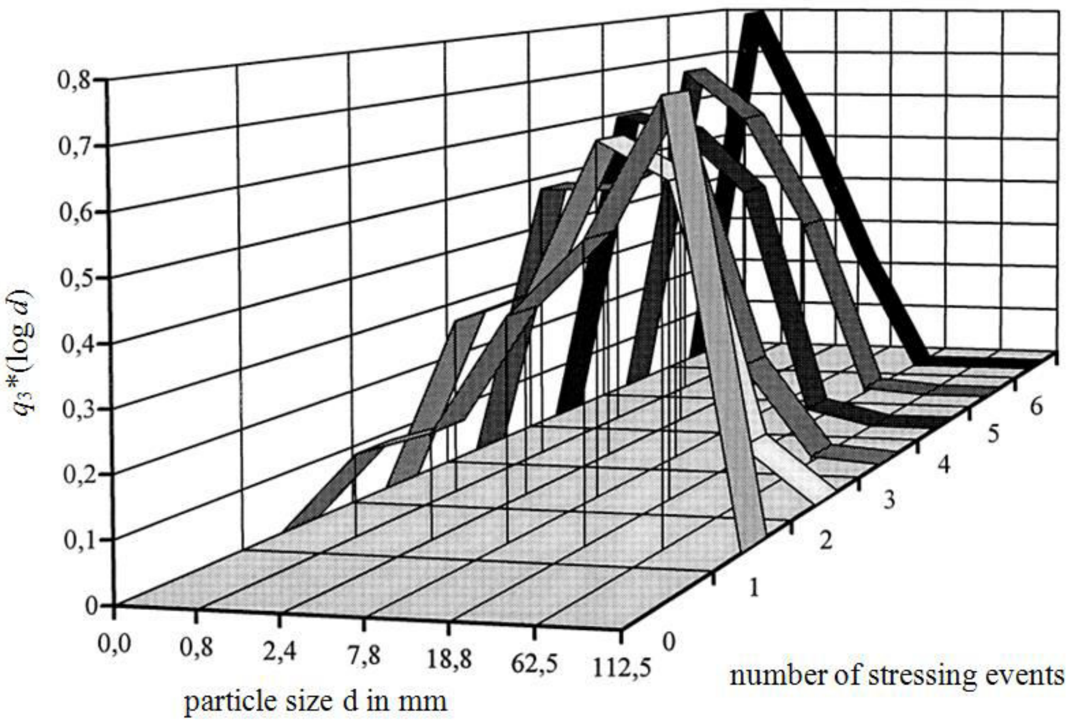

Figure 2.4 Logarithmic normal distribution (multiple stressing, v = 55.0 m/s) [45].

The same DEM simulation method was applied by Antonyuk et al. [29] to investigate granules breakage behavior. The mechanical behavior from elastic to plastic range of γ-Al_2O_3, Zeolite 4AK and sodium benzoate (C_6H_5COONa) was examined. The **Figure 2.5** shows loading unloading behavior of Zeolite 4AK granule.

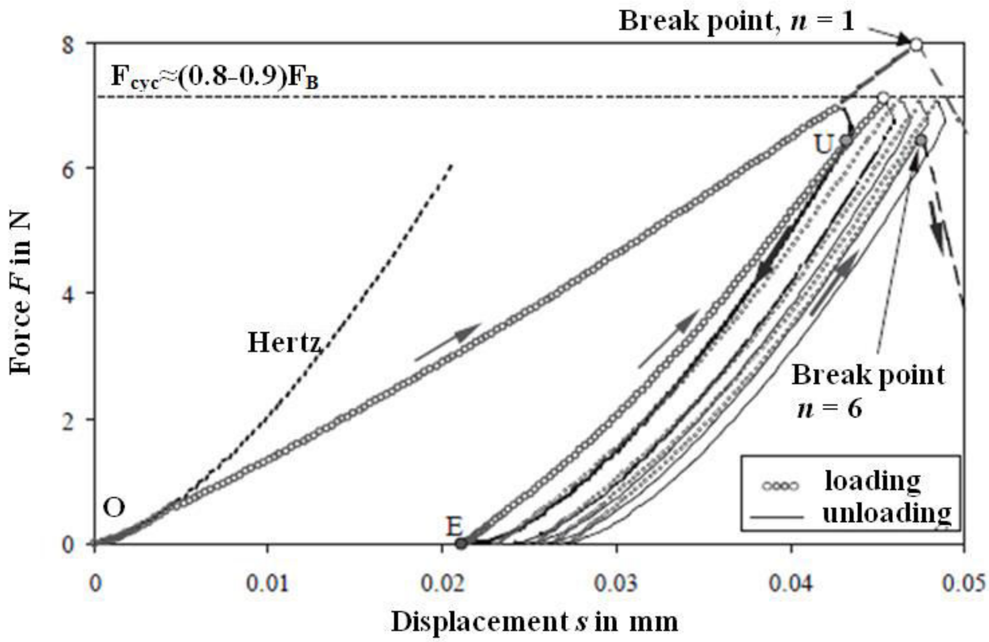

Figure 2.5 Loading–unloading force-displacement curves of Zeolite 4AK granule [29].

A granule was repeatedly loaded and unloaded at a cyclic force F_{cyc}. However, the orientation of the granules to the direction of stressing piston movement remains the same (fixed). That means that granule was stressed at the same point at its surface. A large plastic deformation (O-U) demonstrates elastic–plastic behavior. The unloading curve U–E is similar to the Hertzian curve, however only an elastic deformation disappears during unloading.

The maximum plastic deformation and the highest breakage limit were performed during first cycle. There is a change in the total strain of a granule in each loading cycle until the breakage point. The number of cycles depends on intensity of the loading and the material properties. The reduction of total deformation shows a stiffening effect during loading–unloading cycles.

The important one is, all stressings were conducted in fixed point of stressing direction of a single granule. Repeated stressing generates deformation that leads to crack formation at the contact point of granule. The cyclic stiffening or hardening means the change in structure of the material at the contact points, where the stresses are very high. The density and stiffness in this points increase without any significant change of granules properties outside of contact point. With the increasing of cycle number the microcracks propagate inside.

Granule stores cyclic loading energy and damages are developing during an elastic–plastic deformation, which leads to a lower breakage force than at single loading. However it is only in the fixed position treatment of stressed granules. The result may perform different behavior if granules are rotated granule during testing by repeated stressing.

In addition, Antonyuk et al. [29] calculated the breakage probability of stressed granules by compression test. The breakage probability was calculated by use of Weichert model and fitted with Eq. (2.9). To initiate the fracture at the same probability a higher mass-related energy is required for smaller granules than for larger granules, see **Figure 2.6.**

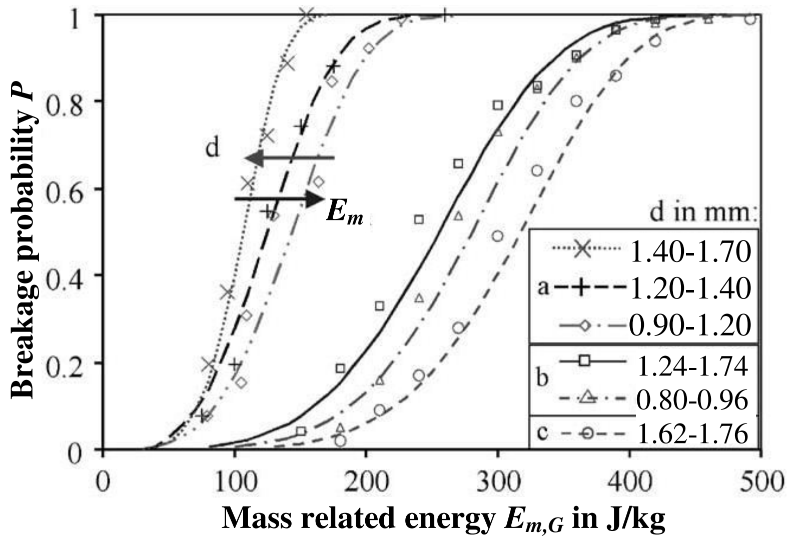

Figure 2.6. Breakage probability P of the different sized examined granulates as a function of mass-related breakage energy E_m: (a) Zeolite® 4AK; (b) sodium benzoate; and (c) $\gamma\text{-}Al_2O_3$ [29].

Result obtained, besides bond strength and orientation the distribution of inhomogeneities are responsible for the breakage behavior.

To consolidate the experimental results with simulation Khanal et al. [46] simulated the stressing conditions and breakage mechanisms of stressed particles compounds. By using finite-element method and DEM, the simulation was carried out with diametrical stressing condition to understand the fracture behavior of particle compounds. The study of the comminution behavior of material emphasized the surface generation distributions relates to the ingredient arrangement by crushing testing.

2.5 The determination of breakage probability by Monte-Carlo Method

In principle, to predict the behavior of particle breakage with a large number of particles the work has to focus on the response of mean quantities. The properties of particle breakage are complex however the breakage probability can be computed by using any modeling method. The results of several researches [20] [24] [47, 48-53] had clearly established the stochastic dynamic of particle fracture and the distribution of the particle fracture strengths. The fracture strength of a particle is considered to be one of the key parameters in relation to its resistance to breakage. This aspect of the breakage behavior of particle is explored in the stochastic modeling of breakage process such as repeated stressing.

In determining the properties of some phenomenon or behavior such breakage of large amount of particles by repeated stressing, one can use Monte-Carlo method. It is a computational algorithms that relies on random sampling to obtain numerical results by generating samples from a probability distribution. In random testing of events such repeated stressing, the breakage is uniformly distributed or followed another desired distribution.

The explained models and experiments above were originally introduced to calculate the breakage probability of spherical particles. For irregularly shaped particles, a distribution function of breakage probability is not precisely defined due to its roughness sensitivity to particle shape and surface (see **Figure 2.7**).

With the help of the particle caps contact model, the deformation behavior of stressed particles or granules can be modeled as hemi-spherical asperities proposed by Tomas et al. [3]. Based on the model of hemi-spherical asperities Aman et al. [23] calculated the breakage probability distribution of irregular shaped particles. The breakage probability distribution by single compression and impact test was calculated by use of Monte-Carlo Method as superposition of the breakage probabilities of asperities with randomly distributed sizes.

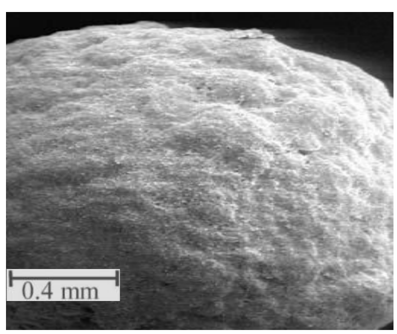

Figure 2.7. Roughness distribution by SEM of a sodium benzoate granule surface [29].

The form of particles was represented as a combination of hemi-spherical asperities. Particles of Dead Sea salt, sugar, basalt and granules of γ-Al_2O_3 were tested. In case of compression test, particle was put on the plate the orientation of the particle to the stressing piston is not random. The breakage of particle occurs as result of fracture of asperities.

The relation between breakage energy distribution and force distribution was obtained. Every distribution was normalized by a mean arithmetic value of breakage energy or force, respectively. The dimensionless normalized distributions were fitted with log-normal functions. The fit function of the normalized force distribution can be transformed into the fit function of the normalized energy distribution and vice versa [23].

The breakage probability distribution of irregularly shaped particles was calculated as a superposition of the breakage probabilities of individual log-normal distributed asperities. The results show the specific features of the resulting breakage probability distribution. The distribution of breakage probability was represented in a simple universal form. In this representation, the breakage depends on the normalized breakage energy only. It does not depend on the particle size and material, see **Figure 2.8.**

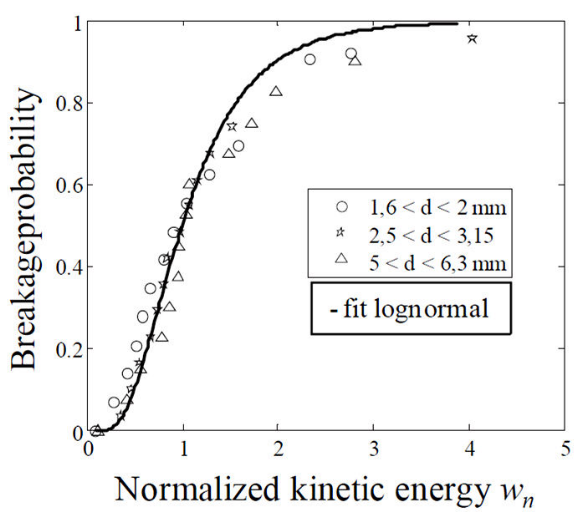

Figure 2.8. Cumulative experimental distributions of breakage probability of basalt particles versus normalized kinetic energy $E_n=E/E_{mean}$ $\cdot E_{mean}$ is equal to 2.56 mJ, 14.8 mJ and 78.3 mJ for particle size d at intervals 1.6<d<2 mm, 2.6<d<3.15 mm and 5<d<6.3 mm, respectively [23].

However, a complete description of physical phenomena that occurs at granules breakage is not available yet. Particularly in predicting breakage behavior of granules regards to the configuration of stressing contact points by repeated stressing.

For example, breakage is history-dependent, i.e. the number of microcracks increases due to previous stressing events [20-23]. As a result, the mechanical properties and breakage parameters vary even by testing the geometrically similar particles of the same size.

Regarding to the inhomogeneous granules, for a given granules size, the fracture stress at the first stressing event varies depending on particle shape.

The mechanical characteristics of the primary particles and the bonding agents are randomly distributed within granules. Even with the identical production process, the strength of the individual granules differs in the microstructure because of the distribution and orientation of bonds, defects and pore size distribution. Besides bond strength and orientation the distribution of in homogeneity pores are responsible for the breakage behavior.

Therefore this thesis will develop a breakage probability model by taking into account the orientation of granules by repeated stressing.

It can be articulated the described models above determine breakage probability by considering some parameters such as:

- Strength distribution within granules.
- The progressive growth of crack-like damage that ultimately leads to fracture of a particle under stresses.
- Number of impacts.
- Damage accumulation.
- Particle shape.
- Particle size.
- Impact velocity.
- Material-specific parameter, and
- Deformation work.

However the previous investigations did not involve the orientation of particle during stressing. The next model will be developed by considering the orientation of particle that is validated by using data from double impact and drop weight testing. This complex behavior can be simulated by use of Monte-Carlo method.

2.6 Statistical data evaluation

2.6.1 Correlation coefficient

For the statistical distribution model, validation of the correlation coefficient or R-square as the statistic probability model is used. The correlation coefficient also known as the fitting parameter used to evaluate the model [54]. Correlation coefficient is 1 minus the ratio of residual variability. When the variability of the residual values around the regression line relative to the overall variability is small, the predictions from the regression equation are good. It can take on any value between 0 and 1, with a value closer to 1 indicating that a greater proportion of variance is accounted for by the model [55].

2.6.2 Normal distribution

The probability distribution function (pdf) $f_n(x)$ represents the probability $p_n(x)$ to find the value x of the normal distributed variable X in interval dx [56]

$$p_n(x) = f_n(x)dx = \frac{1}{\sigma_s\sqrt{2\pi}} exp\left(\frac{-(x-\mu)^2}{2\sigma_s^2}\right)dx \tag{2.20}$$

The parameter μ is the mean or expectation of the distribution. It can be estimated for discrete events as follow

$$\mu = \frac{1}{N}\sum_{n=1}^{N} x_n \tag{2.21}$$

where N is number of elements in X and x_n is mode. The parameter σ_s is standard deviation:

$$\sigma_s = \left(\frac{1}{N}\sum_{n=1}^{N}(x_n-\mu)^2\right)^{\frac{1}{2}} \tag{2.22}$$

It represents the width of distribution.

Function of normal distribution is a symmetrical function with respect to μ and the maximum value of this function will be achieved by $\mu = x_{50} = x_n$. If $\mu = 0$ and $\sigma_s = 1$, the distribution is called the standard normal distribution or the unit normal distribution, and a random variable with that distribution is a standard normal deviate [57].

The normal distribution can be represented in another form as normal cumulative distribution function (cdf)

$$P_n(X < x) = \int_{-\infty}^{x} \frac{1}{\sigma_s\sqrt{2\pi}} \exp\left(\frac{-(t-\mu)^2}{2\sigma_s^2}\right) dt \tag{2.23}$$

Cumulative distribution function (cdf) give the probability that the random variable *X* takes on a value less than or equal to *x*. Due to symmetry of normal distribution function with respect to μ the median value $P_{0.5}$ will be archived at x_{50}=μ.

2.6.3 Relationship between normal and log normal distribution

Two associated random variables *X* and *Y* exhibit the same values of mean value μ and standard deviation σ_s. There are the follow relationships between parameters of the normal and associated lognormal distributions [58]. The lognormal distribution has parameters

$$\mu_{\ln} = \ln\left(\frac{\mu^2}{\sqrt{v+\mu^2}}\right) \quad \text{and } \sigma_{\ln} = \sqrt{\ln\left(1+\frac{v}{\mu^2}\right)} \tag{2.24}$$

Where v_r is variance. The frequency function of this associated lognormal distribution *Y* is

$$p_n(y) = f_n(y)dy = \frac{1}{\sigma_s\sqrt{2\pi}} \exp\left(\frac{-(y-\mu_{\ln})^2}{2\sigma_{\ln}}\right) dy \tag{2.25}$$

where the *y* is a lognormal distributed value with mean value μ_{ln} and standard deviation σ_{ln} [64]. By releasing of value *y*=ln(*x*) [59, 60]

$$p_n(x) = f_n(x)dx = \frac{1}{x\sigma_{\ln}\sqrt{2\pi}} \exp\left(\frac{-(\ln(x)-\mu_{\ln})^2}{2\sigma_{\ln}}\right) dx \tag{2. 26}$$

Figure 2.9 represents probability distribution function for normal and associated lognormal distributions. One can see that the function of normal distribution is a symmetrical function with the maximum by x=μ=10. The lognormal distribution is an asymmetrical function with the maximum that is shifted to lower values of *x* with respect to maximum of associated normal distribution.

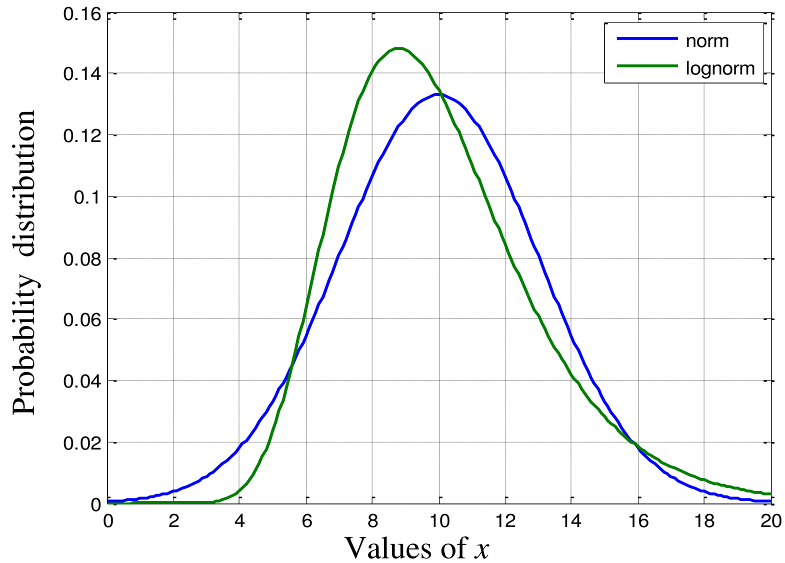

Figure 2.9. Probability distribution for normal and associated lognormal distributions.

Figure 2.10 represents the cumulative probability distribution function for normal and associated lognormal distributions. The median value $P_{0.5,n}$ by cumulative distribution function of normal distribution will be achieved at $x=\mu=10$. Consequently, the median value $P_{0.5,ln}$ by cumulative distribution function of lognormal is shifted to low x.

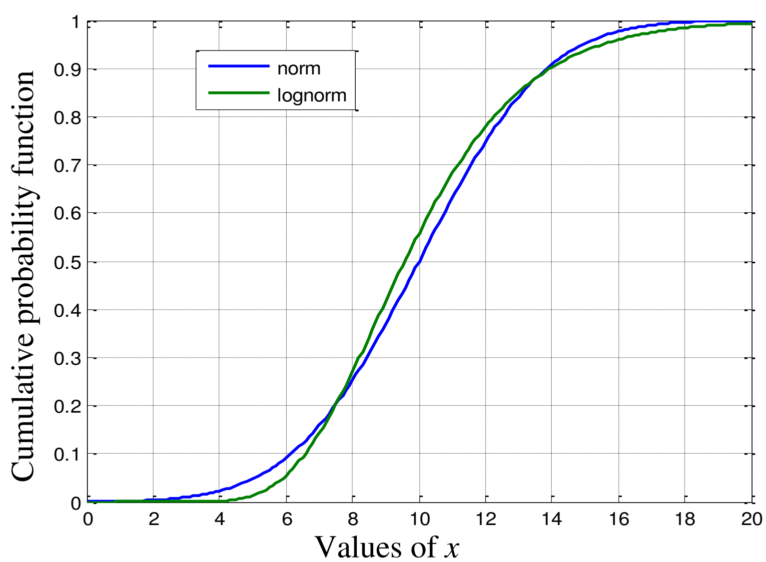

Figure 2.10. Cumulative probability distribution for normal and associated lognormal distributions.

2.7 Materials

Materials that are used in the experiments are gamma Aluminum oxide (γ-Al_2O_3), Zeolite 4AK and Zirconium oxide (ZrO_2).

2.7.1 Gamma - Aluminum Oxide (γ-Al_2O_3)

Aluminum Oxide (Al_2O_3) is a white compound of aluminum and oxygen (see **Figure 2.11**), water-insoluble, loose powder and highly hygroscopic [61]. Hygroscopic particles have porous structure that means the stressing and the absorption behaviour are different from non porous particle.

Modifications occur in Al_2O_3 between 400 and 1000°C as the alumina becomes thermodynamically unstable. Gamma Aluminum oxide (γ-Al_2O_3) is a modified structure transition of Al_2O_3 by thermodynamic treatment. It chemically dissolve in strong acids and in bases [62].

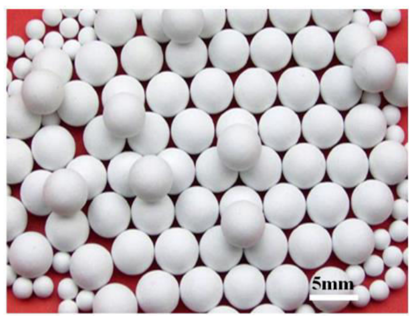

Figure. 2.11 The physical appearance of γ-Al_2O_3granules.

The γ-Al_2O_3 granules are made through a multistep process of boehmite. Boehmite is an aluminum oxide hydroxide (γ-AlO(OH)) mineral, a component of the aluminum ore bauxite [63]. After hydrolyzation of boehmite in an aqueous solution, γ-Al_2O_3 powder can be obtained by spray-drying. The specific surface area decreases with the increasing in calcination temperature. Calcination is a thermal treatment process in absence of air applied to ores and other solid materials to bring about a thermal decomposition, phase transition, or removal of a volatile fraction [63]. By granulation of γ-Al_2O_3 powder, spherical granules are made in different sizes. There are often used spray granulation and sintering [64].

Granules of γ-Al_2O_3 are easy to handle, favorably priced and easy to produce. Moreover, they are available in large quantity. Due to its high surface activity, γ-Al_2O_3 is used as an adsorbent and catalyst material (see **Table 2.1**).

Due to a high internal membrane surface and intermediate layer area they are widely used as an industrial adsorbent catalyst support. Based on their thermal stability, they are used as catalyst carriers and adsorbents in the petroleum and chemical industries. Sintered into porous structures and applied to coarser substrates, nano scale aluminum oxide can also be used for nano filtration (see **Figure 2.12**) [64].

So far, this model material has been selected for numerous scientific works and analyzed in detail due to the beneficial and is defined physical properties [65].

Table 2.1 Properties of γ-Al_2O_3 granules [65]

Properties γ-Al_2O_3	
Molecular formula	γ-Al_2O_3
Industrial size	1.6 - 3.0 mm
Appearance	White solid
Odor	Odorless
Density	3.95–4.1 g/cm^3
Melting point	2072 °C
Boiling point	2977 °C
Solubility	insoluble in diethyl ether, practically
Thermal conductivity	insoluble in ethanol 30 $W \cdot m^{-1} \cdot K^{-1}$
Structure	
Crystal structure	Trigonal
Coordination geometry	Octahedral
Thermochemistry	
Enthalpy of formation	$-1675.7\ kJ \cdot mol^{-1}$
Standard molar entropy	$50.92\ J \cdot mol^{-1} \cdot K^{-1}$

2.7.2 Zeolite 4A

Appearing as small dense pinkish beads, zeolite 4A are highly porous crystalline metal-alumino silicates (see **Figure 2.13**) [66]. The zeolite 4A that is used in these experiments is a commercial trademark produced by "*Chemiewerk Bad Köstritz*", Germany. The product is labeled as "*Köstrolith*® 4AK" with a pore size is 4Å. It allows the end product to be more precise then other desiccants so different pore sizes can be found, each one with a few different properties.

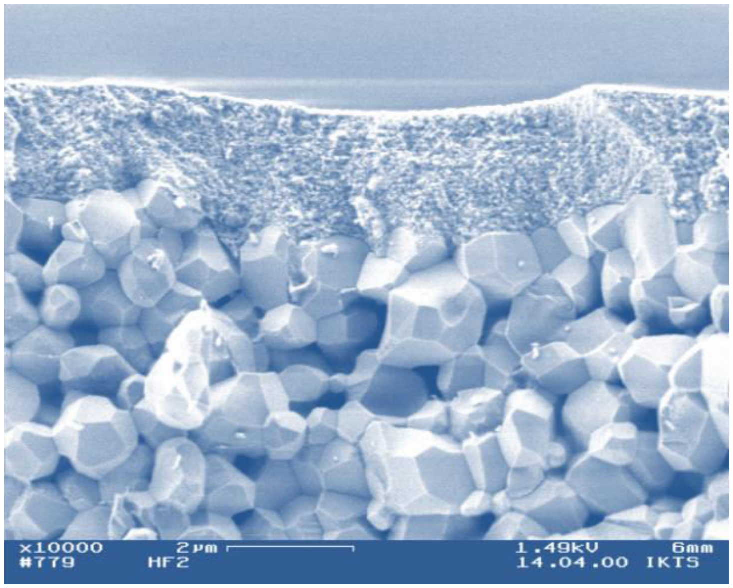

Figure 2.12 The 0.2 μm cover membrane of amorphous Al_2O_3 on an approximately 1 μm intermediate layer of γ-$A1_2O_3$ [64].

Absorption will occur only for molecules with smaller diameters than which have pore size larger molecules being excluded from absorption. Preferentially absorbed are molecules of greater polarity which makes zeolite 4A ideal for absorption of water from liquids and gases as water molecules are both polar and very small. The specific characteristic is shown in **Table 2.2**. Zeolite 4A is classified by its pore size in angstroms, some of the most used are 3A, 4A itself, 5A, 8A (10X) and 10A, also known as 13X. This feature allows the selection of a zeolite 4A which can absorb water yet exclude most of other molecules or other desiccants which will absorb bigger molecules like aromatics or carbon dioxides [67].

Related to those characteristics, some applications of zeolite 4A are as dryer of gases and organic liquids, absorber of carbon dioxide, for water pre-purification, and for bringing the relative humidity in packages down as low as 10% RH [67].

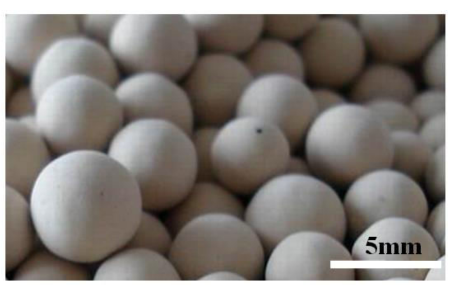

Figure 2.13 The physical appearance of granules zeolite 4A.

Table 2.2 Characteristic properties of zeolite 4A material [67].

Manufacturer	**CWK "Chemiewerk Bad Köstritz", Bad Köstritz**
Chemical composition (%)	85% synthetic zeolite 13X, (30%-Al_2O_3, 51%-SiO_2, 17%-Na_2O, 2%-MgO)
Binder	clay and water
Granules size distribution (mm)	0.90–1.20; 1.20–1.40; 1.40-4.00; 1.40–1.70
Agglomerate density (kg/m^3)	1300
Solid density (kg/m^3)	2100
Specific surface area (m^2/g)	415 (including the surface of micropores)
Pore volume fraction (%)	45 (macropores)
Application	Adsorbent (molecular sieve) for drying processes and cleaning of gas.

2.7.3 Zirconium Oxide (ZrO_2)

Figure 2.14 A typical Zirconium Oxide balls (ZrO_2) type grinding balls.

Zirconia or Zirconium Oxide (ZrO_2) grades are various. They differentiate from each other by the properties of the stabilizing agent which is used. Magnesia-partially-stabilized Zirconia (MgO-PSZ) and yttria-partially stabilized Zirconia (Y-TZP) in particular offer an outstanding resistance to mechanical shocks as well as to flexural load. It is because of their high fracture toughness and relative "elasticity". These two zirconias are advanced ceramics of choice for severe mechanical applications (see **Figure 2.14**) [68].

At high temperature the transformation from tetragonal form to monoclinic is rapid and is accompanied by a 3 to 5 percent volume increase that causes extensive cracking in the material. This behavior destroys the mechanical properties of fabricated components during cooling and makes pure zirconia useless for any structural or mechanical application [69].

The controlled, stress induced volume expansion of the tetragonal to monoclinic inversion is used to produce very high strength, hard, tough varieties of zirconia available from manufacture for mechanical and structural applications [70]. There are several different mechanisms that lead to strengthening and toughness in zirconias that contain tetragonal grains. This is a complex subject matter [70]. Circonias are used in cutting and wear resistant applications due to its reliable and outstanding hardness and toughness as is shown in **Table 2.3** [70].

Table 2.3 Characteristics of Zirconium Oxide, ZrO_2 [70].

Mechanical	Unit	Value
Size	mm	1.5-5.0
Density	gm/cm^3	6
Porosity	%	0
Color	—	ivory
Flexural Strength	MPa	900
Elastic Modulus	GPa	200
Compressive Strength	MPa	1800-4820
Hardness	N/mm^2	1300
Fracture Toughness K_{IC}	$MPa.m^{1/2}$	13
Thermal Conductivity	W/m.°K	2

2.7.4 Characteristics of granule structures

A single granule is built by primary particles, internal pores in the primary particles and binder. Binder performs solid bridge bonds (see **Figure 2.15**).

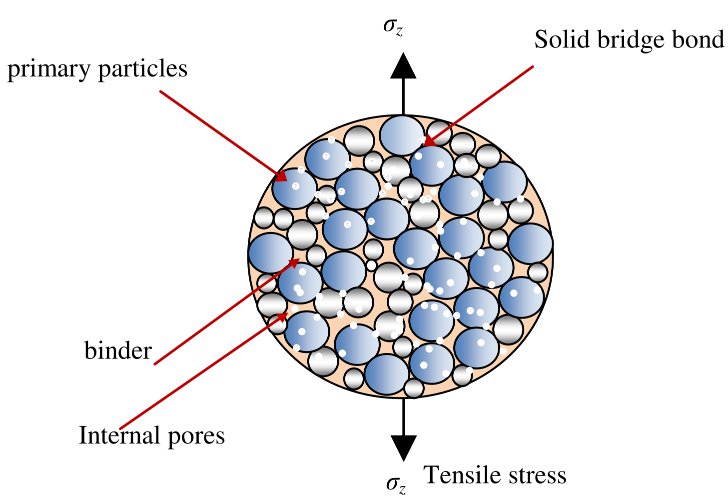

Figure 2.15. Schematic structure of a granule and possible breakage path [29].

The solid bridge (parallel) bond stiffness is more or less a kind of a solid state bond between the particles (see **Figure 2.16**). It describes the constitutive behaviour of a finite-sized piece of cementitious material deposited between two particles [29]. These bonds can transmit both forces (normal and shear) and moments between particles. Adhesive contact bonds transmit forces (tensile normal and shear), frictional rolling and torsional moments acting at very small contact area compared to particle sizes.

Solid bridge bonds are physically strong contact bonds with constant normal and shear stiffness. They uniformly distributed over either a circular or rectangular cross section lying on the contact plane and centered at the contact point [29].

Once stress reaches the bond strength of the particle, bonds between the particles will break. Bonds between particles are failure by tensile strength. At the start of each time-step, the set of contacts is updated from the known particle and wall positions. Stressing generates a relative motion at the primary particle contact. It causes the normal force $F_{b,n}$ and shear bond forces $F_{b,s}$ and a cross sectional moment M_B to develop within the bond material as a result of the solid bridge bond stiffnesses.

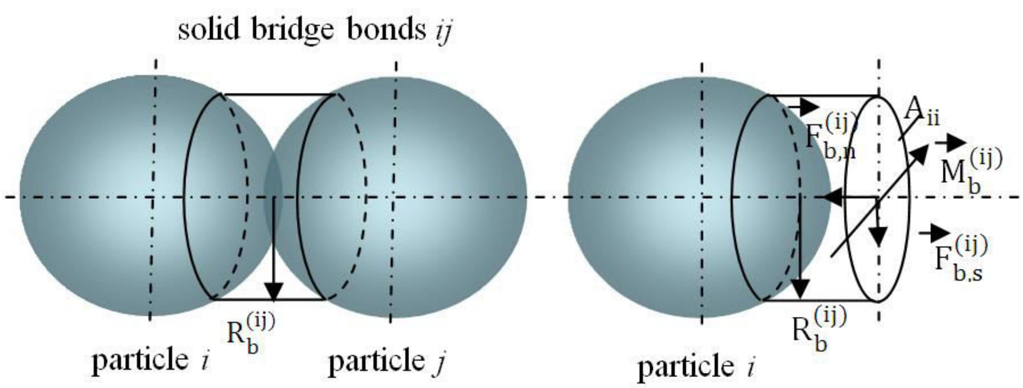

Figure 2.16. Solid bridge bond model for DEM calculation [24].

Force and moment acting on the two bonded particles can be reduced to the normal and shear stresses acting within cross sectional area of the solid bridge bond A_{ij} with R_B is the radius of the solid bridge bond. If either of these stresses reaches its corresponding bond strength, the solid bridge bond breaks [24].

Those forces and moments act on the two bonded particles (particle i and particle j) and can be related to the maximum normal and shear stresses acting within the bond material at the bond periphery. Fracture occurs on a plane normal to the tensile stress direction and that the particles intersected by this plane come apart without themselves contributing to the strength [24].

The smooth round surface of primary particle with a thin shell is identified by **Figure 2.17**. The shell covers irregularities. Repeated stressing like during production and transportation leads to local damages of the shell. The damage mostly initiates defects. Size and position on the surface of the granules have a large influence on the granules failure strength and breakage probability during repeated stressing [29]. By stressing, the surfaces of the pores have substantially higher tension than elsewhere, which increase the probability of breakage at these domains.

Granules of γ-Al_2O_3, behave elastic-brittle during stressing. This is indicated by meridian cracks generation. The cracks initiate from the perimeter of a circular contact area, where a maximum tension stress appears. With a rapid propagation of cracks (divergent to the impact axis) by repeated stressing, the grains will be separated into several meridian fragments [29].

The smooth area of the meridian cracks through the porous γ-Al_2O_3-granules clearly refers to a brittle fracture, without plastic deformation.

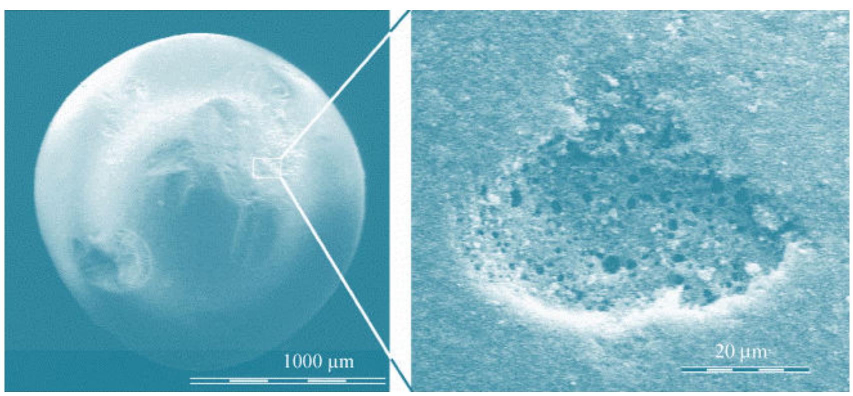

Figure 2.17. SEM of a local damage at the surface of a γ-Al_2O_3-granule after an impact [29]

In addition many small cracks within the cone of fines occur, where the energy density is very high at the moment of impact [29]. The crack propagates from one pore to another pore.

As a result, many fine particles are formed within the range of 0.5–100 µm, where the lower limit is equivalent to the average distance between two pores. At high fired granule velocity, secondary cracks are formed and they are perpendicular to the direction of impact [29].

Digital images of different optical enlargements of the surface structure of the granules have been recorded with scanning electron microscopy as shown in **Figure 2.18**. The granules exhibit a high sphericity and a smooth surface. Highly enlarged images reveal the structural composition of the granules consisting of primary particles of different sizes and random orientation bonded together by solid bridge bonds [31].

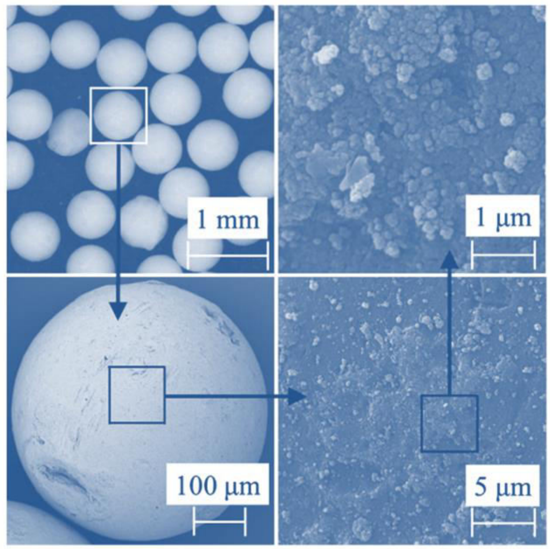

Figure 2.18. Digital images of the surface of a granule γ-Al_2O_3 (d_{50} = 0.6 mm) recorded using scanning electron microscopy [31].

Granules consist of solid microscopic primary particles bonded by adhesion forces, liquid or solid bridges [71]. Liquid at the primary feed particles perform binding among the contacts of the primary particles or capillarization in the internal pores. This adhesion forces influence the breakage probability of granules by stressing [72].

Inhomogeneity of granules is influenced by granulation. It depends considerably on micro and macrostructures of the granules, which are formed during the production process [71].

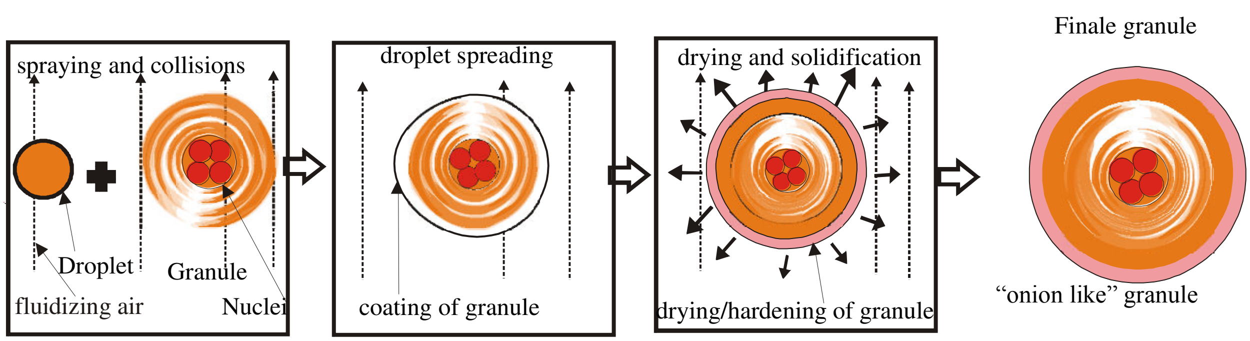

Figure 2.19.Granule growth by coating from the principle of fluidized bed spray granulation [71].

Zeolites for instance are produced by the fluidized bed granulation (**Figure 2.19**). The process consists of the multiple spraying, spreading and solidification of the droplets on the nuclei [71]. The performance of granule surface is depending on granulation technique.

CHAPTER 3

MONTE-CARLO ANALYSIS OF GRANULE BREAKAGE

3.1 Description of Monte-Carlo Analysis

To describe the breakage behavior of granules by repeated stressing one can use Monte-Carlo analysis [73]. It is a computational algorithm that used a sampling of random distributed numbers to obtain the results of numerical tests. The Monte-Carlo analysis can be successful applied when the analyzed system is infeasible to apply a deterministic algorithm. In this context, the Monte-Carlo methods are very useful for simulating of behavior of granule systems contain large number of granules with random distributed parameters. The application of Monte-Carlo method is particularly promising in case of repeated stressing of inhomogeneous granulates where the strength is distributed inside of granules and depends on history of granule stressing. For example, there is a simple procedure that can be used to calculate the breakage probability distribution. On the one hand, the strength distribution of granules can be modeled by generating random distributed numbers - breakage forces. On the other hand the force applied to granules can be modeled with other set of random distributed numbers. The breakage probability distribution can be calculated by means of comparing of the applied force and breakage force of granule. The parameters of distributions and its temporal behavior can be easily varied depending on granule properties and applied forces.

There are follow grounds to apply the Monte-Carlo analysis for breakage test:

a) The Monte-Carlo for testing is a numerical test that can be carried out under conditions likely to condition of real breakage experiment,
b) The parameters of Monte-Carlo simulation can be easily changed to take into account a change of granule properties depending on stressing history,
c) The Monte-Carlo method can be applied for multi-modal distributions. In this way an effect of different combinations of granules properties on its breakage behavior can be investigated.

A Monte-Carlo numerical method is equivalent to the real experiments. It requires careful planning and analyzing the results. Because Monte-Carlo method deals with multiple conditions and massive amounts of resultant data, the careful identification of properties of analyzed granules and selection of simulation parameters is the scope of the planning of simulation.

3.2 Monte-Carlo analysis of breakage behavior of granules

It is assumed that the strength of granules varies not rapidly along the granules surface. Due to this a finite number of stressing locations, N can be introduced to characterize their breakage behavior. Inside of single location with number i the breakage force $F_{b,i}$ does not change. The set of locations represent a strength distribution along the surface of granules, see **Figure 3.1.** As result, the surface of granules can be divided into finite number N of locations where the breakage behavior can be tested by means of Monte-Carlo analysis. The applied method is similar to described by Aman et al. [73] where combination of the finite number of hemispherical asperities was used to simulate the breakage behavior of irregular shaped granules.

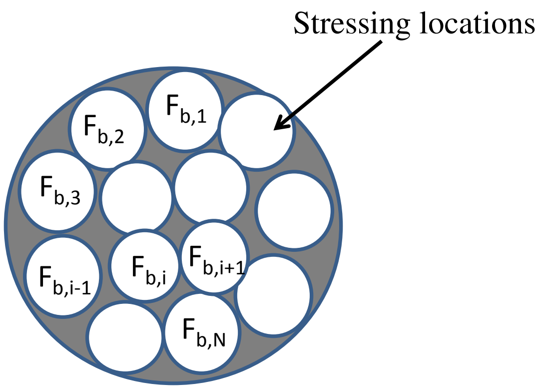

Figure 3.1.The distribution of test location on the surface of granules.

There are simple steps in Monte-Carlo simulation that can be easily implemented in MATLAB to simulate the repeated testing of granules.

Step 1: Generation of breakage force distribution. Set of i random distributed breakage forces $\{F_{b,i}\}$ is generated, see **Figure 3.2**. Every value of breakage force $F_{b,i}$ corresponds to the test location (point) with the number i at granules surface. The type of distribution can be chosen depending on the granule properties.

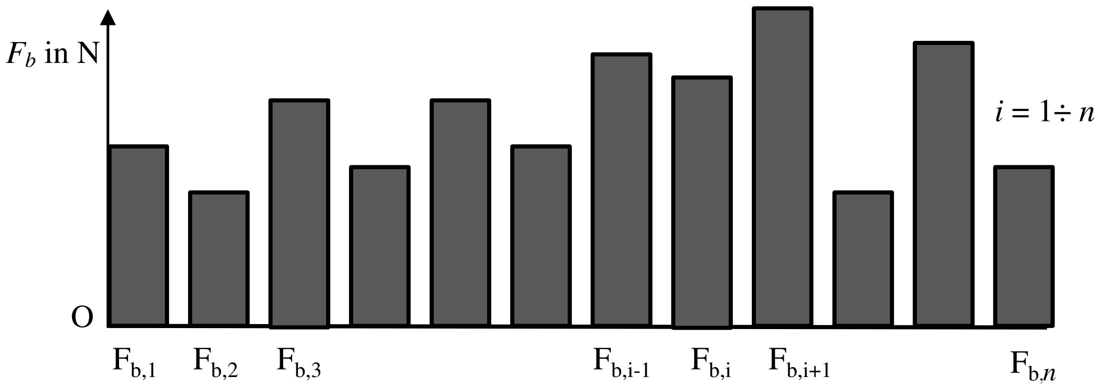

Figure 3.2. The strength distribution of the test location.

Step 2: Generation of applied force distribution. Set of j random distributed stressing forces $\{F_j\}$ was generated. The element of set F_j corresponds to force applied to the granule by the stressing event with number j, see **Figure 3.3.**

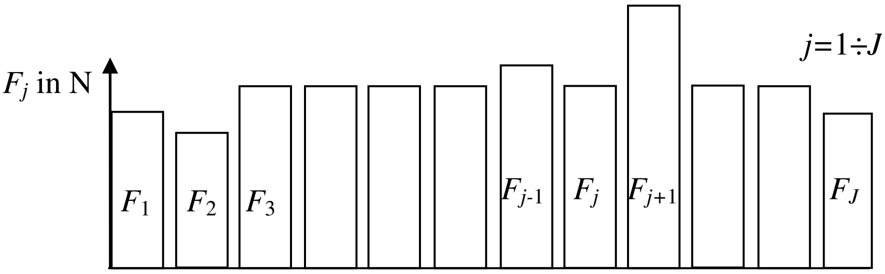

Figure 3.3. The distribution of applied forces.

Step 3: Breakage test i.e. comparing of applied and breakage forces. There are to distinguish four different types of breakage tests.

Fixed contact point by stressing on the granule surface

a) A repeated force from set $\{F_j\}$ is applied to one test point on the granule surface. In this particular case the number i from breakage forces set $\{F_{b,i}\}$ is the number of tested granule. If the current force F_j is higher than $F_{b,i}$ then the breakage condition is fulfilled and breakage occurs. The breakage force number, i.e. number of stressing events until breakage j, is saved. If the breakage does not occur by applied force F_j then the next force F_{j+1} is applied, see **Figure 3.4.** The test is repeated until the breakage occurs or all J generated forces would be tested. After breakage of granule with number i a new force set $\{F_j\}$ is generated to test the next granule with number i+1.

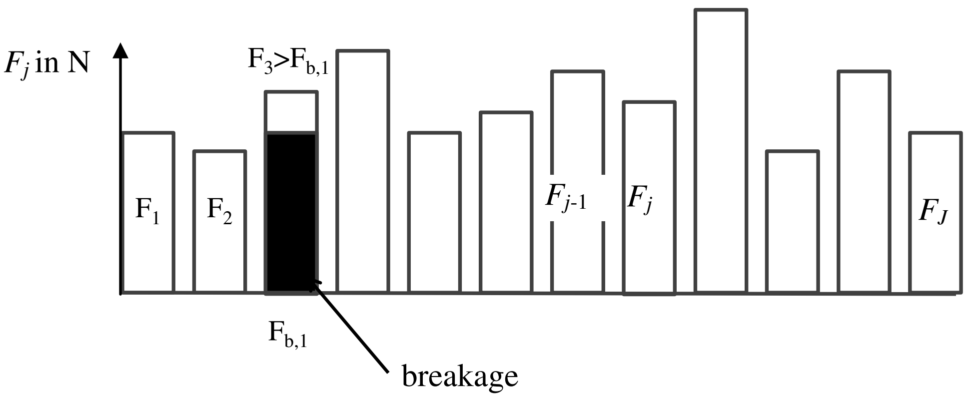

Figure 3.4. The test of granule strength by means of applied forces. The breakage of granule at the test location with number 1 ($F_{b,1}$) occurs by the testing events number 3 (applied force F_3), where the breakage condition $F_3 > F_{b,1}$ is fulfilled.

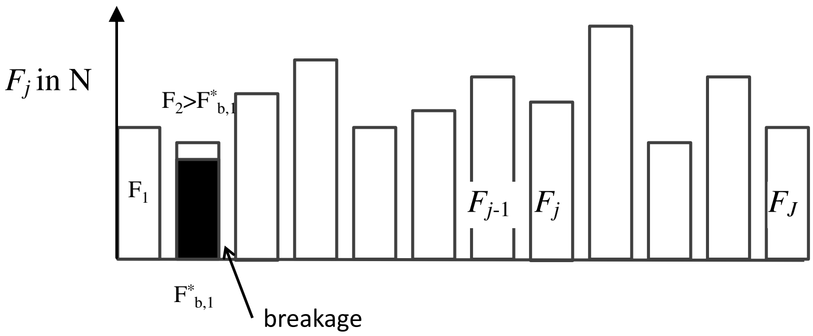

Figure 3.5. The breakage force $F_{b,1}$ is reduced due to the force application during the test number 1. The reduced breakage force of granule $F_{b,1}{}^*$ is lower than the applied force F_2. The breakage occurs by applied force F_2.

b) Like the procedure described in sub section **a**), the force set $\{F_j\}$ is applied to the same point until the breakage occurs. However, in difference to the test procedure described in the subsection **a**), the strength of granule is affected by the repeated loading. If the next test occurs at the same surface location as previous, then the breakage force would be reduced, see **Figure 3.5**.

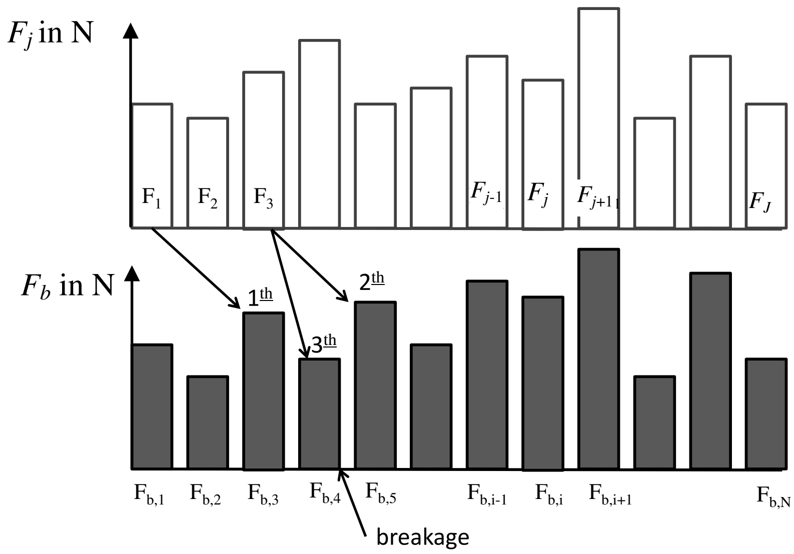

Figure 3.6. The force F_1 was applied at first to the test points 3. Then the force F_3 to the test point 5. However, the breakage condition $F_2>F_{b,4}$ is fulfilled by 3th stressing. The breakage occurs at the test point 4 by application force F_3.

Random contact points of stressing on the granule surface

c) Force from set $\{F_j\}$ with random number j is applied to the random chosen locations on the surface of tested granule. After breakage the stressing number corresponding to breakage is saved and granule is removed from set of tested granules. By next test the tested granule is randomly chosen from remained granule. The strength of granule at given location will not be changed by the application of repeated force, see **Figure. 3.6**.

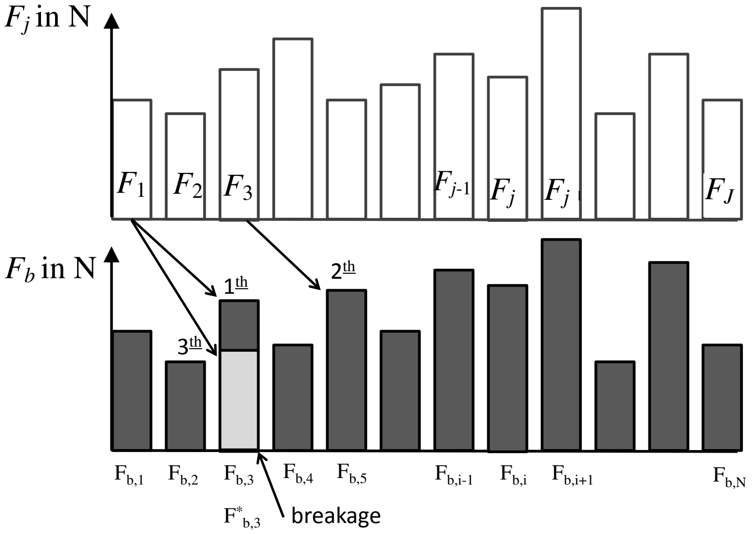

Figure 3.7. The breakage occurs by the 3th stressing. The strength of point 3 was reduced after the 1th stressing.

d) Like the procedure described in **section c)**, the random force is applied to the different points on the granule surface. If the next test occurs at the surface location tested before, then the breakage force has to be reduced, see **Figure 3.7**.

Step 4: The distribution of breakage numbers is analyzed to obtain the breakage probability distribution depending on the test number i.e. on the number of stressing events before breakage occurs.

3.3 Results of Monte-Carlo test with normal (Gaussian) distributed breakage forces

The parameters of breakage and applied force distributions were chosen to model the real condition of granule tests, see **Table 3.1**.Usually, the applied forces are depending on type of stressing equipment, only. Based on this fact, it can be assumed that the applied forces are normal distributed and are not changed during the experiments. The test can be carried out in the dimensionless form i.e. by using arbitrary units that can represent both – the forces and stressing energies that are necessary for granule breakage.

The **Figure 3.8** represents the results of Monte-Carlo simulation fitted by means of degradation model. The degradation model was developed to fit the results of Monte-Carlo simulation. It was taking into account that the granule properties i.e. breakage probability can be changed during the repeated stressing. The breakage probability $w(1)$ by the first stressing is about of 0.5. Indeed, the parameters of applied and breakage forces distributions are the same.

Table 3.1. The condition of breakage test with normal distributed breakage forces.

Type of breakage test	Breakage force distribution ($F_{b,i}$) in N	Applied force distribution (F_j) in N
Fixed stressing location. Test condition accor-ding to section **a)**	Normal distribution with mean force $F_{b,i,\ mean}$=10 N and standard deviation S=3 N. Number of breakage forces i.e. tested granules I=1000.	Normal distribution with mean force $F_{j,mean}$=10 N and standard deviation S=3 N. Number of applied forces J=10 .

To characterize the degree of granule the degradation parameter q is introduced. After every stressing events of number i the breakage probability is reduced in to simple rule:

$$w(i) = w(i-1)\cdot q = w_0 \cdot q^i \quad i = 1..n \tag{3.1}$$

Wherew_0 is the initial breakage probability.

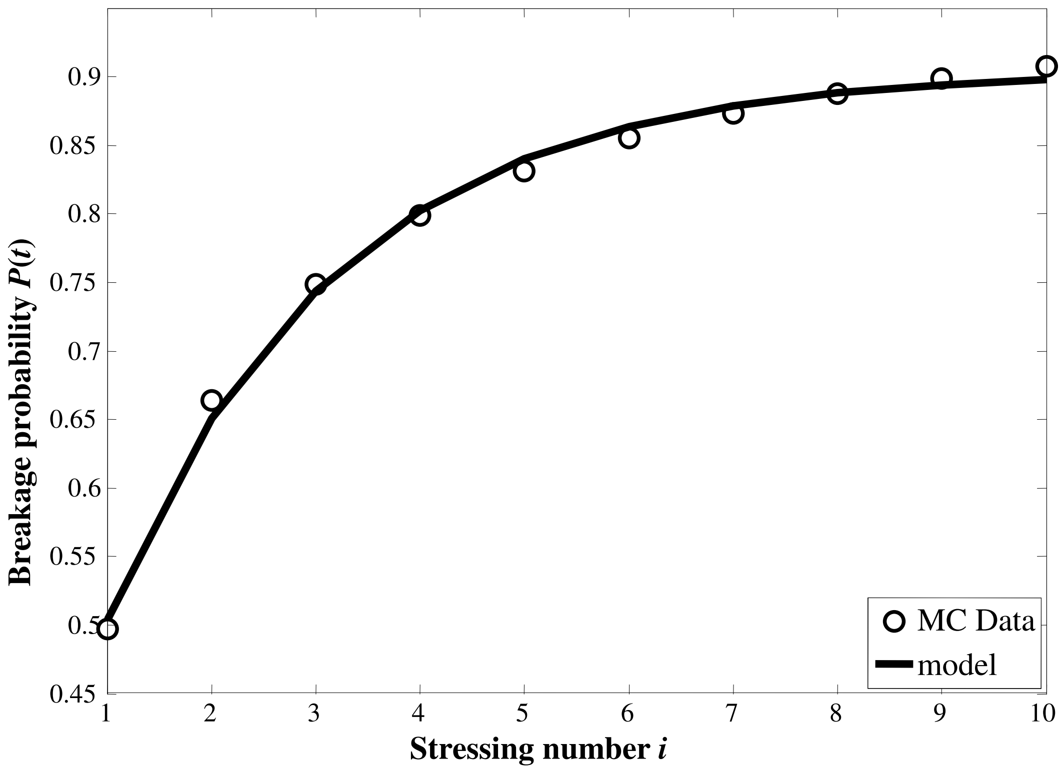

Figure 3.8. The results of Monte-Carlo simulation fitted by means of degradation model. The granule degradation parameter q=0.796. Correlation coefficient R^2=0.984. The breakage probability and applied forces are normal distributed.

For every granule the probability to be broken during the stressing events with number i can be calculated based on this assumption. In terms of developed model the number of nonbroken granules N_{nb} after the first stressing:

$$N_{nb} = N_0 \cdot (1 - w_0 \cdot q) \quad (3.2)$$

Where N is the total number of tested granules.

The number of nonbroken granules after the second event and the stressing events with number i can be found as:

$$N_{nb} = N_0 \cdot (1 - w_0 \cdot q) \cdot (1 - w_0 \cdot q^2) \quad (3.3)$$

$$N_{nb}(i) = N_0 \prod_{j=1}^{i} \left(1 - w_0 \cdot q^{j-1}\right) \quad (3.4)$$

Consequently, the number of broken granules $N_b(i)$ and the breakage probability $P(i)$ result in:

$$N_b(i) = N_0 \prod_{j=1}^{i} \left(1 - \left(1 - w_0 \cdot q^{j-1}\right)\right) \quad (3.5)$$

The result in general equation is:

$$P(i) = \frac{N_b(i)}{N_0} = 1 - \prod_{j-1}^{i} \left(1 - w_0 \cdot q^{j-1}\right) \quad (3.6)$$

To develop a model of kinetic the decreasing number of nonbroken granules dN_{nb} per time increment dt is proportional to the number of nonbroken granules N_{nb}

With N_b=N-N_{nb} (see **Figure 3.9**),

$$\frac{dN_{nb}}{dt} = -kN_{nb} \quad (3.7)$$

$$\ln N_{nb} = (C - k \cdot t) \quad (3.8)$$

$$N_{nb} = C \exp(-kt) \quad (3.9)$$

$$N_{nb}(t = 0) = N_0 \quad (3.10)$$

$$N_b = N_0 - N_{nb} = N_0 - N_0\, exp(-kt) \quad (3.11)$$

Where k is the degradation rate constant with unit time^{-1}. The solution of Equation (3.11) is

$$N_b(t) = N_0 (1 - \exp(-k \cdot t)) \quad (3.12)$$

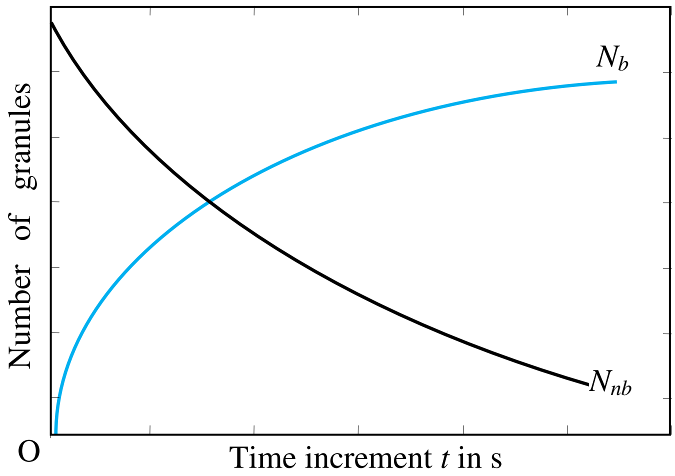

Figure 3.9. The disproportional of broken N_b and nonbroken N_{nb} granules by means of the time increment.

To rewrite the Equation (3.12) in terms of discrete stressing events the time t is replaced by stressing number i:

$$i = S_F . t \tag{3.13}$$

and k through dimensionless constant α. Where

$$i = S_F . t \tag{3.14}$$

$$t.k = \frac{i}{S_F} \cdot k \cong i.\alpha \text{ with } \alpha = \frac{k}{S_F} \tag{3.15}$$

The S_F is stressing frequency in unit time^{-1}. As result, the breakage probability $P(i)$ can be represented as:

$$P(i) = 1 - \exp(-i \cdot \alpha) \tag{3.16}$$

This form of breakage probability dependence on the stressing number corresponds to model proposed by Vogel and Peukert [38] (**Table 1.1** in **Chapter 1**). There is a connection between Equation (3.1) and Equation (3.16). Therefore the probability of granule breakage during the stressing with number i:

$$w(i) = \frac{dP(i)}{di} = \alpha \cdot \exp(-i \cdot \alpha) \tag{3.17}$$

and the ratio

$$\frac{w(i+1)}{w(i)} = \frac{\alpha \cdot \exp(-\alpha(i+1))}{\alpha \cdot \exp(-\alpha \cdot i)} = \exp(-\alpha) = q \tag{3.18}$$

Hence q as function of α given in **Table 3.2**:

Table 3.2 The tendency of α and q values correspond to the strength behavior.

α	q	Breakageprobability	Strengthbehavior
>1	<1	Breakageprobabilitydecreases	Stressing number and strength of granule increase
= 0	= 1	Saturation	Strength of granule remains the same
< 0	≥ 1	Breakageprobabilityincreases	A progressive weakening or loss of granule strength due to damage accumulation occurs.

On the other hand, according to Equation (3.16) the granule behavior by repeated stressing can be fitted by means of variable q.

The limits for $i = f(q, w_0)$ for $q > 1$, according to Equation (3.6), generates cumulative breakage probability function that is derived as:

$$P(i,q,w_0) = N_b / N_0 = 1 - \prod_{j=1}^{i} \left(1 - q^{j-1} \cdot w_0\right) \tag{3.19}$$

To calculate the limits at $P(i) = 1$, i.e. all granules were broken, and asking for $i = f(q, w_0)$ for $q > 1$.

For q = constant the cumulative breakage probability function results in:

$$P(i,q,w_0) = N_b / N_0 = 1 - \prod_{j=1}^{i} \left(1 - q^{j-1} \cdot w_0\right) = 1 - \left(1 - q^{i-1} \cdot w_0\right)^{i} \tag{3.20}$$

For the limit $P(i,q,w_0) = 1$ that all stressed particles break one obtains:

$$\left(1 - q^{i-1} \cdot w_0\right)^{i} = 0, \quad 1 - q^{i-1} \cdot w_0 = 0, \quad q^{i-1} \cdot w_0 = 1, \quad (i-1) \cdot \ln q = \ln 1 / w_0,$$

$$i = 1 + \frac{\ln 1 / w_0}{\ln q} \tag{3.21}$$

Thus

$$i(q,w_0) = 1 - \frac{\ln w_0}{\ln q} \text{ for } q>1 \tag{3.22}$$

By this form, it does not work for q=1, ln1 = 0. But for q<1 $P(i)$ is approaching $P(i \to \infty) \to 1$ e.g. for:

$w_0 = 0.5$ and $q = 1.05$ follows $i = 15.2 \approx 15$ events are necessary to obtain $P(i{=}15) = 1$

$w_0 = 0.5$ and $q = 1.10$ follows $i = 8.27 \approx 8$ events are necessary to obtain $P(i{=}8) = 1$

$w_0 = 0.5$ and $q = 1.20$ follows $i = 4.80 \approx 5$ events are necessary to obtain $P(i{=}4) = 1$

The limit i number related to q values are exhibited in **Figure 3.10**.

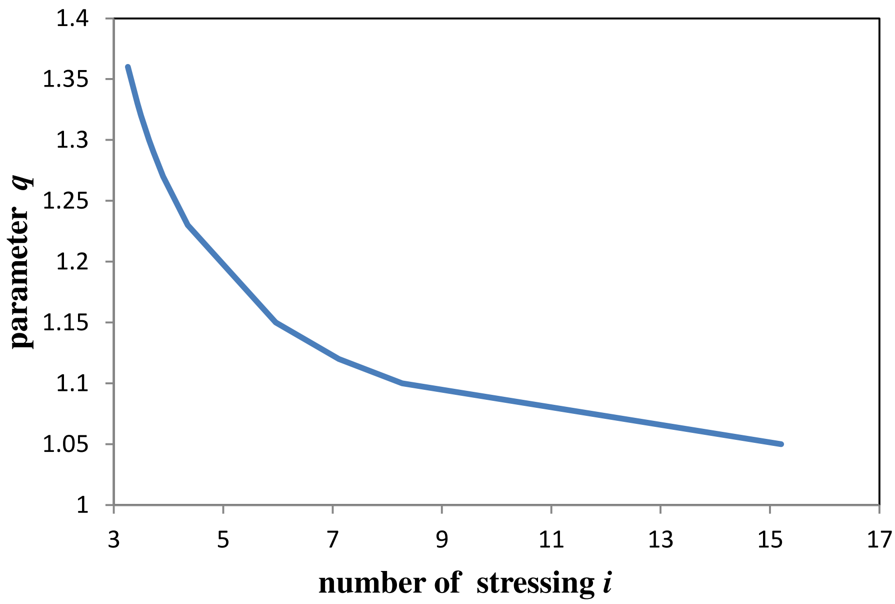

Figure 3.10. The number of stressing i can be reached by diverse values of $q>1$.

The fitting by use of q includes both tendencies in granule behavior progressive weakening due to damage accumulation and increasing of granule strength. One can see that the simple model that uses only one parameter q can be successful applied to fit the data of Monte-Carlo analysis by normal distributed breakage force, i.e. normal distributed strength of granule. Thus, it is reasonable to test the breakage behavior for others types of granule strength distributions i.e. lognormal, random and Weibull.

3.4 Monte-Carlo simulation with lognormal distributed breakage forces

The parameters of applied force distribution are the same as parameters used in **section 3.3**. On the other hand, the breakage forces used in this test are lognormal distributed according to Kolmogorov [60]. However, the mean value of breakage force $F_{b,mean}$=10 N and its standard deviation S=3 N are the same as parameters on normal distribution used in **section 3.3**. The parameters mean of log normal distribution $F_{\mathrm{mean},ln}$ and variance of log normal distribution $\sigma_{\ln}$ that are associated with lognormal distribution are calculated as in Equations (3.4) and (3.5). The lognormal and associated normal distributions from **Figure 2.9** and **2.10** (see **Section 2.6.3, Chapter 2**) with mean force F_{mean}=10 N and standard deviation S=3 N is represented in **Table 3.3**.

Table 3.3 The condition of breakage test with lognormal distributed breakage forces.

Type of breakage test	Breakage force distribution (F_b) in N	Applied force distribution (F_j) in N
Fixed stressing location. Test condition according to section **a)**	Lognormal distribution with mean force $F_{b,mean}$= 10 N and standard deviation S=3 N. Number of breakage forces i.e. tested granules I = 1000.	Normal distribution with F_{mean}= 10 N and standard deviation S = 3 N. Number of applied forces J = 10.

The **Figure 3.11** represents the breakage behavior by repeated stressing of granules with lognormal distributed strength. By this figure there is a little difference between the breakage behavior of lognormal and associated normal distribution. The fitting parameters q are 0.796 and 0.764 for normal and lognormal distribution, consequently. However, the $w(1)$ in case of lognormal distribution is about of 0.582 that is higher compared with normal distribution.

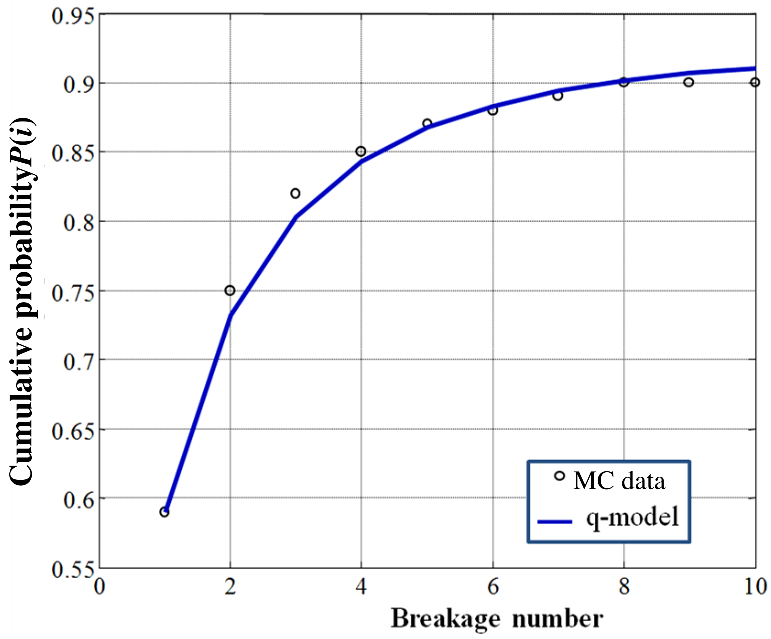

Figure 3.11. The breakage behavior of granules with lognormal distributed strength. The fit parameter q=0.764. Correlation coefficient R^2=0.957.

3.5 Monte-Carlo analyzes with random and Weibull distributed strength of granules

The two next types of breakage force distributions were chosen to test the change in breakage behavior depending on initial stress distribution by the same condition of granule tests i.e. applied forces, see **Table 3.3.**

Table 3.4 The condition of breakage test with Weibull and random distributed breakage forces.

Type of breakage test	Breakage force distribution (F_b) in N	Applied force distribution (F_j) in N
Fixed stressing location. Test condition according to section **a)**	a) Weibull distribution with mean force F_{mean}=10 N and standard deviation S=3 N. The width of distribution =4. b) Random number distribution with mean force F_{mean}=10 N and standard deviation S=3 N. Number of breakage forces i.e. tested granules I=1000.	Normal distribution with mean force F_{mean}=10 N and standard deviation S=3 N. $x_{t,63}$ quantile of 63%

The **Figure 3.12** shows the normal and two associated breakage distributions –random and Weibull cumulative distributions. The mean force F_{mean}=10 N and standard deviation S=3 N are the same for all three represented distributions. The cumulative Weibull distribution of breakage forces is presented as used by Weichert [20]:

$$P = 1 - \exp\left(1 - \frac{F_b}{F_{b,63}}\right)^{k_S} \qquad (3.23)$$

Where $F_{b,63} \rightarrow F_b$ at P= 0.63, where k_s> 0 is the shape parameter.

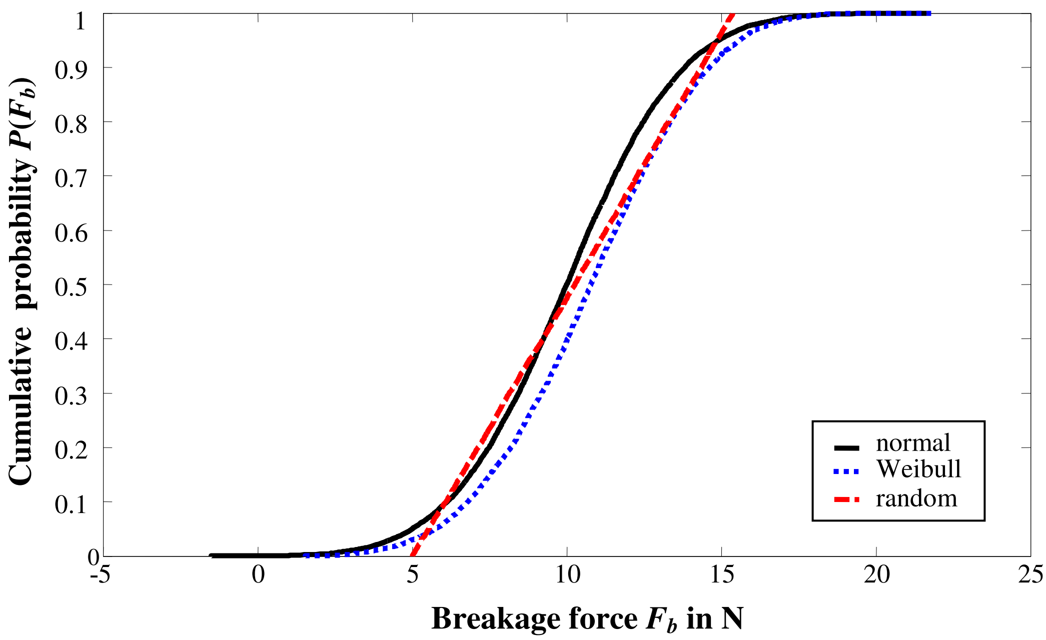

Figure 3.12. Associated normal, Weibull and random breakage forces distributions with mean force F_{mean}=10 N and standard deviation S=3 N.

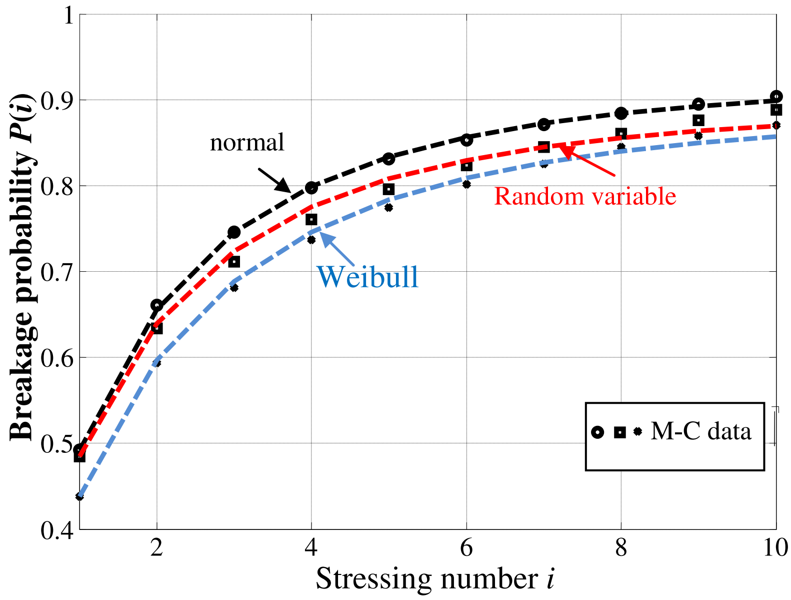

Figure 3.13. The breakage behavior of granules with normal, random and Weibull distributed strength. The data of Monte-Carlo (M-C) simulations were fitted in terms of degradation model with q parameter. Correlation coefficient R^2 is about 0.97 for all three distributions.

The **Figure 3.13** shows the breakage behavior of normal, random and Weibull cumulative distributions. The data obtained by means of Monte-Carlo simulations were fitted in terms of q-value. The breakage probability of granules with normal distributed strength is higher compared to random and Weibull distributed strength. The fitting parameters q are 0.780 and 0.806, consequently. They are not significantly changed depending on the type of initial granule strength distribution.

Thus, the Monte-Carlo simulation shows that the degradation model can be applied to describe the breakage behavior of granules with different initial strength distributions – normal, lognormal, random and Weibull.

3.6 Reduction of breakage probability by testing the survived granules

By high strength of granules the breakage does not occur after application of all J generated forces from set $\{F_j\}$. In this case the breakage force is saved, see subsection **a**) in **3.2**.Due to this the generation of a new set $\{F_{b,n}\}$ of breakage forces with increased strength takes place. The next test of granule breakage behavior is carried out at the same parameters of applied forces distribution i.e. normal distribution with mean force $F_{j,mean}$=10 N and standard deviation S=3 N. The initial distribution of breakage forces is normal distribution, too. **Figure 3.14** represents the results of 5 repeated tests of breakage behavior. One can see that the breakage probability decreases with test number. The degradation model is applied to fit the breakage behavior by repeated test.

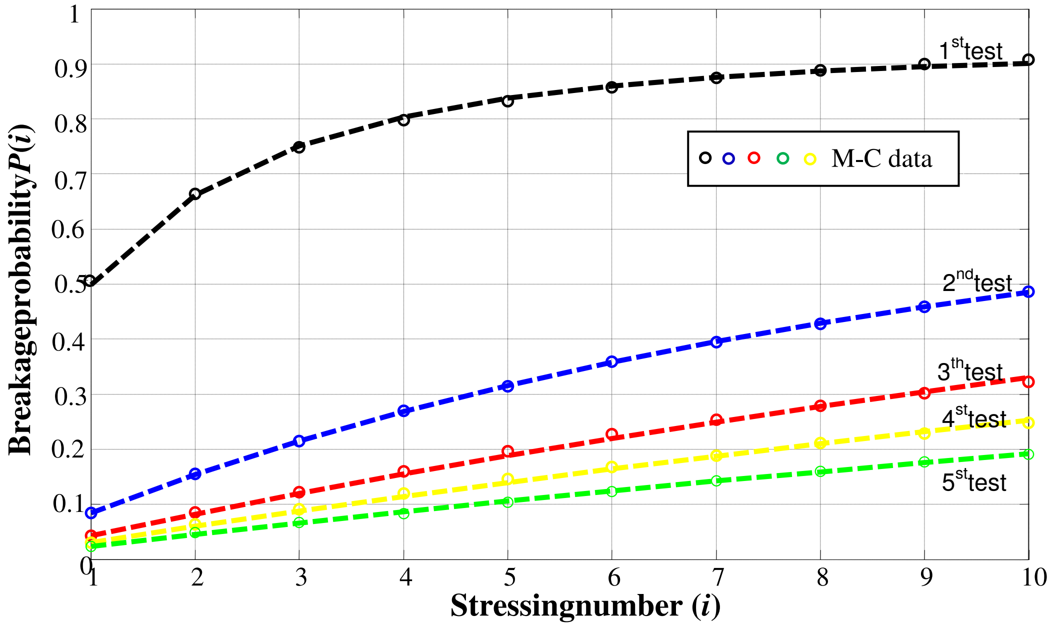

Figure 3.14 The breakage behavior of granules by repeated test. Breakage probability is drastically reduced with test number due to the selection of granules with increased strength.

3.7 The damage accumulation effect

The test was carried out under condition described in **section 3.2**. The force is applied to the same point on the granule surface.

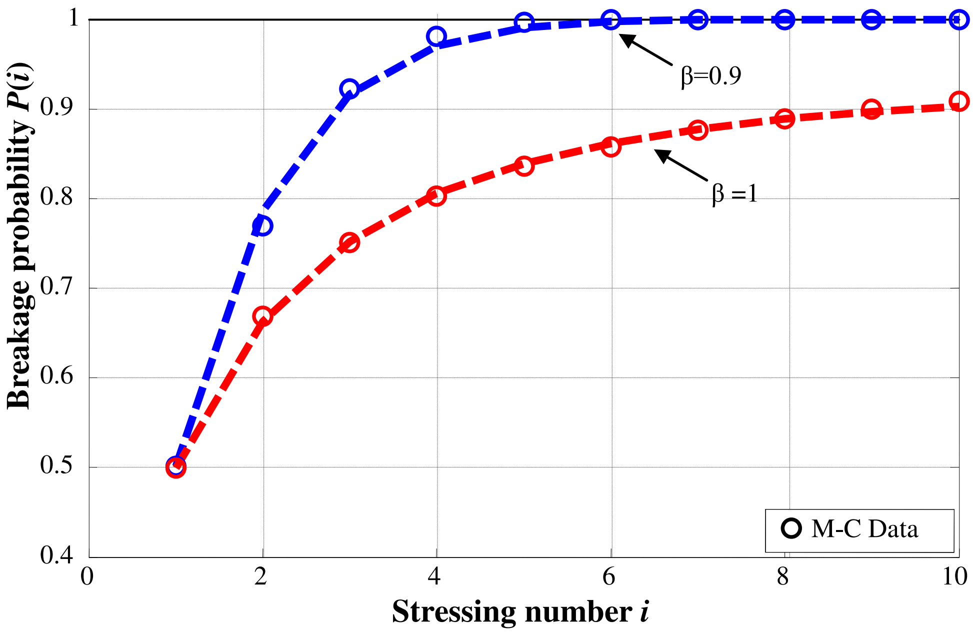

Figure 3.15. The breakage behavior of granules by repeated test. Breakage probability is increased with test number due to damage of granules with reduced strength. Correlation coefficient R^2 is about of 0.98.

However, the strength of granule is affected by the repeated loading. After every stressing event the granule degradation parameter q is reduced again:

$$q(i) = q(i-1) \cdot \beta \tag{3.24}$$

Where $\beta \leq 1$ is constant.

Figure 3.15 shows the change of breakage probability due to damage accumulation. The damage accumulation was modeled by means of the reduction of parameter q (β=0.9). In this case the breakage probability increases compared to model with the constant parameter $q(\beta=1)$. In terms of damage accumulation model, the breakage of all granules occurs before 10 stressing events.

3.8 Stressing of random chosen location on the surface of tested granule

The breakage test is carried out according to **subsection (c)**, **Step 3**, see **section 3.2**. Force from set $\{F_j\}$ with random number j is applied to the random chosen location on the surface of tested granule.

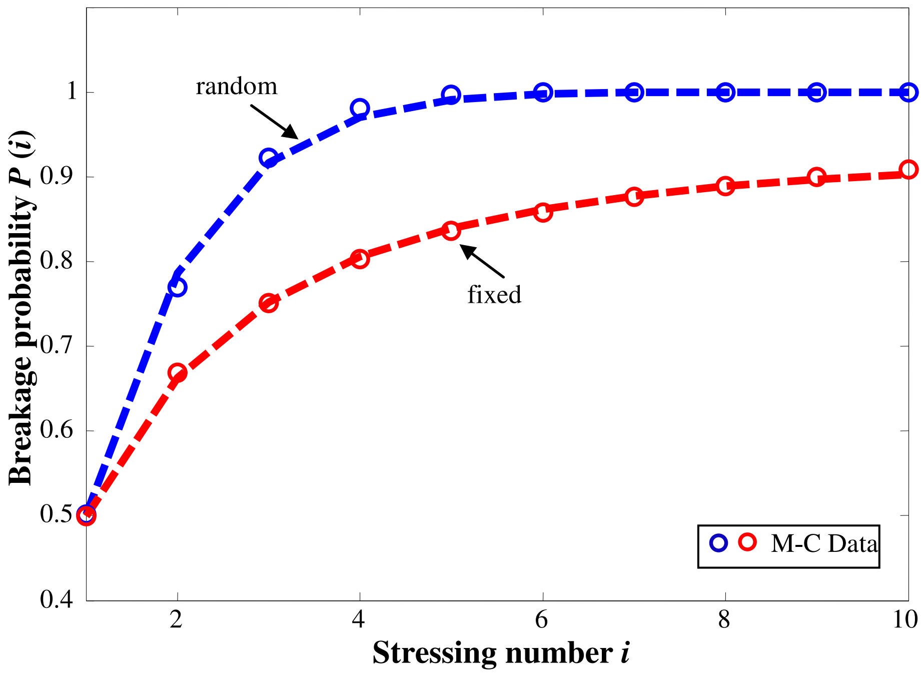

Figure 3.16. Breakage probability by test of random chosen locations is higher compared with fixed locations test. The degradation model was used to fit data from Monte-Carlo simulation. Correlation coefficient of R^2 is about of 0.98.

The number of tested locations is equal to the number of applied forces. After breakage the stressing number is saved and granule is removed from set of tested granules. By random chosen locations the probability to find the weak location increases. Consequently, the breakage probability is higher compared to fixed point test carried out by the same stressing conditions, see **Figure 3.16**. The strength of granule at given location will not be changed by the application of repeated force.

3.9 Damage accumulation on random chosen location on the surface of tested granule

The breakage test is carried out according to **section (d)**, Step 3 (see **section 3.2**). Force from set $\{F_j\}$ with random number j is applied to the random chosen location on the surface of tested granule. After breakage the stressing number is saved and granule is removed from set of tested granules. The strength of granule i.e. breakage force $F_{b,i}$ at given location is reduced by force application with 50% of breakage force $F_{\mathrm{b},50}$:

$$F^{*}{}_{b,i} = F_{b,i} \cdot \left(1 - \varphi * \frac{F_j}{F_{b,50}}\right) \tag{3.25}$$

Where $F^{*}{}_{b,i}$ the magnitude of breakage force after application of force F_j and φ=0.1 is structure change parameter.

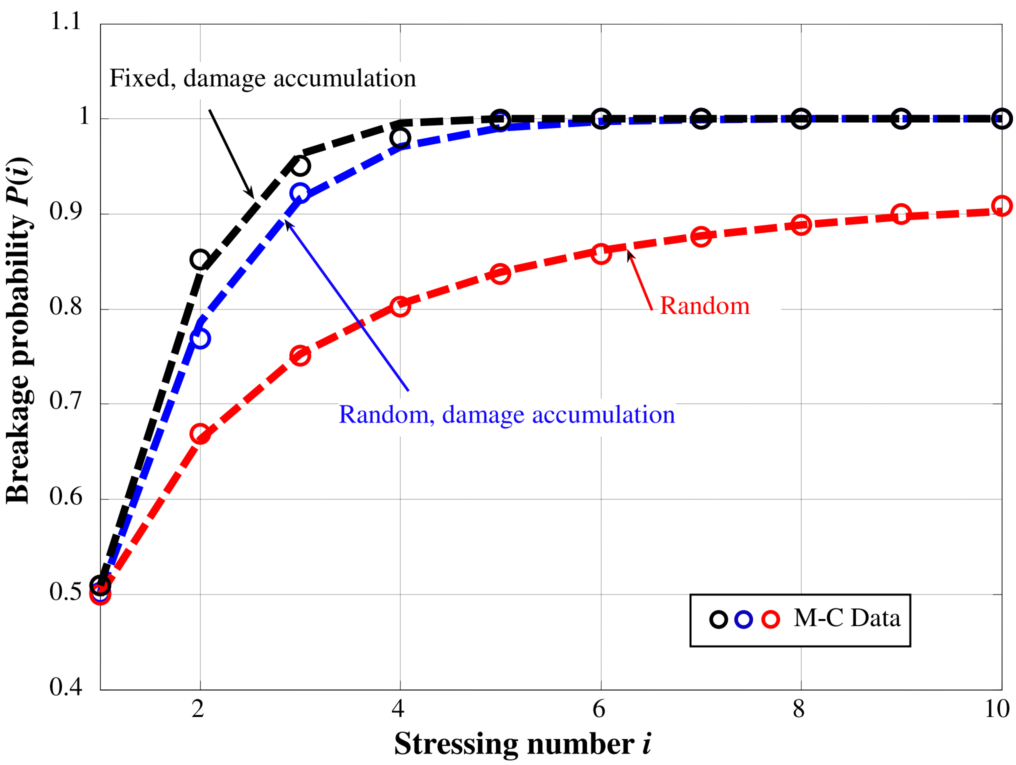

Figure 3.17. Breakage probability by test with damage accumulation. The effect of damage accumulation by fixed locations is larger compared with random distributed locations. The degradation model was used to fit data from Monte-Carlo simulation. Correlation coefficient R^2 is about of 0.95.

Figure 3.17 represents the increasing of the breakage probability due to damage accumulation in random chosen locations. The effect of damage accumulation by fixed locations is larger compared with random distributed locations.

3.10 Conclusions of Monte-Carlo analysis of granule breakage

The degradation model can be tested by means of fitting the data obtained by Monte-Carlo analyzes. This model can be applied as well to test the breakage behavior of granules with normal, lognormal, random and Weibull strength distributions. A simple equation was proposed to take into account the damage accumulation.

CHAPTER 4
REPEATED STRESSING OF GRANULES BY COMPRESSION TEST

4.1. Stressing by compression test with low stressing rate

Repeated stressing often much better describes the real events of stressing frequency in industrial processing than a single stressing. However a complete understanding of particle breakage behavior by repeated stressing is not generally accomplished. Unless they are analyzed in the most elementary breakage event, which is a single particle subjected to stresses.

Several researchers investigated the breakage behavior of a single particle with low stressing rate by compression test. By applying a nonlinear mechanism the formation and propagation of damages during repeated stressing of a single particle until fracture was observed by Antonyuk et al. [1]. With considering the influence of particle sizes Aman et al. [73] investigated the microstructure on material resistance against cyclic loadings. Different temperatures and stressing velocities were observed by Ghadiri et al. [37], and with different agglomerates in [38-44]. The other studies also described the strength behavior of granules regard to the moisture content in [1,2] and [31,32].

However these earlier studies did not take into account the distribution of mechanical properties inside of inhomogeneous particles i.e. distributed strength of granules by repeated stressing. Theoretically, there are different results that possibly obtained by repeated stressing of granules depending on fixed or stochastic orientation of granules regarding to the applied force and stressing test point. The different effects that may take place by repeated stressing are represented in **Chapter 3.** The breakage behavior of granules by compression test may perform a certain behavior depending on test location by cyclic stressing. This chapter presents the result of compression tests for granules by taking into account the stressed point during testing.

4.2 Description of uniaxial compression tester

The spherical granules of γ-Al_2O_3 and synthetic Zeolite 4AK are used as test materials. The compression equipment produced by Etewe GmbH, Karlsruhe (**Figure 4.1**) was used.

During repeated compression test, the punch moves towards the upper fixed plate side and presses the granule up to the defined force or deformation. Then, the punch moves downward, thus the unloading of the granule takes place. The stressing process is recorded with a CCDcamera. Granules were examined in each experiment at low stressing velocity v_B in the range of 0.02–0.15 mm/s.

The experiments are divided into two types. The type one, granules are tested in a fixed contact point regarding to direction of piston movement, and the type two, granules are stressed in rotated configuration i.e. in randomly chosen contact points.

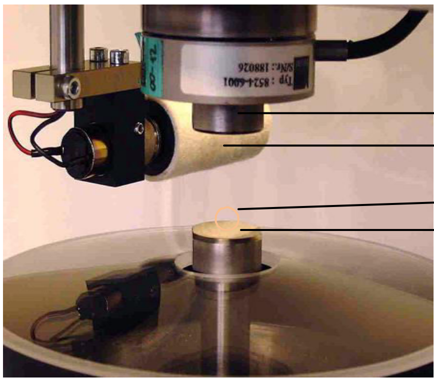

Figure 4.1 Uniaxial compression test device

4.3 Theoretical approach of deformation

During compression of a comparatively soft spherical granule with a smooth stiff punch (flat surface) the contact area between them deforms as a circle with radius r_k (**Figure 4.2a**). The contact radius and internal pressure distribution p depends on the granule radius r and stiffness of the two contacting materials.

4.3.1 Elastic contact deformation

In this case, a circular contact area of a radius $r_{k,el}$ is built with an ellipsoidal pressure distribution $p(r_k)$. Hertz [74] has found the maximum contact pressure in the centre of the contact at the depth, shown by point K as

$$p_{max} = \frac{3F_{el}}{2\pi r_{k,el}^2} = \frac{3}{2} p_m \tag{4.1}$$

Where p_m is the averaged contact pressure. All three principal stresses in point K, are calculated as pressures according to Eq. (4.1) [75, 76]. At this point K, all the stresses have nearly the same magnitudes. They are compressive stresses and generate approximately an isostatic stress state [24] and [76], whereby tension is shown by negative sign and compression by positive one.

$$\sigma_1 = p_{max}, \tag{4.2}$$

As a consequence, no cracks can be observed at this state. The maximum tensile stress $\sigma_{t,\max}$ arises at the contact perimeter and can be calculated according to Eq. (4.3) [77]. For particle with Poisson ratio $v_1 = 0.28$, one obtain $\sigma_{t,max} = -0.15\ p_{max}$

$$\sigma_{t,max} = -\frac{1-2v_1}{3} p_{max} \tag{4.3}$$

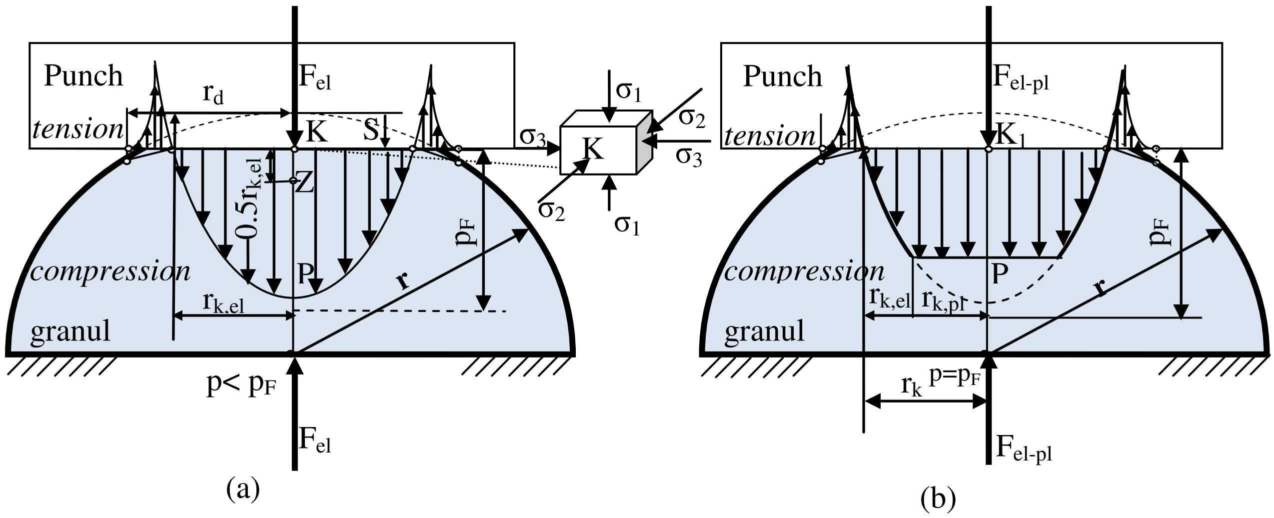

Figure 4.2. Characteristic particle contact pressure $p(r_k)$ on a plate–sphere contact during elastic deformation (a) and elastic–plastic deformation (b) [3].

The maximum shear stress on the principal axis occurs at the depth of $K–Z \approx 0.5r_{K,el}$ (point Z in **Figure 4.2a**). The principal stress in this point is given by Eq. (4.4). The shear stress can be calculated with Tresca failure criterion, Eq. (4.5), as proposed by Gross and Seeling [78]. It is larger than the maximum tensile stress, according to Eq. (4.3), and is responsible for the crack generation, especially for plastic materials.

$$\sigma_1 = 0.8\ p_{max,} \tag{4.4}$$

$$\sigma_2 = \sigma_3 \approx 0.18 p_{max}. \tag{4.5}$$

$$\tau_{max} = \frac{\sigma_1 - \sigma_3}{2} = 0.31 p_{max}. \tag{4.6}$$

The radius of elastic contact is given by Hertz [74]

$$r_{K,el}^3 = \frac{3rF_{el}}{2E^*} \tag{4.7}$$

According to Huber [77] the tensile region outside the perimeter of the contact zone is responsible for surface bending, displacement and distortion. Due to this distortion at the radius of totally deformed area is larger than the contact radius: $r_d \geq r_{K,\mathrm{el}}$ [79]. The effective modulus of elasticity E^* of both particle (index 1) and punch (index 2) ($E_2 \gg E_1$, $E_2 \rightarrow \infty$) is given as

$$E^* = 2\left(\frac{1-v_1^2}{E_1}+\frac{1-v_2^2}{E_2}\right)^{-1} \approx \frac{2}{1-v_1^2}E_1. \tag{4.8}$$

The effective shear modulus $G_i = E_i/(2(1+v_i))$ for i=1,2, is given by

$$G^* = 2\left(\frac{2-v_1}{G_1}+\frac{2-v_2}{G_2}\right)^{-1} \approx \frac{2}{2-v_1}G_1. \tag{4.9}$$

The relation between elastic contact force and deformation is non-linear as found by Hertz [74]

$$F_{el} = \frac{2}{3}E^*\sqrt{\frac{d}{2}s^3} \tag{4.10}$$

Due to the parabolic curvature $F(s)$, the contact stiffness in normal direction increases with increase in deformation and particle diameter as described by Tomas [3]

$$k_{N,el} = \frac{d\,F_{el}}{ds} = E^*\sqrt{\frac{d}{2}s} = \left(\frac{F_{el}\,d}{4D^2}\right)^{1/3} \tag{4.11}$$

The elastic constant determines here the averaged compliance of both contact materials as expressed by Lurje [80]

$$D = \frac{3}{4}\left(\frac{1-v_1^2}{E_1}+\frac{1-v_2^2}{E_2}\right) \approx \frac{3(1-v_1^2)}{4E_1} \tag{4.12}$$

4.3.2 Elastic–plastic contact deformation

For elastic–plastic material behavior, an elastic deformation is generated at the limit, where the pressure is smaller than the yield point, and plastic deformation is closer to the centre of the contact (**Figure 4.2b**). The maximum pressure p_{max} in the contact centre K_1 lies below the plastic yield strength p_F (the stress at the beginning of plastic yielding). Because of a confined stress field the micro yield strength p_F is higher than the macroscopic yield strength for tension $p_F/\sigma_E \approx 3\ldots5$ [81]. The stiffness is proportional to the radius r of the granule and micro yield strength, p_F given by Tomas [24]

$$k_{N,el-pl} = \frac{dF_{el-pl}}{ds} = \pi r p_F\left(\frac{2}{3}+\frac{1}{3}\frac{A_{pl}}{A_K}\right) \tag{4.13}$$

$$= \pi r p_F\left(1-\frac{1}{3}\sqrt[3]{\frac{s_F}{s}}\right) \tag{4.14}$$

Where s_F is a contact deformation at yield point. Furthermore, at this point $p_{el} = p_{max} = p_F$ is valid.

The ratio of plastic deformed contact area A_{pl} to the total contact deformation area $A_K = A_{pl} + A_{el}$ can be used to define the elastic–plastic deformation and lies between 0 and 1. The ratio is 0 for perfectly elastic and 1 for perfectly plastic deformation.

4.3.3 Plastic contact deformation

The whole contact area deforms plastically for a perfectly plastic material. In this case, the contact circle radius is given by

$$r_k^2 = r^2 - \left(r - s_{k,1}\right)^2 = 2rs_{k,1} - s_{k,1}^2 \approx d \cdot s_{k,1} \tag{4.15}$$

Where $s_{k,1}$ is the plastic deformation at the contact 1, as shown in **Figure 4.3**. Having assumed that the plastic deformation at the two contacts is equal ($s_{K,1} = s_{K,2}$, $s = s_{K,1} + s_{K,2}$ and $r_{k,1} = r_{k,2}$), one obtains

$$r_k^2 = r \cdot s \tag{4.16}$$

The repulsive force against plastic deformation is calculated as proposed by Tomas [24],

$$F_{pl} = p_F A_K = \pi r_K^2 p_F = \pi\, d\ \cdot S \cdot\ p_F \tag{4.17}$$

With Eqs. (4.1), (4.6) and (4.14) the yield strength p_F is calculated

$$p_F = \frac{E^*}{\pi}\sqrt{\frac{s_F}{r}} \tag{4.18}$$

The contact stiffness is constant for a perfectly plastic yielding material:

$$k_{N,pl} = \frac{dF_{pl}}{d_s} = \pi d \cdot p_F \tag{4.19}$$

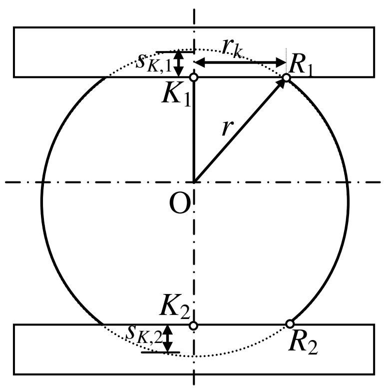

Figure 4.3 Contact geometry by plastic deformation [24].

4.4 Description of repeated compression results

Compared to crystalline solids, within one contact or distributed contact a granule consists of primary particles, which stick together by adhesion forces at their randomly distributed contacts (see **Figure 4.4**). Depending on the granulation process the internal adhesion forces are influenced by the superposition of different interactions e.g. capillary or solid bridges, high-viscous binder, organic macromolecules, and sintering or interlocking of granules [1, 26-28, and 31].

The mechanical behavior of granules is strongly determined by these randomly distributed micro binding mechanisms [24]. This breakage is influenced by distribution of strength within granules. Therefore it supposed to the configuration of contact point performs distributed deformation behavior as well.

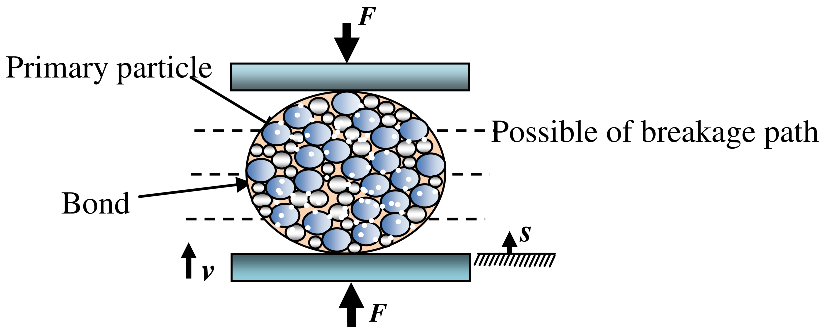

Figure 4.4 Principle of granule compression test [3].

4.5 Results and discussion of fixed and randomly distributed stressed granules

The repeated stressing under compression test was set up at the force about 15 percent of breakage force. In the way of fixed granules the elastic-plastic deformation was performed at first stressing (s_1) (see **Figure 4.5**). The Hertz line for successive stressing (n-Hertz) depends on the yield point Y_p values and they nearly the same after first stressing. It is demonstrated by Y_n.

The reduction of deformation shows a stiffening effect. It occurs by repeated stressing which is obviously represented by the stressing series $s_{1\text{-}5}$. The cyclic stiffening (K_i) denotes the change in structure of the material that is especially high at the fixed contact points, where the stresses are strongly concentrated. The increasing of cycle number, also increase the failure of solid bridge that propagate within the specimen and consolidate the structure. A large plastic deformation (O–E) demonstrates elastic–plastic behavior of granules.

The contact stiffness in the elastic and elastic-plastic deformation ranges increases with increasing number of cycles. The smallest stiffness is exhibited in the first stressing and performs an extreme change to the second cycle. A further increase of the curve slope can only be observed during the first stressing. All loading curves for $n>2$ are located on the same curve O−U_n, which approaches the corresponding Hertz curve practically up to the maximum force (point U_n).

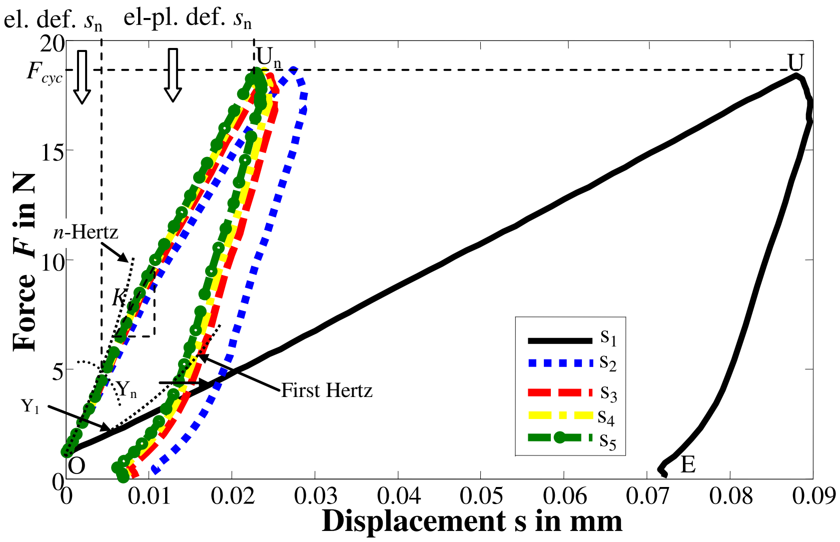

Figure 4.5 Force-displacement curves by repeated compression of fixed granules (γ-Al_2O_3, d=1.8 mm). The index $s_{1\text{-}5}$ represents the stressing series. The O–Y_n and F–U_n are elastic deformation and elastic–plastic deformation at n stressing respectively.

The hysteresis loops detected between unloading and reloading curves are gradually decreased with the progress of stressing cycles. After some cycles no plastic deformation arises and the unloading curves return to the loading origin, i.e. a contact consolidation state is reached. However, small viscoelastic deformations occur during the cyclic loading in the contact consolidation state. As a result, the area of the hysteresis loop does not fully disappear; see the loop between the loading-reloading curves of the 2th and 5th cycles.

Repeated stressing force generates a chance of losing the contact (bonds broken) between many primary particles at a same time. When the particles experience the stress which is equal to their own strength, they delete the contacts from their bonds of primary of particles. The primary particle looses the contacts with its neighbors due to breakage of solid bridge bonds and thus, the primary particles are compacted each other (see **Figure 4.6**).

The breakage of solid bridge at primary reduces the stiffness. The plastic yielding of solid bridge bond leads to a certain consolidation of fixed granule. The local density and stiffness of granules increases.

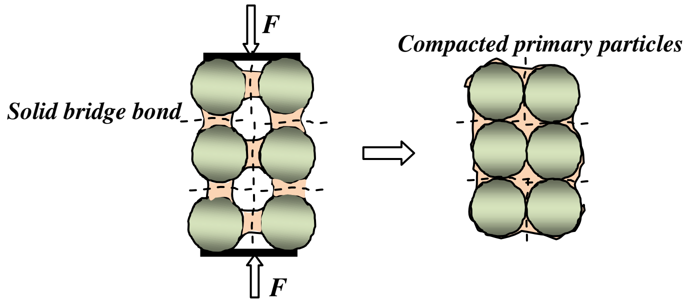

Figure 4.6 Breakage and deformation of solid bridge bond of primary particles.

The elastic-plastic deformation behavior depends on the stressing point and is not strongly affected by third, fourth, and fifth cycle, s_3 to s_5, by the number of stressing events (see **Figure 4.7**). Different with the fixed granules, the Hertz lines at randomly distributed contact points of stressed granules vary depending on local mecahnical properties of stressing points.

A different deformation behavior is characterized by randomly distributed contact points of stressed granules. The stiffness of randomly distributed contact points of stressed granules tends to be distributed randomly. Only a weak area is affected by the stressing. Due to this, the elastic and elastic plastic deformation behavior for randomly distributed contact points of stressed granules is more or less similar at all stressing events. Apparently, the curves of stressing series $s_{1\text{-}5}$ were distributed randomly, as well as the Hertz behavior.

The elastic-plastic deformation behavior is similar to the elastic-plastic deformation behavior at first stressing s_1 at fixed granules.

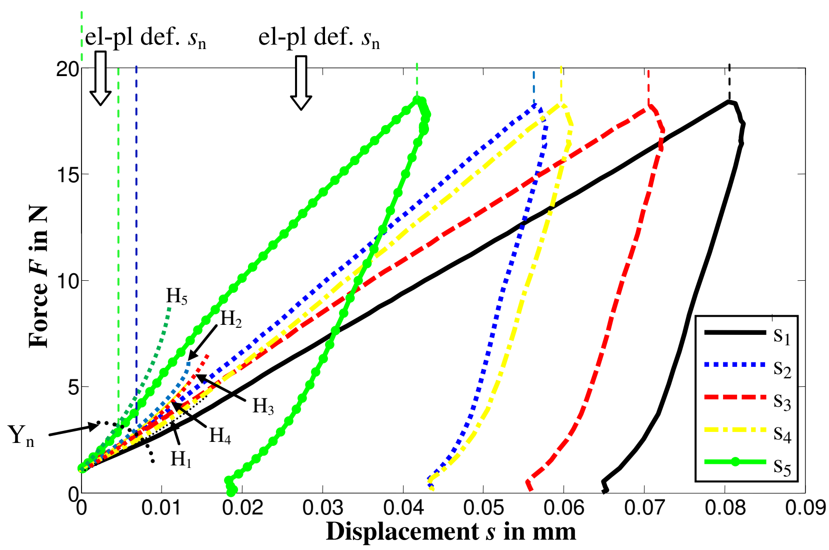

Figure 4.7 Force-displacement curves by repeated compression of randomly distributed contact points of stressed granules (γ-Al_2O_3, d = 1.8 mm) at F_{cyc} = 17 N with varied elastic plastic deformation (el-pl def.) area and Hertz line behavior ($H_{1\text{-}5}$).

The cyclic loading of randomly distributed contact points of stressed granules does not change significantly the common structure of the material at the contact points. The increase of stressing number by rotating configuration does not intensively generate failure of solid bridge. Therefore, it renders large breakage probability in fixed granules than at the randomly distributed contact points of stressed granules. There is a typical breakage by repeated stressing that performs damage accumulation in fixed granule (**Figure 4.8a**) and distributed deformation in randomly distributed contact points of stressed granule (**Figure 4.8b**).

With varied granule sizes (d = 1.8 -3.0 mm) and forces (F_{cyc} = 18, 19 and 73 N) for both γ-Al_2O_3 and Zeolite 4 AK granules, the largest elastic-plastic deformation was also exhibited at first stressing (s_1).

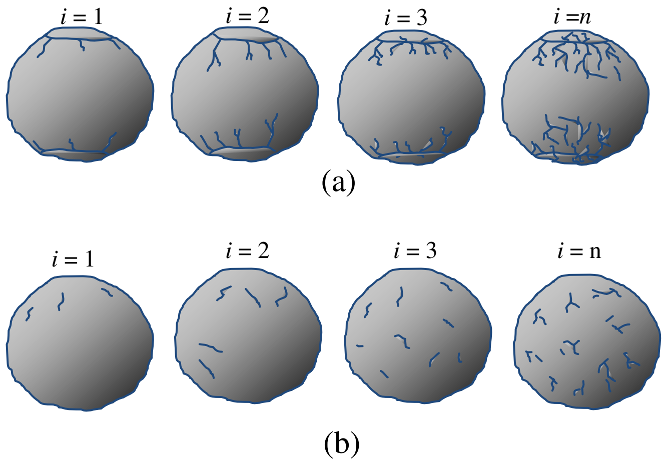

Figure 4.8 Damage accumulation by repeated stressing in fixed granule (a) and distributed deformation by repeated stressing in randomly distributed contact points of stressed granule (b).

After several stressings at the same contact point the reduction of deformation demonstrates a stiffening effect as well (see **Table 4.1-4.2**).

At fixed granule, stiffness increases i.e. damage accumulation effects are higher for small size granules. After repeated stressing of γ-Al_2O_3 granules with sizes 1,8 mm, 2,5 mm and 3 mm the stiffness increases consequently.

One can observe the same behavior of the Zeolite 4AK granules by repeated stressing. For low size granules the contact area is lower compared with larger size. Consequently, the stress is higher and damage accumulation is more substantial.

For randomly distributed contact points of stressed granules, with different forces, granule sizes and types, deformation for all stressing of stressed granules is distributed randomly within granules. Moreover, they tend to be similar with the elastic-plastic deformation behavior at first stressing s_1 in the fixed granules. It is because stressings at randomly distributed contact points of stressed granules do not generate significant breakage solid bonds at bounded primary particles.

Table 4.1 The deformation properties of repeated stressing of fixed and randomly distributed contact points of stressed γ-Al_2O_3 granules at varied sizes and cyclic forces.

γ-Al_2O_3(d = 1.8 mm, F_{cyc} = 17 N)

	Fixed						Random					
	ΔF_{fix} in N	Δs_{fix} in mm	K_{fix} N/mm	E_{st} in µJ	Y_p in N	E^* in GPa	ΔF_{rot} in N	Δs_{rot} in mm	K_{rot} N/mm	E_{st} in µJ	Y_p in N	E^* in GPa
s_1	17	0.088	193.18	1.496	8.04	2.99	17	0.081	209.88	1.377	9.85	2.75
s_2	17	0.065	261.54	1.105	11.74	2.21	17	0.057	298.25	0.969	10.25	1.93
s_3	17	0.023	739.13	0.391	11.77	0.78	17	0.071	239.44	1.207	10.03	2.41
s_4	17	0.022	772.73	0.374	11.80	0.74	17	0.058	293.10	0.986	9.95	1.97
s_5	17	0.022	772.73	0.374	11.82	0.74	17	0.042	404.76	0.714	10.95	1.42

γ-Al_2O_3 (d = 2.5 mm, F_{cyc} = 19 N)

	Fixed						Random					
	ΔF_{fix} in N	Δs_{fix} in mm	K_{fix} in N/mm	E_{st} in µJ	Y_p in N	E^* in GPa	ΔF_{rot} in N	Δs_{rot} in mm	K_{rot} in N/mm	E_{st} in µJ	Y_p in N	E^* in GPa
s_1	19	0.0154	1168.83	0.2926	4.05	0.59	19	0.0700	257.14	1.330	4.91	2.66
s_2	19	0.0082	2194.12	0.1558	4.98	0.31	19	0.0210	857.14	0.399	4.81	0.80
s_3	19	0.008	2250.00	0.1520	4.99	0.30	19	0.0180	1000.00	0.342	4.85	0.68
s_4	19	0.0056	3214.29	0.1064	4.98	0.21	19	0.0165	1090.91	0.313	4.98	0.63
s_5	19	0.0057	3157.89	0.1083	4.99	0.22	19	0.0116	1551.72	0.220	5.11	0.44

γ-Al_2O_3 (d = 3.0 mm, F_{cyc} = 73 N)

	Fixed						Random					
	ΔF_{fix} in N	Δs_{fix} in mm	K_{fix} in N/mm	E_{st} in µJ	Y_p in N	E^* In GPa	ΔF_{rot} in N	Δs_{rot} in mm	K_{rot} In N/mm	E_{st} in µJ	Y_p in N	E^* in GPa
s_1	73	0.0655	1099.24	4.781	9.25	9.56	73	0.0510	1411.76	3.723	9.30	7.45
s_2	73	0.0385	1870.13	2.810	9.32	5.62	73	0.0648	1111.11	4.730	8.79	9.46
s_3	73	0.0351	2051.28	2.562	9.33	5.12	73	0.0430	1674.42	3.139	9.30	6.28
s_4	73	0.0335	2149.25	2.445	9.32	4.89	73	0.0530	1358.49	3.869	9.80	7.74
s_5	73	0.0320	2250.00	2.336	9.33	4.67	73	0.0630	1142.86	4.599	7.56	9.20

Table 4.2 The deformation properties of repeated stressing of fixed and random stressed Zeolite 4AK granules at varied sizes and cyclic forces.

Zeolite 4AK (d = 1.6 mm, F_{cyc} = 5 N)

	Fixed						Random					
	ΔF_{fix} in N	Δs_{fix} in mm	K_{fix} in N/mm	E_{st} in µJ	Y_p in N	E^* in GPa	ΔF_{rot} in N	Δs_{rot} in mm	K_{rot} in N /mm	E_{st} in µJ	Y_p in N	E^* in GPa
s_1	4	0.0251	159.36	0.100	2.85	0.20	4.1	0.0159	256.41	0.064	2.56	0.13
s_2	4	0.0150	266.67	0.060	2.86	0.12	4.2	0.0260	161.54	0.104	2.70	0.21
s_3	4	0.0130	346.15	0.052	2.87	0.10	4.2	0.0126	333.33	0.050	2.90	0.10
s_4	4	0.0126	357.14	0.050	2.87	0.10	4.2	0.0157	267.52	0.063	2.85	0.13
s_5	4	0.0125	320.00	0.050	2.85	0.10	4.2	0.0123	341.46	0.049	2.83	0.10

Zeolite 4AK (d = 2.0 mm, F_{cyc} = 7.5 N)

	Fixed						Random					
	ΔF_{fix} in N	Δs_{fix} in mm	K_{fix} in N/mm	E_{st} in µJ	Y_p in N	E^* in GPa	ΔF_{rot} in N	Δs_{rot} in mm	K_{rot} in N/mm	E_{st} in µJ	Y_p in N	E^* in GPa
s_1	7.5	0.02500	280.00	0.188	2.75	0.38	7.5	0.0151	468.65	0.113	2.80	0.23
s_2	7.5	0.01525	459,02	0.114	2.87	0.23	7.5	0.0158	449.37	0.119	2.75	0.24
s_3	7.5	0.01520	500.00	0.114	2.88	0.23	7.5	0.0254	279.53	0.191	2.50	0.38
s_4	7.5	0.01512	502.65	0.113	2.87	0.23	7.5	0.0156	454.13	0.117	2.90	0.23
s_5	7.5	0.01501	499,67	0.113	2.88	0.23	7.5	0.0280	253.57	0.210	2.50	0.42

Zeolite 4A (d = 2.5 mm, F_{cyc} = 9 N)

	Fixed						Random					
	ΔF_{fix} in N	Δs_{fix} in mm	K_{fix} in N/mm	E_{st} in µJ	Y_p in N	E^* in GPa	ΔF_{rot} in N	Δs_{rot} in mm	K_{rot} in N/mm	E_{st} in µJ	Y_p in N	E^* in GPa
s_1	8	0.0356	224.72	0.285	3.80	0.57	8	0.0409	195.60	0.327	4.30	0.65
s_2	8	0.0210	380.95	0.168	4.20	0.34	8	0.0309	258.90	0.247	4.25	0.49
s_3	8	0.0206	388.35	0.165	4.23	0.33	8	0.0408	196,08	0.326	4.15	0.65
s_4	8	0.0200	400.00	0.160	4.25	0.32	8	0.0204	392.16	0.163	4.90	0.33
s_5	8	0.0190	421.05	0.152	4.30	0.30	8	0.0390	205.13	0.312	4.50	0.62

Compression behavior with only one stressing at varied forces (F = 25, 45, 65 and 73 N) gives also a certain deformation as shown in **Figure 4.9**. A large displacement was obtained at F = 73 N with varied elastic and/or elastic-plastic deformation (el-pl def.). However the increasing force does not change the stiffness significantly. That means, there is no need for large extended forces to change the structure. It is indicated by small yield point value.

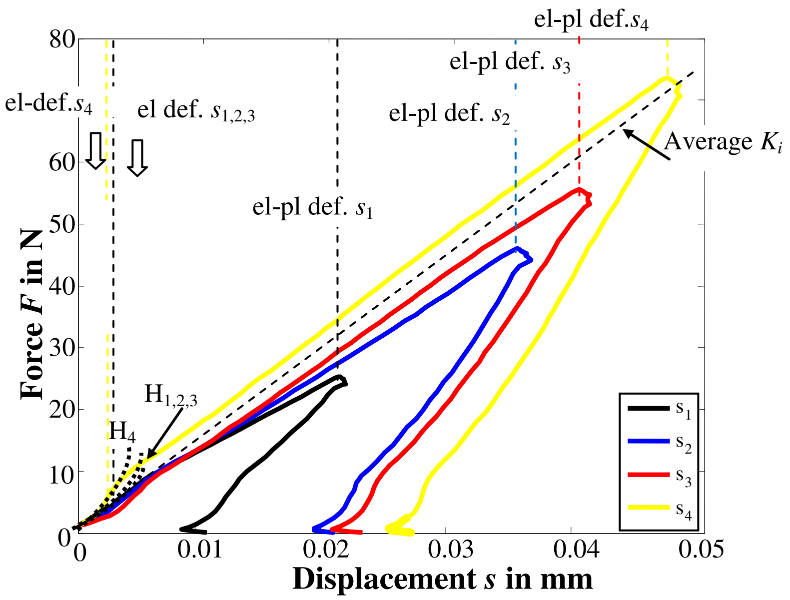

Figure 4.9 Single stressing fixed of γ-Al_2O_3 granules (d = 3.0 mm) at varied forces with Hertz (H) behavior.

It is because the stiffness does not so much vary depending on the force. After a single stressing with varied forces, stiffness is considered to remain nearly the same. This result confirms the damage accumulation due to repeated stressing events at low energy that is described also in **Chapter 5**. This damage accumulation is verified by degradation parameter model and validated by double impact experiments in **Chapter 5** and **6**.

4.6 The variation of contact radius

The trace of stressing both in fixed and randomly distributed contact points of stressed granules is distinguished visually by using microscope. The images compare the trace stressing at the contact point of fixed granule of γ-Al_2O_3 after some stressing (see **Figure 4.10).** The figure represents the change of contact area depending on the stressing number.

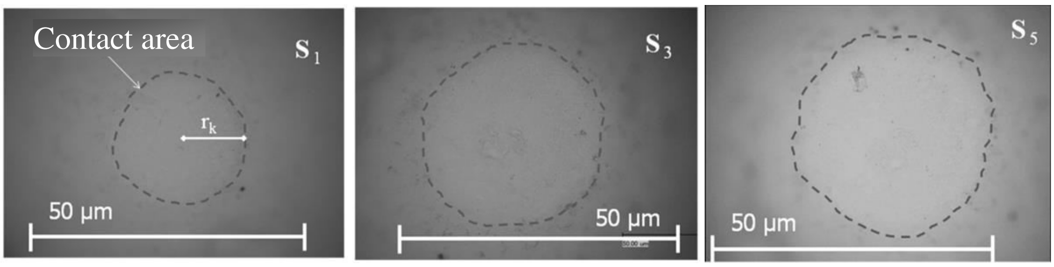

a b c

Figure 4.10 The increasing flattened contact area and cyclic stiffening of fixed γ-Al_2O_3 granule for stressing series s_1, s_3 and s_5.

One concedes the contact or deformation radius (r_k) increases with stressing number. The contact radius at stressing s_1 is increasing r_{k1} = 11.92 µm, r_{k3} = 15.48 µm, and r_{k5} = 17.53 µm. However with rotating granules the stressing obviously performs a different form of r_k. The successive r_k areas in **Figure 4.11** are considered constant. At stressing s_1, r_{k1} = 12.15 µm, at s_3, r_{k3} = 12.20 µm, and at s_5, r_{k5} = 12.18 µm.

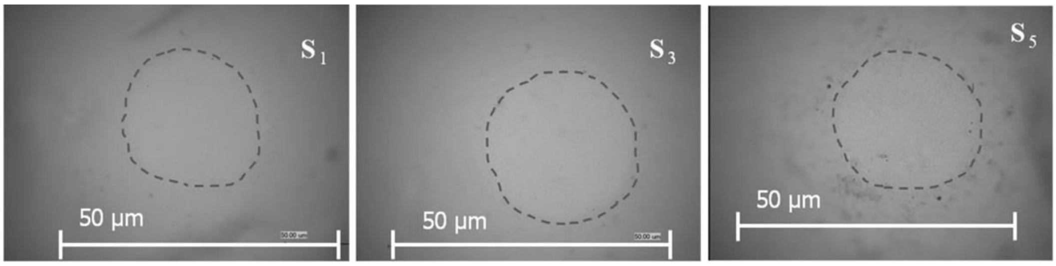

a b c

Figure 4.11 The randomly distributed flattened contact area of randomly distributed contact points of stressed γ-Al_2O_3 granule for stressing series s_1, s_3 and s_5.

From this examination, the stiffness of fixed granules at the first stressing is low, but increases between at second and third cyclic and remains nearly the same for more than 5 cycles. The stiffness increases due to compression and compaction of solid bridge bonds. However in randomly distributed contact points of stressed granules stiffness and strength are distributed randomly. It indicates that the damage accumulation for fixed granules is significant and has to be taking into account by repeated stressing regarding to particle breakage probability.

4.7 Conclusions repeated stressing of granules by compression test

Repeated stressing force generates a chance of losing the contact (bonds broken) among primary particles. It renders the contact area of stressed granule is more compacted and eventually increase the stiffness in the contact zone.

The stiffness of fixed granules by repeated stressing increases with the number of compression due to compaction of solid bridge bonds. While, at randomly distributed contact points of stressed granules, stiffness are distributed randomly.

The damage accumulation for fixed granules is generated significantly and has to be taking into account by repeated stressing for calculating to breakage probability. While in randomly distributed contact points of stressed granules deformation is distributed randomly that reduces the cumulative breakage probability.

CHAPTER 5

REPEATED DOUBLE IMPACT OF GRANULES BY DROP WEIGHT APPARATUS

5.1 Degradation model with parameter *q* approach

The validation of model by stressing experiments is required to obtain the agreement between the model and real experiment. **Chapter 3** developed model to calculate the breakage probability by repeated stressing of inhomogeneous granules. This specific developed distribution is identified as degradation model with a parameter q. Where this parameter may refer to the particle shape, distributed strength at contact point of granule, and material properties.

The breakage probability distribution is approached by this model. Degradation refers to the possibility of breakage probability decreasing. This model is used to fit the experimental data to validate the theoretical results of breakage probability distribution by repeated stressing.

This chapter analyzes the breakage probability of repeated stressing of granules depending on stressing number by using drop weight test. The test is considered as a fast compression where the stressing rate is larger than at compression test (see **Chapter 4**).

The rotation of granules during stressing is the essential consideration in this experiment. It demonstrates a significant difference of breakage probabilities with the fixed point. The height arrangement of the equipment enables to lead the expected number of stressing in observing breakage probability.

5.2 Material tests and description of double impact by drop weight apparatus

5.2.1 Material tests

The granules of γ-Al_2O_3 (1.8-3.0 mm), Zeolite 4 AK (1.8-4 mm) that represent porous particles and ZrO_2 (2.5-3 mm) for non porous are used.

5.2.2 Description of double impact test by drop weight apparatus

The drop weight test is one of the simplest and most commonly used method for investigating breakage characteristics of materials [6].

The equipment consists of striker, line guider, anvil and displacement sensor (see **Figure 5.1a** and **5.1b**). Equipment is arranged to provide the control of the granules orientation in each stressing. The granules can be fixed on a plate bed and does not change the position i.e. stressing point during testing. This is accomplished by using a bit paraffin to fix the granule on the anvil.

The impact energy is arranged by selecting the appropriate combination of drop heights or net drop height h_0. This distance between two plates can be varied to realize the fine adjustment of impact energy. The impact energy is calculated according to velocity record in releasing of drop weight.

The procedure principle, the weight (striker), from a known height, against a granule positioned on top of a hard anvil. The distance between the bottom of the drop weight and the top of granules is arranged. When weight is released the striker immediately hit granule that is set at the hot plate anvil. The displacement sensor at the top indicates the falling velocity of the load.

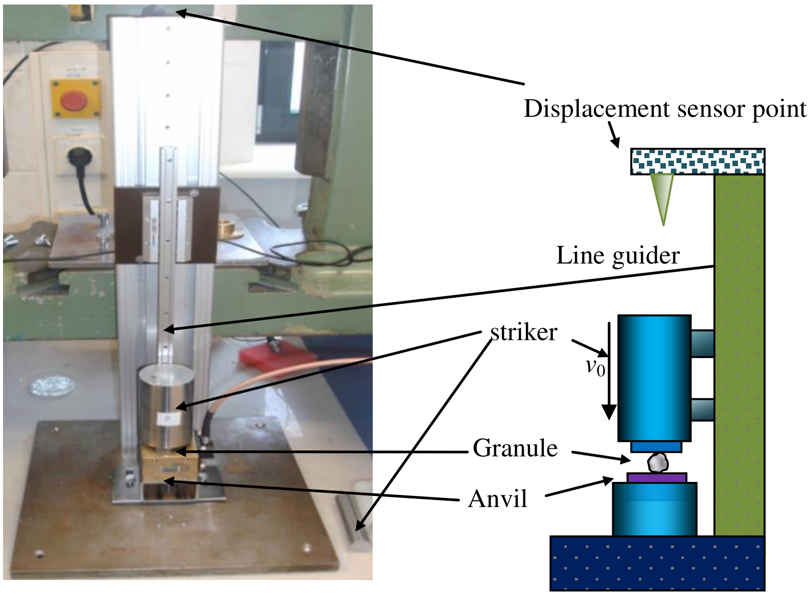

(a) (b)

Figure 5.1 The equipment (a) and schematics drawing of the drop weight tester (b) that corresponds to double impact stressing between two stiff solid plates.

The guiders well-designed, which have low frictional losses. Velocity of the striker in the instant of collision is measured by displacement time of wiper depending. The displacement sensor is a linear position transducer that is frequently used for measuring linear position or displacement up to 0.72 m (see **Figure 5.2**).

Displacement sensor converts linear motion into a changing resistance that can be converted directly to voltage and current signals. The movement causes the resistance value between the wiper and the two end connections to change giving an electrical signal output. The variation of resistance corresponds to the free fall distance and period. The movement can be synchronized to basic velocity principle $v = s/t$.

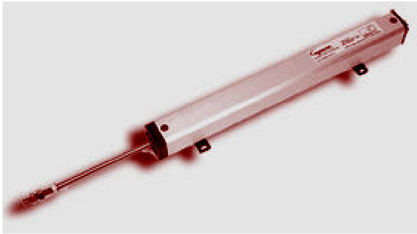

Figure 5.2 A linear position transducer for measuring displacement.

Once the striker reaches the granule surface, the input energy becomes equal to the kinetic energy. The proportional correlation between v_0 and h_0 is shown in **Figure 5.3**.

The input energy corresponds to the mass of the weight m_b and h_0. The test rigs in proved to be effective with spheres [6] Hence, the potential input energy is given by

$$E_{pot} = m_b g h_0 \tag{5.1}$$

When guider is used [6] to control the position of the falling weight, momentum may occur due to friction, so that the kinetic input energy is more appropriately calculated by

$$E_{kin} = {}^{1}\!/_{2}\, m_b {v_0}^2 \tag{5.2}$$

Equations (5.1) and (5.2) are equivalent to the frictionless free-fall conditions prevail, where the impact velocity is given by

$$v_0 = \sqrt{2gh_0} \tag{5.3}$$

Related to the average mass of granule m_G the granule mass related energy is

$$E_{m,b} = \frac{m_b}{m_G} g h_0 \tag{5.4}$$

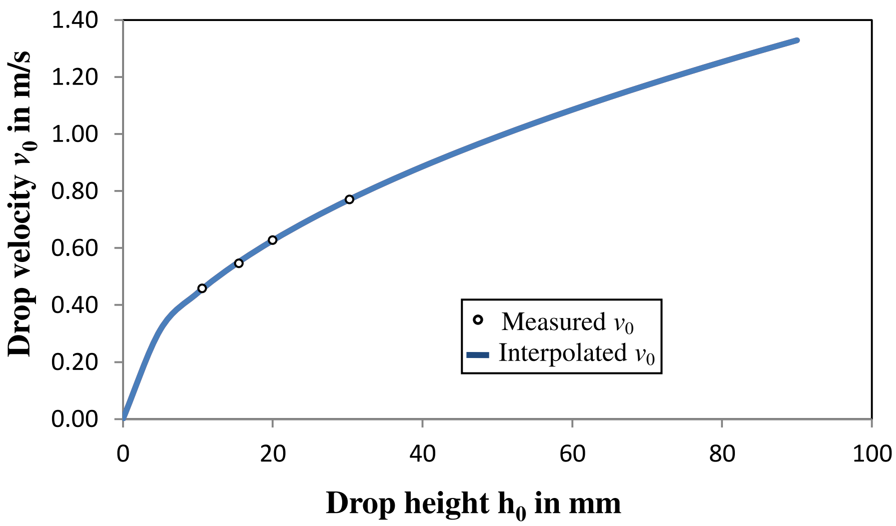

Figure 5.3 The measured drop velocity v_0 at different drop distance or height h_0 in drop weight test is equipped with a linear guiding system.

In this experiment the equipment is developed to measure breakage probability of repeated stressing of granules by taking into account the stressing point. The contact point of granules during testing is arranged in two positions —fixed and random position of stressing *s* (see **Figure 5.4**).

The experiment is accomplished with equipment setup in which the height of striker is arranged to meet the appropriate collision. The striker is released and immediately taps the granule beneath that is mounted between the static load and the anvil.

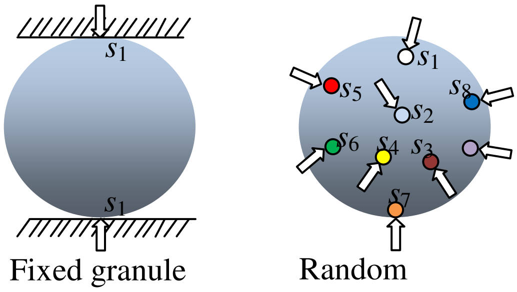

Figure 5.4 Fixed and random configuration of granules by repeated stressing.

5.3 Discussion of double impact test by drop weight apparatus results

5.3.1 Stressing energy

The limit h_0 is about 100 mm thus the maximum stressing energy that can be reached is only about 0.06 J. Considering the v_0 dependence on the drop distance, obviously this test may only be used to study fracture of granules at reasonably low strength. Since free-fall conditions are met in such tests, the stressing energy follows the simple expression as described in Equation (5.1) with impact velocities up to 1.4 ms^{-1}.

The remaining energy is dissipated by the collision stage, which results in secondary fracture of the initial progeny and possibly several further stages of sequential fracture as well [6]. The load m_b put on a free-fall condition prevail of the system. It means guider system that is used to control the drop of the falling weight, receives a loss of momentum that may occur due to friction. For well-designed guiding systems, they have low frictional losses, result in impact velocities between 95% and 99% of free-fall velocity [6] so that Equation (5.4) is enable to be used to estimate the energy input with reasonable accuracy (see **Figure 5.5**).

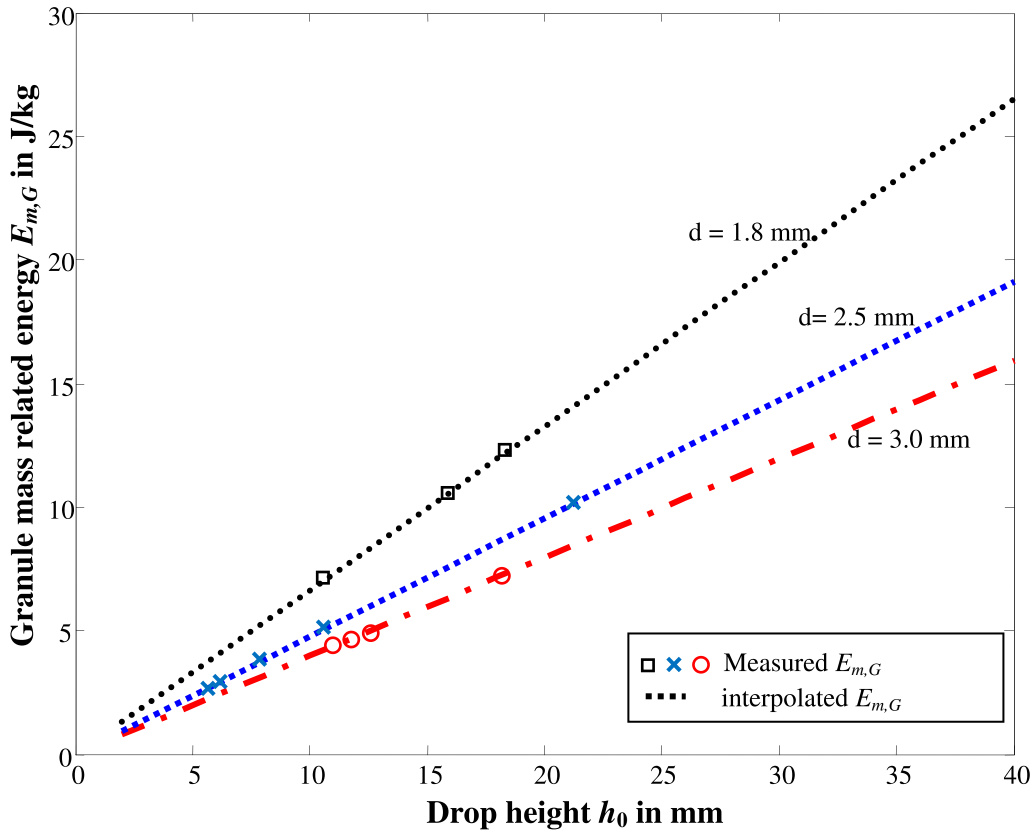

Figure 5.5 Granule mass related energy $E_{m,G}$ as a function of h_0 for different sizes γ-Al_2O_3 granules.

5.3.2 Result and discussion of breakage probability by drop weight testing

The cumulative breakage probability P(i) by repeated stressing was fitted by using degradation model with parameter q depending on the number of stressing. The model calculation is applied for fixed and random points.

5.3.2.1 Breakage probability of γ-Al_2O_3 and Zeolite 4AK granules as function of granule mass related energy $E_{m,G}$

The appropriate selected height h_0 is arranged with the values shown in **Table 5.1.** This certain height is chosen to render a repeated stressing in testing or to allow an appropriate collision in such away that the stressing does not generate breakage at initial stressing.

At a very small ($E_{m,G} < 2$ J/kg) collision energy, the repeated stressing does not break the granules. Meanwhile, at higher collision energies ($E_{m,G} > 60$ J/kg), repeated stressing is not performed either due to fracture at initial stressing.The unbroken granules at low energy are

Table 5.1. Percentage of breakage by repeated stressing of granules at varied drop height h_0.

Granule	D in mm	h_0 in mm	$E_{m,G}$ in J/kg	Percentage of breakage in %		Percentage of breakage in %	
				Fixed	Random	Fixed	Random
γ-Al_2O_3	3	11.0	4.38	17	16	36.4	36.0
		12.4	4.94	26	23	86.9	87.0
		13.0	5.18	29	28	100	100
		18.0	7.17	32	32	100	96
	2.5	5.8	2.77	10	10	71	69
		8.7	4.15	12	12	100	100
		10.8	5.16	35	35	99	100
		12.2	5.83	37	37	100	100
	1.8	10.8	7.17	3	5	100	100
		15.8	10.48	9	7	100	100
		19.6	13.00	28	30	100	100
Zeolite 4 AK	2.5	23.3	14.69	35	34	90	92
		19.0	11.98	19	19	56	63
	4	10.8	4.38	21	21	61	66
		13.8	6.59	25	25	90	92
		14.9	7.11	33	34	83	73
ZrO_2	3	13	21.26	29	28	99	100
	2.5	32.9	53.79	20	20	100	100

Table 5.2 The breakage probability increments $p(i,E_{m,G})$ in %, by drop weight for γ-Al_2O_3 (d = 2.5 mm) at varied h_0.

h_0 in mm	Configuration	Stressing sequence									
		1	*2*	*3*	*4*	*5*	*6*	*7*	*8*	*9*	*10*
5.8	Fixed	10	3	12	6	4	8	8	9	6	5
5.8	Random	10	6	3	8	10	5	6	8	7	6
8.7	Fixed	12	27	25	18	11	3	1	2	0	1
8.7	Random	12	30	27	11	8	3	7	1	1	0
10.8	Fixed	18	37	24	7	3	7	2	1	0	0
10.8	Random	18	50	19	7	1	3	1	0	0	1
12.8	Fixed	37	51	6	3	2	1	0	0	0	0
12.8	Random	37	50	8	2	2	0	1	0	0	0

obtained by small h_0, in this test for instant, the repeated stressing at h_0 (γ-Al_2O_3, d = 3 mm) lower than 11 mm ($E_{m,G}$ = 4.38 J/kg) does not generate breakage. These unbroken γ-Al_2O_3 granules also exist at h_0 below 5.8 mm (d = 2.5 mm ($E_{m,G}$ =2.77 J/kg) and d = 1.8 mm (h_0 =10.8 mm, $E_{m,G}$=7.17 J/kg)). The breakage probability increments is depending on the stressing series and drop high h_0. The increasing number of stressing generates small number of breakage see **Table 5.2** and **5.3.**

Table 5.3 Breakage probability increments $p(i,Em,G)$ in % of drop weight for γ-Al_2O_3 (d = 3.0 mm) at varied h_0.

h_0 in mm	Configuration	Stressing sequence									
		1	*2*	*3*	*4*	*5*	*6*	*7*	*8*	*9*	*10*
11	Fixed	17	4	1	3	3	0	2	4	1	2
11	Random	16	1	2	2	2	5	2	2	3	1
12.4	Fixed	26	11	7	13	7	9	3	5	1	4
12.4	Random	23	14	10	7	11	6	4	2	7	3
13	Fixed	29	21	11	15	11	5	2	4	0	1
13	Random	28	15	24	7	12	3	4	1	3	2
18	Fixed	32	21	24	15	5	3	0	0	0	0
18	Random	32	21	17	12	14	3	1	0	0	0

Different breakage probability behavior for fixed and random points is demonstrated in this test. Repeated stressing at a fixed point leaves "memory effect". Meanwhile this behavior is not generated in the random points. Therefore in measuring the breakage probability it is important to take into account the properties change that caused by repeated stressing.

This change of material properties is represented by a parameter as identified as degradation model with parameter q for fitting model as shown in Equation 3.12 (**Chapter 3**). However before going further, it is better to compare the breakage probability result regardless to the change of granules properties (the equation is described in Equation (6.7), **Chapter 6**). Without taking into account this change or un-applying parameter q as a fitting model, the typical result of cumulative breakage probability of fixed and random γ-Al_2O_3 granules (d = 3.0 mm) is depicted in **Figure 5.6**. In this way the model calculation is considered q = 1.

One can see that the model is not appropriate to represent the repeated stressing test for fixed and random points. The measured cumulative breakage probability is not fitted well by calculation. In this term the breakage probability distribution necessity to involve a parameter that also denotes the change of particle properties by repeated stressing. The change of particle properties (particularly the strength) occurs due to the orientation of contact point of stressing. This orientation contact point in this experiment is arranged by rotating the granules during stressing.

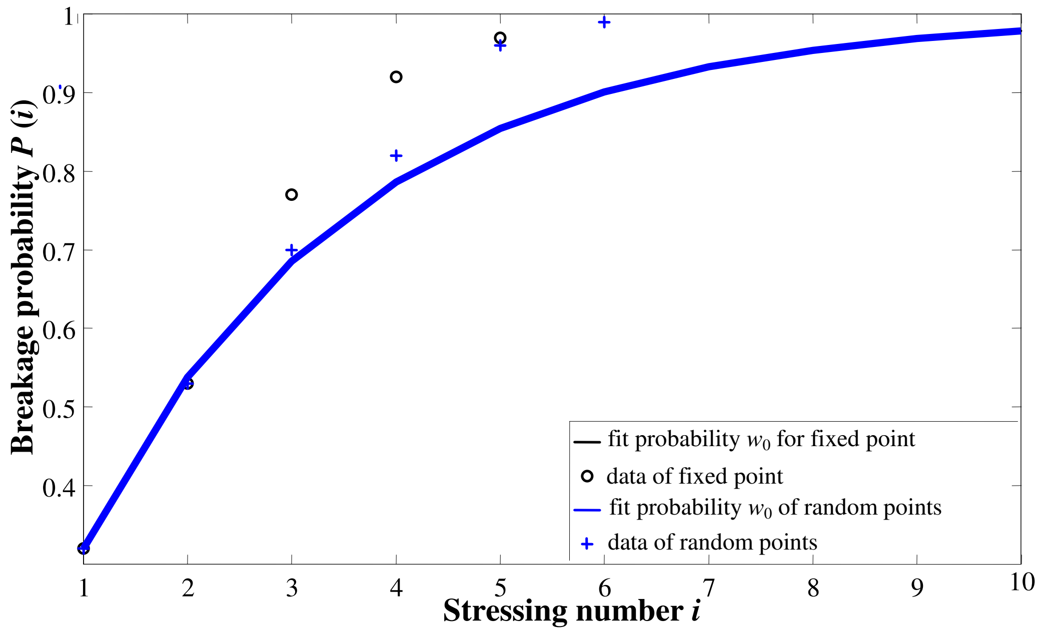

Figure 5.6 The cumulative breakage probability $P(i)$ of γ-Al_2O_3 granules (d = 3 mm) at h = 18.0 mm as a function of the number of stressing i without taking into account the change of granules properties during stressing (see Eq. (6.7), **Chapter 6**).

The rotation that causes a variance of cumulative breakage probability is represented by degradation model with parameter q. This parameter fits the distribution of breakage probability as a function of the stressing number. The **Figure 5.7** shows fitting of experimental data distribution of γ-Al_2O_3 granules (d = 3 mm) at h_0 = 18.0 mm, $E_{m,G}$ = 7.17 J/kg.

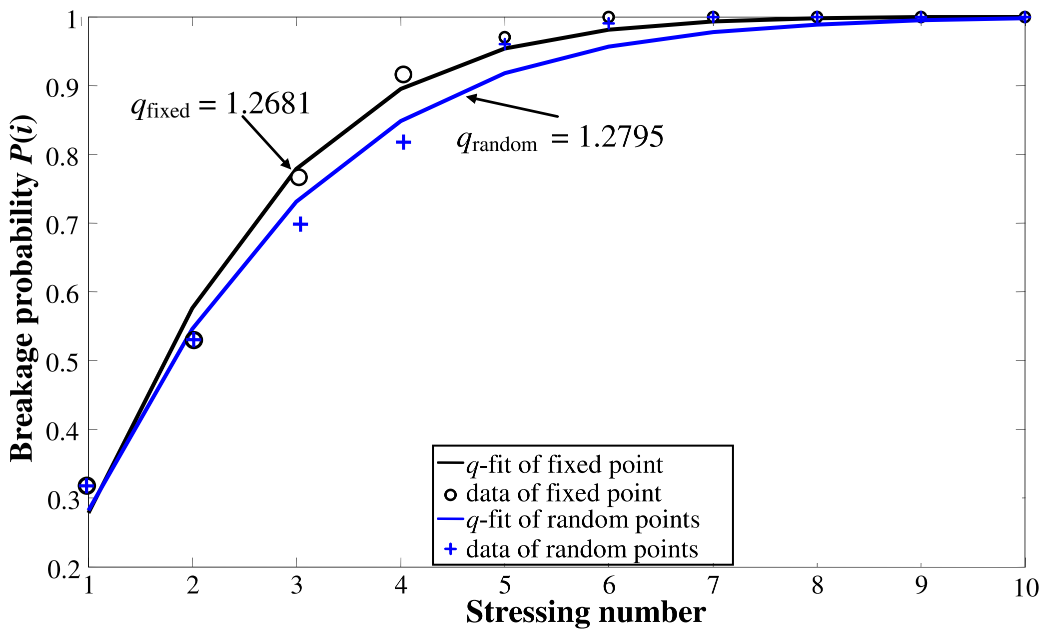

Figure 5.7 The fitted data according to degradation model q. The cumulative breakage probability is measured for fixed and random γ-Al_2O_3 granules (d = 3 mm) at h_0 =18.0 mm with $E_{m,G}$ = 7.17 J/kg.

For fixed point, at initial stressing, the striker hit isotropic granule. The initial stressing corresponds approximately to the resistance of unstressed surface of granules. The stressing area renders plastic strain during the initial cycle. The advanced stressing is applied at the same axis or stress direction and the same dropping height. The cycle retains practically the same shape as the move along the isotropic deformation axis.

There is a 'memory effects' which can be characterized by the maximum value of the cyclic stress amplitude. Its increasing is associated with significant plastic deformation [16, 17]. If the stress path is situated entirely within this region, the cycles will provide a progressive compaction even for initially dense materials. When it crosses the boundary of the region during each cycle, then it generates advanced compaction and dilation. If the average level of the cycle lies within the contractant domain, cyclic stressing produces a consolidation and hardening [18].

In acquisition the stressing by model calculation, the fit model demonstrates varied values of degradation model with parameter q depending on type of the contact test, materials, granules size d, drop height h_0, and mass related energy $E_{m,G}$ (see **Table 5.4**). The difference of degradation model with parameter q increases with applied stressing energy. The deformation of fixed point at the certain contact point increases by means of repeated stressing. By a micro scale observation it was found that the elastic plastic deformation decreases due to repeated stressing [12]. There is a formation and propagation of damages of the solid bridge bonds between primary particles. Due to this, the stiffness of spherical granules increased with the increasing number of stressing cycles up to the point where a final consolidation of the plastic deformation is reached [12] and see also **Chapter 4**.

The validated degradation model with parameter q has confidence bounds 95% and q value has the tendency as follows:

- The values of q for large particle size are less than that small size.
- Small granules initiates high $E_{m,G}$ and eventually generates high $P(i)$ that is proportionally with values of q.
- Regarding to the configuration of granules by selecting the stressing point the values of $q_{\text{fixed}} > q_{\text{random}}$ by repeated stressing.

The tendency of q affirms the damage accumulation events that occurs by repeated stressing particularly at low stressing energy. The values of q tend to q>1. This means the damage

Table 5.4 Parameter q at varied granule sizes and drop heights (h_0).

Granules	d in mm	h_0 in mm	config.	$E_{m,G}$	q_{min}	q	q_{max}	*R-square*
γ-Al_2O_3	3	11.0	fixed	4.38	0.6565	0.7165	0.7765	0.8541
			random		0.7408	0.8168	0.8928	0.8725
		12.4	Fixed	4.94	0.8910	0.9645	1.0380	0.9869
			Random		0.9120	0.9674	1.0227	0.9927
		13.0	Fixed	5.18	1.0205	1.0751	1.1298	0.9953
			Random		0.9847	1.0583	1.1319	0.9909
		18.0	Fixed	7.17	1.2163	1.2681	1.3199	0.9970
			Random		0.5783	1.2795	1.9807	0.8790
	2.5	5.8	Fixed	2.77	1.0394	1.1003	1.1611	0.9930
			Random		1.0436	1.0987	1.1539	0.9942
		6.8	fixed	3.65	0.9509	1.0828	1.2146	0.9808
			random		1.0007	1.1148	1.2289	0.9876
		8.7	fixed	4.15	1.2942	1.4188	1.5434	0.9930
			random		1.0799	1.2471	1.4143	0.9801
		10.8	fixed	5.16	1.0422	1.2128	1.3834	0.9721
			random		1.1248	1.3557	1.5866	0.9589
		12.2	fixed	5.83	1.1319	1.3103	1.4887	0.9518
			random		1.1432	1.3123	1.4814	0.9572
	1.8	10.8	fixed	7.17	1.1651	1.2123	1.2595	0.9964
			random		1.0510	1.0992	1.1474	0.9892
		15.5	fixed	10.48	1.2039	1.3008	1.3978	0.9950
			random		1.0291	1.0908	1.1525	0.9933
		19.6	fixed	13.00	1.2023	1.3268	1.4512	0.9842
			random		1.1835	1.3621	1.5408	0.9695
Zeolite 4AK	4.0	10.8	fixed	4.38	0.7913	0.8421	0.8928	0.9813
			random		0.8198	0.9108	1.0019	0.9626
		13.8	fixed	6.59	0.9172	0.9729	1.0286	0.9930
			random		0.9086	0.9563	1.0041	0.9943
		14.9	fixed	7.11	0.7389	0.8097	0.8806	0.9656
			random		0.6450	0.7243	0.8036	0.9143
	2.5	23.3	Fixed	14.69	0.8133	0.8872	0.9611	0.9785
			random		0.8168	0.9397	1.0625	0.9582
		19.0	Fixed	11.98	0.8183	0.8425	0.8667	0.9961
			random		0.9966	1.0620	1.1275	0.9936
ZrO_2	3	13	Fixed	21.26	1.0205	1.0751	1.1298	0.9953
			random		0.9847	1.0583	1.1319	0.9909
	2.5	32.9	Fixed	53.79	0.9974	1.1128	1.2283	0.9840
			random		1.1821	1.2958	1.4094	0.9902

accumulation occurs by increasing of stressing number. The breakage probability increments decreases that confirms the selection event that occurs by repeated stressing. The intensity and the frequency of stressing and the microstructure influence material resistance against cyclic stressing [12].

The same behavior of stressed γ-Al_2O_3 granules is also exhibited in stressing of Zeolite 4 AK granules. However there is another phenomena, the breakage behaviour begins to change when the stressing sequence reaches the 4th of stressing sequence. This change point is identified as a transition point (see **Figure 5.8**).

At a lower velocity stressed granules are not broken, due to hardening events. The increasing number of stressing generates stronger granules as described above. Overall either for γ-Al_2O_3 or Zeolite 4 AK, at the result, the breakage probability of fixed tend to be larger than that random points depending on stressing number.

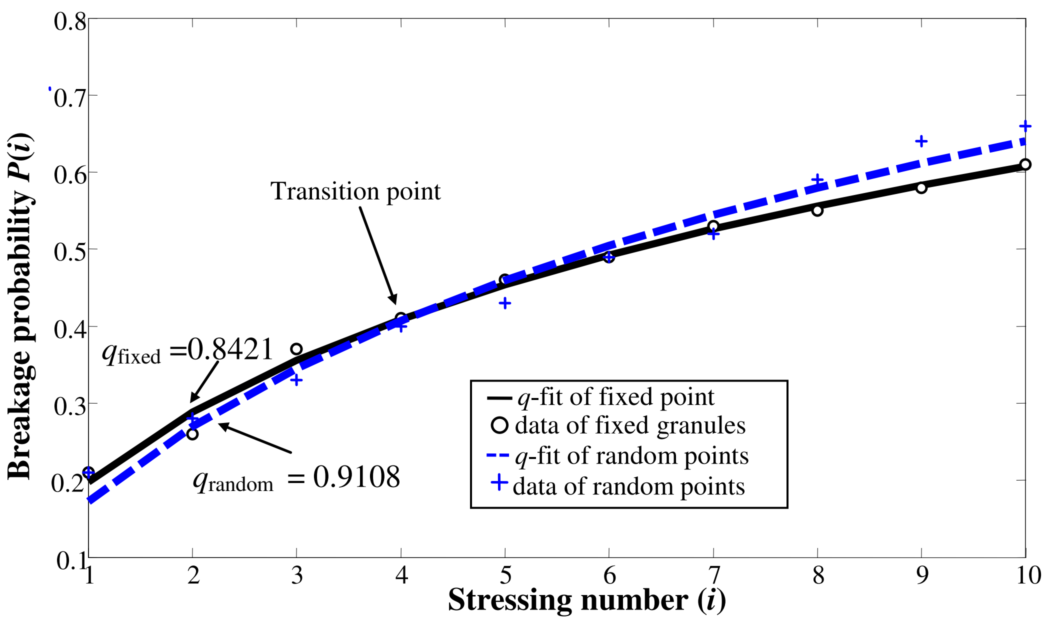

Figure 5.8 Fit according to degradation model with parameter q model of zeolite 4AK granules (d = 4.0 mm) at h_0 = 10.8 mm, with $E_{m,G}$ =4.38 J/kg.

Similar with γ-Al_2O_3 behavior, the breakage probability of fixed zeolite 4AK granules is larger than the random points. Zeolite 4AK consists of several layers to build the body during stressing, hence when it is stressed it does not break immediately, but rather the granule is eroded gradually (see the brief description of **Figure 2.17**, **Chapter 2**). The stressing at the same point by fixed stressing propagates damage accumulation at the contact point (see **Figure 5.9**).

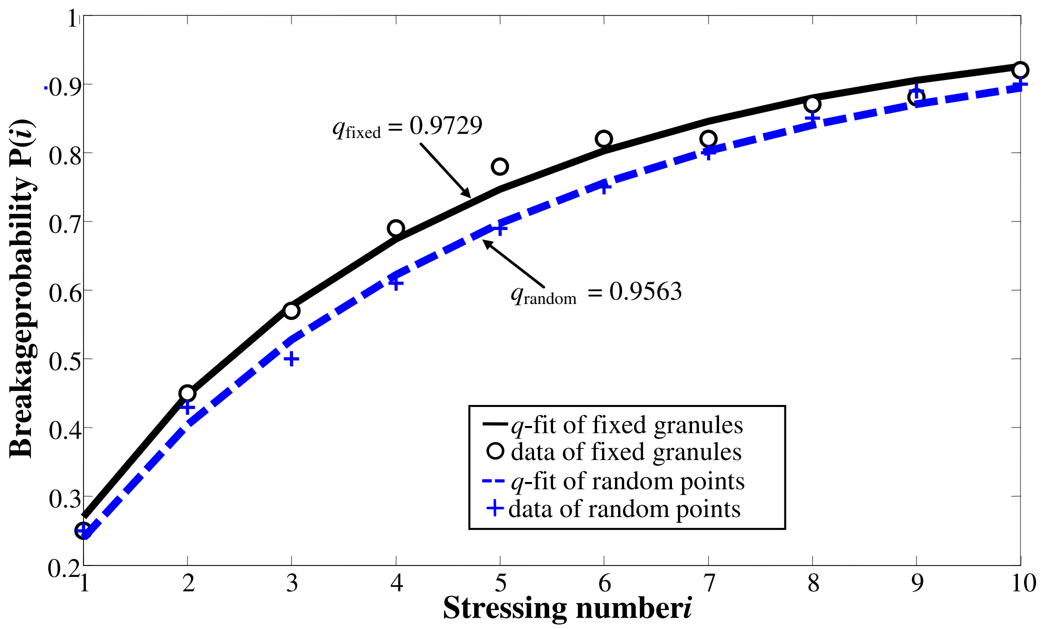

Figure 5.9 Breakage probability by degradation model with parameter q as a fitting model of zeolite 4AK granules (d = 4.0 mm) at h = 13.8 mm, with $E_{m,G}$ = 6.59 J/kg.

5.3.2.1 Breakage probability of ZrO_2 granules

It is important also to apply the drop weigh test upon ZrO_2 as a non porous particles. The testing only can be established at minimum velocity v_0 = 0.16 m/s or a limited input energy, that is done at h_0 = 20 mm (see **Figure 5.10**). There is no breakage below this velocity.

The result shows different behavior from γ-Al_2O_3 and Zeolite 4AK as porous materials. For fixed and random points tend to have similar breakage probability behavior. This is because at fixed point there is a typical Hertzian ring and cone cracks, which are usually performed at the first failure of solid granules. This breakage occurs with increasing number of stressing.

During the post-stressing phase, additional cracks which form inside the main Hertzian ring are associated with deformation processes such as densification where density increase at the deformed zone [21]. However this deformation does not lead to fracture at a static input energy [21]. Small increasing in impact velocity leads to the detachment of a small amount of material around the impact zone, and increase oblique cracks.

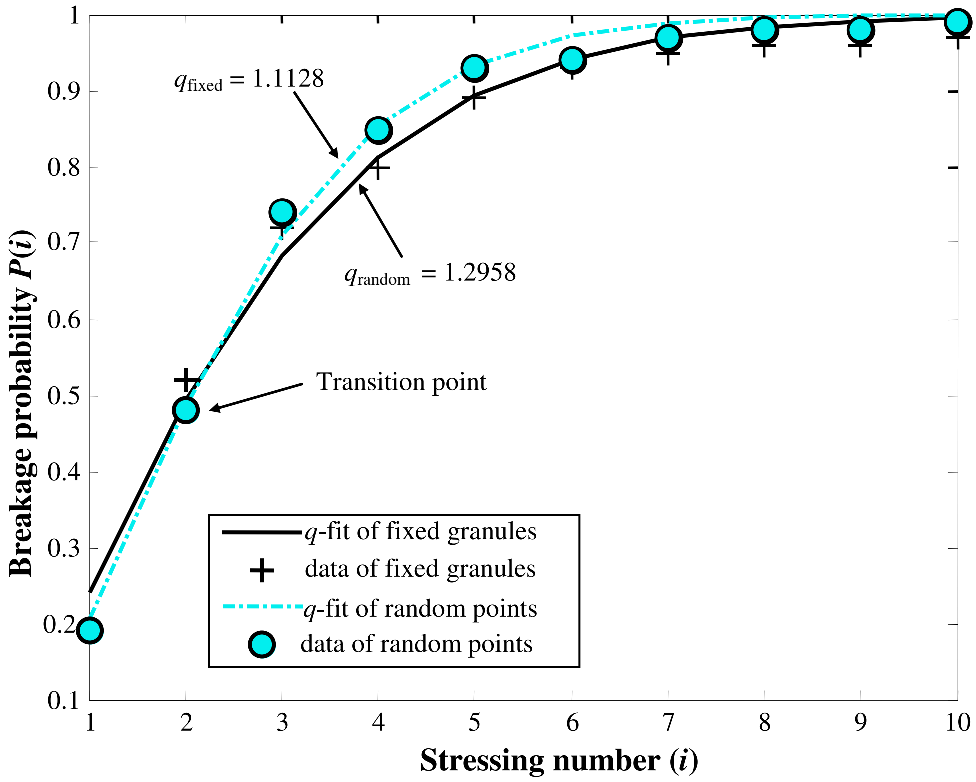

Figure 5.10 The data fitted according to degradation model with parameter q model. The cumulative breakage probability is measured for fixed and random of ZrO_2 granules (d = 2.5 mm), with $E_{m,G}$ = 53.79 J/kg.

It is problematical to describe the repeated stressing of a hard solid material like ZrO_2. Because at low energy there is no breakage, meanwhile at high velocity regarding to the free fall distance, repeated series is not performed very well, where granules broke at initial stressing. ZrO_2 granules have better resistance against cyclic stressing than that γ-Al_2O_3 and Zeolite 4AK.

5.3.4 The breakage probability depending on the specific energy

The breakage probability by repeated stressing of granules by using drop weight is strongly influenced by h_0. Varied h_0 generates different input energy that is identified as granules mass related energy ($E_{m,G}$) and eventually correspond to the cumulative breakage probability $P(E_{m,G})$. This behaviour is depicted at **Figure 5.11** and **5.12** that the higher h_0 the higher $P(E_{m,G})$ which it corresponds proportionally with q. It verifies the degradation effect by cyclic stressing. Thus the values of q can be used to examine $P(i)$.

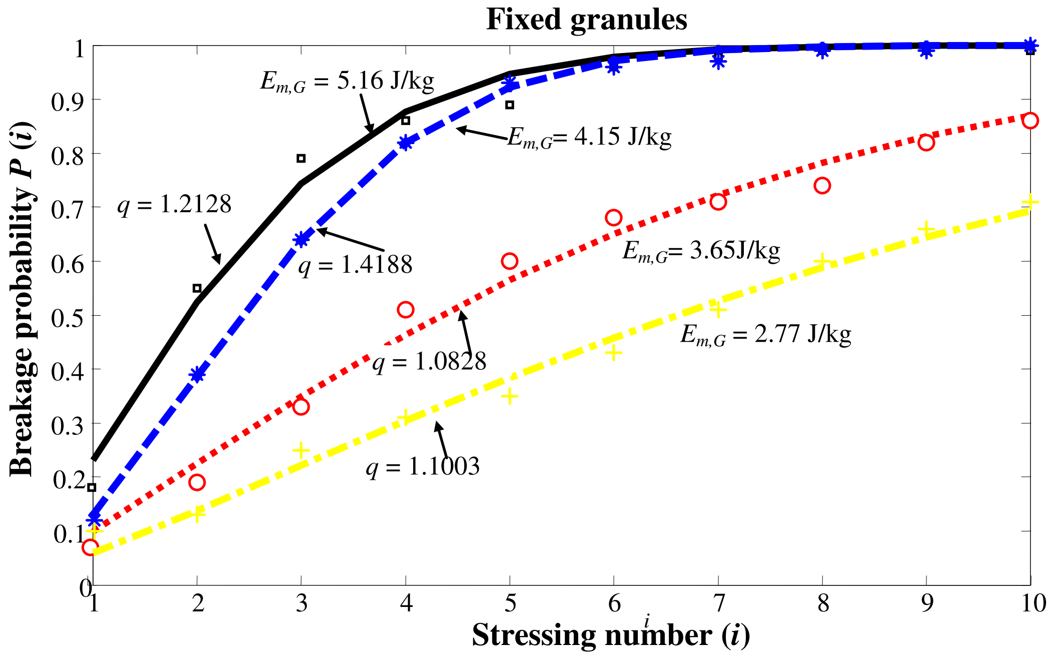

Figure 5.11 The fitted data according to degradation model with parameter q. The cumulative breakage probability is measured for fixed γ-Al_2O_3 granules (d = 2.5 mm) depending on the mass related $E_{m,G}$.

The same breakage probability behavior with γ-Al_2O_3 are also exhibited by Zeolite 4AK. Varied h_0 generates certain breakage probability as well. At high h_0, the equipment demonstrates large input energy and it allows large number of breakage by repeated stressing. For all h_0 values, the cyclic stressing represents a hardening effect in fixed point.

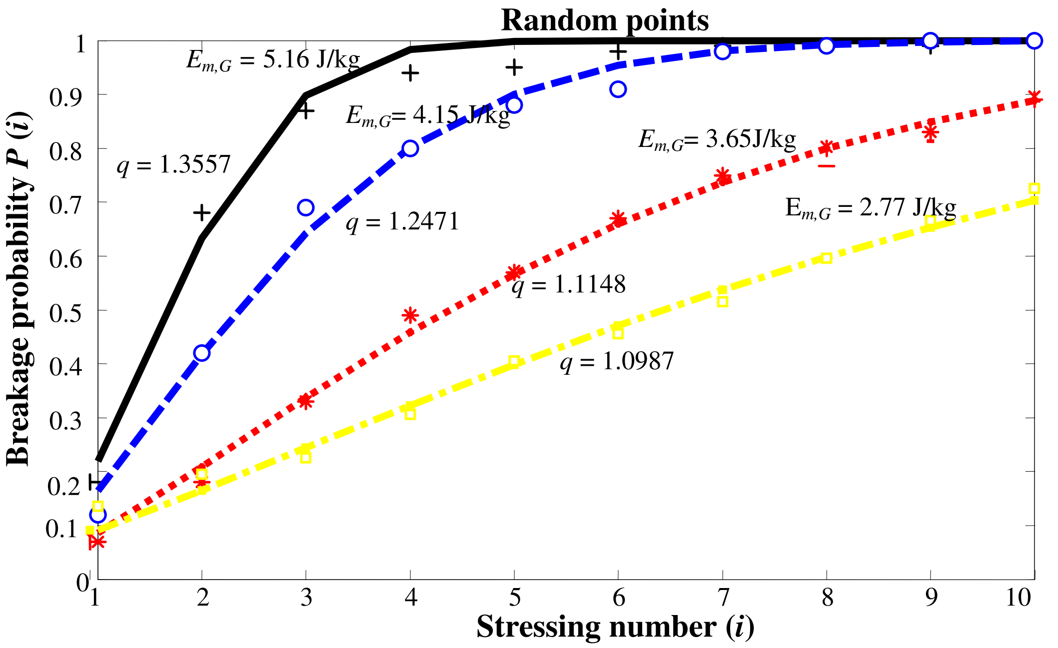

Figure 5.12 The fitted data according to degradation model with parameter q. The cumulative breakage probability is measured for random γ-Al_2O_3 granules (d = 2.5 mm) depending on the mass related energy $E_{m,G}$.

5.4 Conclusions of repeated stressing by drop weight test

Double impact by drop weight experiment with selecting stressing contact by fixed and random points has a significant influence on the breakage probability behavior. The experiment datas are fitted by degradation model with parameter q for calculating the cumulative breakage probability related to stressing number. The model denotes the change of granules strength by repeated stressing.

The degradation model with parameter q has the tendency where the with high $E_{m,G}$ the q also large consequentially increases $P(i)$. The consistent values q>1 implies damage accumulation occurs during repeated stressing.

With the increasing number of stressing, the breakage probability increments decrease consecutively. This behavior represents the hardening effect by cyclic stressing (it is also obtained in **Chapter 4**). Therefore, the cyclic stressing produce either damage accumulation effect or the other one, selects the stronger granules to be survived.

CHAPTER 6
REPEATED DOUBLE IMPACT STRESSING BY PENDULUM APPARATUS

6.1 Equipment with low energy impact

From the previous chapters, the number of stressing and the varied contact points have a major effect on the damage behavior particularly breakage probability of granules. Repeated stressing disregards the solid bridge of primary particles together with progressive hardening within stressed granule. This hardening is propagated due to damage accumulation that is performed in fixed point (see conclusions in **Chapter 4** and **5**).

The configuration of contact point during cyclic stressing provides a possibility to find the weak points on granule surface, where the strength is low (see subsection 4.6, Ch**apter 4**). The behavior is examined in this chapter by using pendulum as the double impact test.

Similar with drop weight the equipment is also considered for fast compression. It provides a possibility to examine the parameters of breakage probability by different stressing conditions. This equipment can be operated at low impact energy that is hardly performed in such drop weight test. The validation of degradation parameter q is carried out to fit the experiment data to determine breakage probability.

6.2 Experiment

6.2.1 Material tests

About 200 the γ-Al_2O_3 granules with diameter 1.62–2.50 mm are used as material tests to investigate the breakage probability by pendulum double impact.

6.2.2 Description of pendulum double impact equipment

The equipment is developed to examine granules behavior during repeated stressing regarding to the stressing point (see **Figure 6.1a**). The part of equipment can swivel or tip on a fixed point at a fulcrum. The stem and the fulcrum are mounted in adequate position at the middle so that the stem can go up and down (**Figure 6.1b**). Granule is impacted by releasing the leveling load at a predetermined height. The granule is put on a hard metal plate that is made from tungsten carbide material (**Figure 6.1c**). It allows arrangement of granule configuration into two ways – with fixed and random position.

(a) normal position

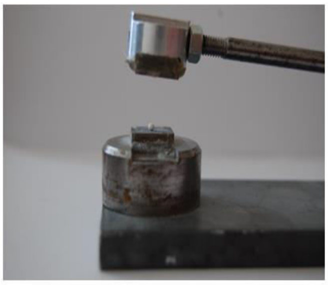

(b) with falling distance

(c) contact with granule

Figure 6.1 Selecting an appropriate combination of drop height in pendulum impact. The device at normal position (a), with falling distance (b) and weight contact with granule (c).

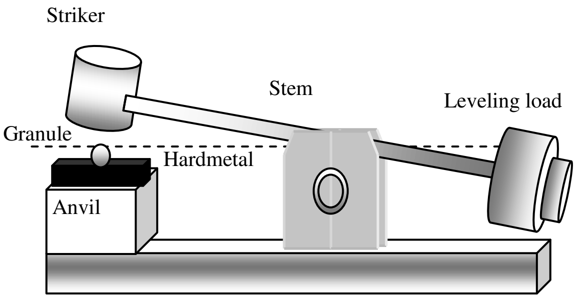

(a)

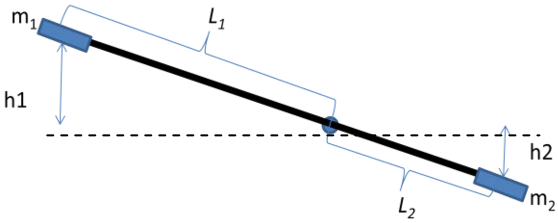

(b)

Figure 6.2. Setup of pendulum impact and the schematic representation.

The mechanical principle of double impact test is explained according to **Figure 6.2.b**. The striker is not in the centre but close to the end of the stem. Simply by pushing down the right side the load is lifted immediately at the same time. The potential energy of a falling striker is:

$$E = m_1 g h_1 - m_2 g h_2 + \frac{m_{st} g}{2(L_1 + L_2)} L_1 h_1 - \frac{m_{st} g}{2(L_1 + L_2)} L_2 h_2 \tag{6.1}$$

or

$$E = m_1 g h_1 - m_2 g h_2 + \frac{m_{st} g}{2(L_1 + L_2)} (L_1 h_1 - L_2 h_2) \tag{6.2}$$

But by similar triangle

$$\frac{h_1}{L_1} = \frac{h_2}{L_2} \tag{6.3}$$

$$E = g h_1 \{ m_1 - m_2 \frac{L_2}{L_1} + \frac{m_{st}}{2L_1(L_1 + L_2)} (L_1^{\,2} - L_2^{\,2}) \} \tag{6.4}$$

Where m_{st} is mass of stem. The m_1 and m_2 are the mass of the striker and leveling load respectively. The h_1 is the height of the dropping striker. In this experiment m_1 = 0.01368kg, m_2 = 0.038895 kg, and lever arm length L_1 = 168.50 mm, and L_2 = 82.00 mm are used.

6.3 Discussion of test result by pendulum impact

6.3.1 Breakage probability increments

Configuration of contact point by fixed and random points exhibits a unproportional correlation between the number of stressing and the breakage probability increment $p_{i,d}$. At the initial stressing, the $p_{i,d}$ is large and the same behaviour also occur at the same $E_{m,G}$ (0.5297 J/kg) or h_0 = 15 mm (see **Table 6.1**).

After 10 stressings the $p_{i,d}$ decrease according to simple rule at Equation (3.5) in **Chapter 3.**

The measured breakage probability at the first stressing (w_0) is considered the same for fixed and random points. However, the low difference (about 2%) in initial $p_{i,d}$ increase due to repeated multiplication that takes place by calculation.

Table 6.1 The $p_{i,d}$ of γ-Al_2O_3 granules (d =1.80 mm) by fixed and random configuration in pendulum impact test.

Granules configuration	Number of broken granules depending on stressing event number										$E_{m,b}$ in J/kg
	1	2	3	4	5	6	7	8	9	10	
Fixed	29	22	25	14	13	8	10	6	6	2	0.5297
Random	31	11	16	20	9	6	10	8	8	11	0.5297

From the regression analysis, the correlation coefficient for fixed and random points is about of 0.98. Confidence bounds value is 95% for both configurations that indicate the reliability of an estimate is accepted. The range of value (interval), act as good estimates of the unknown parameter. In this way, 95% of the observed confidence intervals will hold the true value of the parameter.

6.3.2 Cumulative breakage probability

The cumulative breakage probability or simply entitled as breakage probability $P(i)$ of stressed granules is calculated in to two ways: model without and with degradation parameter. The applied degradation parameter q as a fitted model in this calculation is the same with in **Chapter 5**.

The height of dropping striker h_1 is measured as 12.0 mm. It is obtained w_0 = 0.15. The stressing that occupies a region at initial stressing on surface is denoted as s_1. The next stressing series (s_2 to s_{10}) are applied along the same axis or stress direction.

Equation (6.2 - 6.7) calculate the breakage probability regardless the change of granule properties for fixed and random points.

$$N_b(1) = N_0 . w . \quad (6.5)$$

Where N_0 is the number of initial granules and w is the breakage probability at the any events. The number of nonbroken (N_{nb}) granules after the first stressing is:

$$N_{nb}(1) = N_0 \cdot (1-w). \quad (6.6)$$

The $N_{nb}(2)$ after the second stressing is:

$$N_{nb}(2) = N_0 \cdot (1-w)^2. \quad (6.7)$$

The number of granule that remains nonbroken after n stressing events $N_{nb}(n)$ is:

$$N_{nb}(n) = N_0 \cdot (1-w)^i \cdot \quad (6.8)$$

Consequently the number of broken (N_b) granules is:

$$N_b(n) = N_0 - N_{nb}(n) = N_0(1-(1-w)^i) \cdot \quad (6.9)$$

And the cumulative breakage probability after i stressing events $P(i)$ results is:

$$P(n) = N_b / N_0 = 1-(1-w)^i \cdot \quad (6.10)$$

This equation is used to calculate breakage probability which the data result is shown in **Figure 6.3**. However, it does not fit well the experiment data. There is no a good agreement between the fit and experiment data.

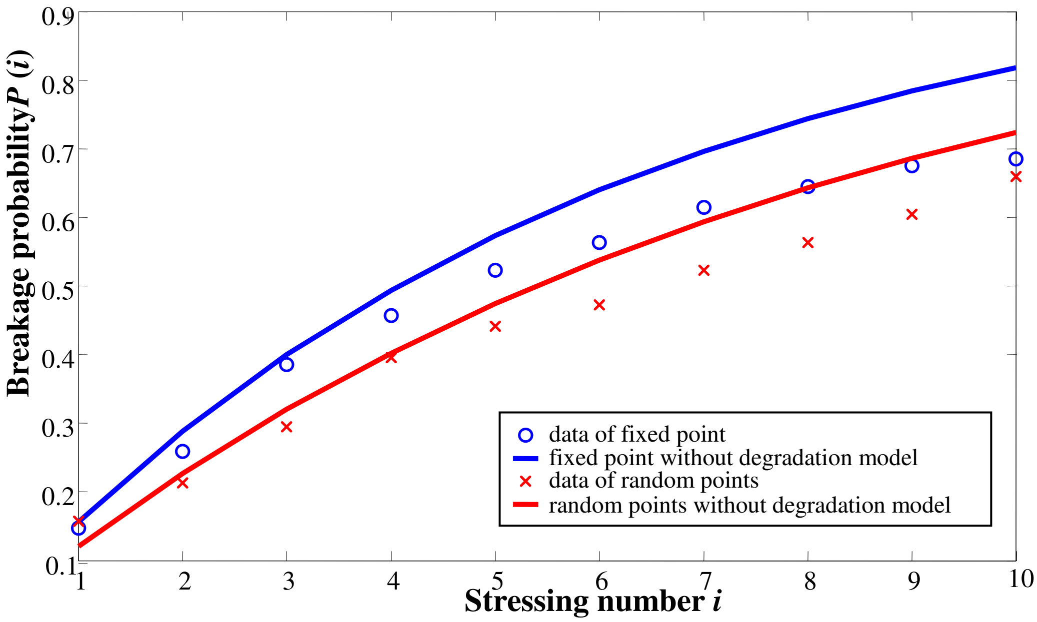

Figure 6.3.Breakage probability of repeated stressing by pendulum impact test with fitted without degradation paramater q of γ-Al_2O_3 granules (d =1.80 mm).

Therefore, the breakage probability must be calculated by using fit parameter that refers to the change of granules properties by repeated stressing. In repeated stressing an evolution of the deviatoric strain is occurred. It changes gradually the strength value of granule. The explanation of this model is presented in Equation 3.12, **Chapter 3**. The parameter denotes the memory effect or the orientation of granules and the change during cyclic stressing. As the result, for fixed point, there is a progressive weakening within stressed granule due to the breakage of solid bridge bond between primary particles during repeated stressing. This weakening is propagated due to damage accumulation that is performed in this fixed configuration.

In a different way, for random points, stressing that is established at the selected stressing points does not correspond to stressing history. During cyclic stressing a reorientation of the contacts takes place. That affects the breakage behavior. Therefore, by involving parameter q, in the calculation the breakage probability can be observed that is gradually changed at every stressing series. The breakage probability increments decrease with the increasing number of stressing. Consequently, repeated stressing of granules affects the cumulative breakage probability (see **Figure 6.4**).

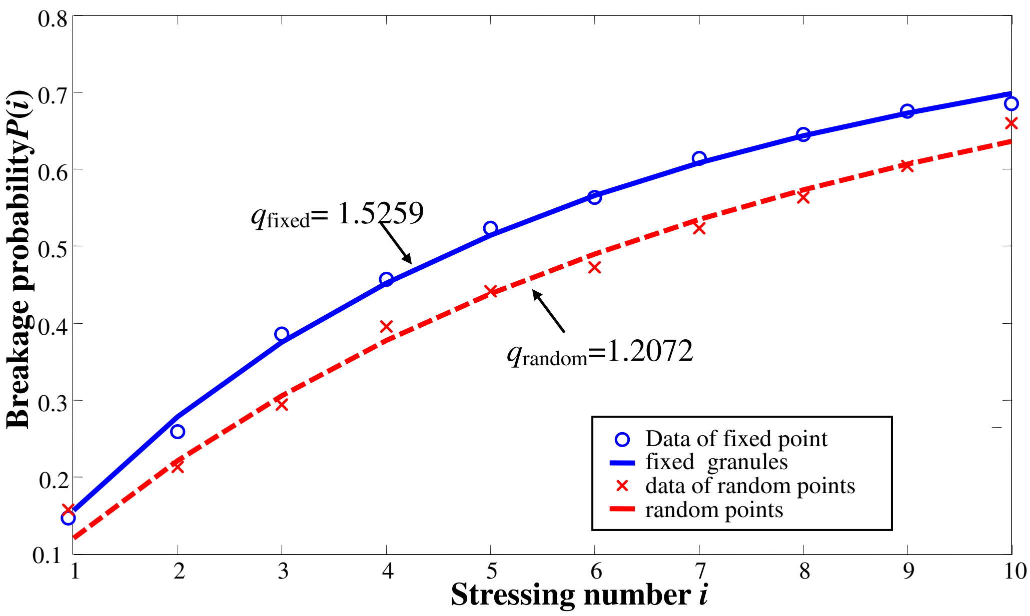

Figure 6.4. Breakage probability of fixed and random contact points of γ-Al_2O_3 granules (d = 1.8 mm) that is fitted by degradation parameter q.

There is a good correlation of both fixed and random points data and the fitting model. With increasing of q the breakage probability increases. The q is consistently $q > 1$ for all experiments. It indicates damage accumulation occurs by repeated stressing. Breakage probability of fixed point is larger than at random points. This result confirms the previous result in **Chapter 5**. The value of q and w_0 are described in **Table 6.2**.

Table 6.2 The degradation paramater q as a function of the breakage probability at initial stressing of individual granule (w_0) of γ-Al_2O_3 granules (d =1.80 mm).

Config.	q	R_{square}	w_0
Fixed	1.5259	0.9183	0.1873
Random	1.2072	0.9047	0.1207

The $p_{i,d}$ of stressed granules by double impact is examined by selecting $h_{1,2}$. Its input energy is related to $h_{1,2}$ that is obtained by using Equation 6.1. It depends on parameters mass $m_{1,2}$ and $h_{1,2}$ of striker (see **Table 6.3**).

Table 6.3 The input energy by means of varied pendulum high and mass of γ-Al_2O_3 granules (d =1.80 mm).

Test	$p_{i,d}$ **in %**	h_1 **in mm**	h_2 **in mm**	E **$*10^{-1}$ in μJ**	$E_{m,G}$ **in J/kg**
1	8.30	12.0	13.81	0.4014	0.4237
2	48.12	15.6	11.67	3.3441	0.5509
3	48.75	15.4	11.56	3.2312	0.5438
4	49.80	15.9	11.82	3.3940	0.5615
5	61.4	16.3	8.96	7.6858	0.5756
6	82.0	16.8	8.85	8.4440	0.5933

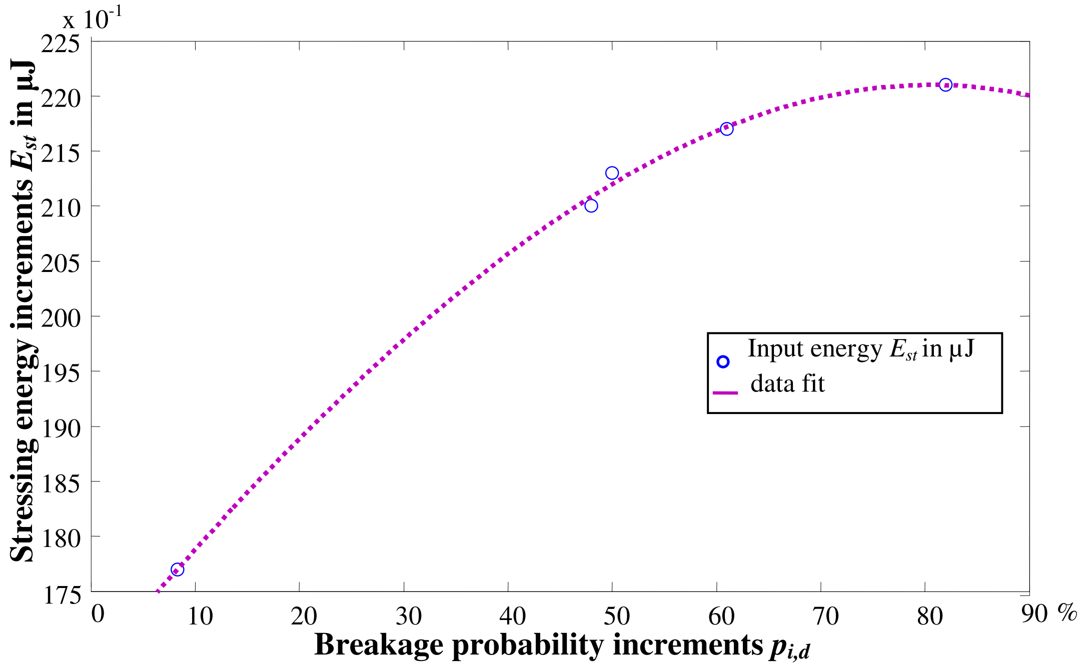

Figure 6.5 The stressing energy increments (E_{st}) of stressed granules at different $p_{i,d}$ of γ-Al_2O_3 granules (d =1.80 mm).

Varied h_1 generates a certain result of $p_{i,d}$. The larger h_1 the more possibility to be broke, eventually generates larger input energy as well (see **Figure 6.5**).

By brittle fracture observation of fragments, there is no difference in fragment form between fixed and random points by pendulum impact (see **Figure 6.6**).

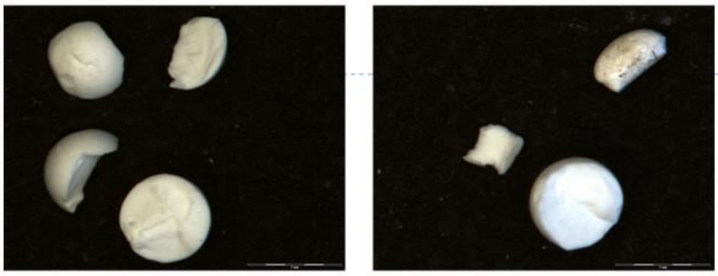

(a) (b)

Figure 6.6.The fragment form of fixed (a) and random points (b) γ-Al_2O_3 granules (d = 1.8 mm) by pendulum impact test.

At this double impact experiment, however, as described above the fixed point perform larger $P(i)$ than that at the random points. It is because the progressive weakening or damage accumulation occurs at the stressing point renders granules more easily to break. Damage accumulation of granules that is represented by q values by repeated stressing for both fixed and random points was discussed in **Chapter 4** and **5**.

6.4 Conclusions of repeated stressing by double impact with pendulum

- There is a significant result of repeated stressing of granules by pendulum impact. A progressive weakening occurs within stressed fixed granule. This weakening is propagated due to damage accumulation that is not generated in random points.
- However the by increasing number of stressing the $p_{i,d}$ is decreasing.
- The $P(i)$ of fixed point is larger than at random points.
- The $P(i)$ by fitted parameter q is obtained consistently with $q > 1$ which implies the damage accumulation effect.
- The increasing number of stressing does not change the q values, or it is obtained constant. This result confirms the same behavior with experiment that is described in **Chapter 5**.

CHAPTER 7
BREAKAGE PROBABILITY OF STRESSED GRANULES BY IMPACT TEST IN AN AIR CANON APPARATUS

7.1 Stressing at large impact velocity

The failure of particles or granules due to free impact is another important test to be observed. In industrial practicing, the free impact along with multiple impact stressing takes the most part in processing where particles are collided many times with wall [8].

This is the main difference between single impact test (that is carried out in a large input energy) and the tests in **Chapter 4**, **5** and **6** (in a low input energy).

In this test the free impact stressing is carried out by air canon apparatus. A single granule is fired toward hard metal target. There is a free space at the opposite side of the contact test or contact point on the surface of granules. Hence, this free impact definitely generates different breakage behaviour, compared to the tests at low input energy and established by stressing from the two sides/double impact test.

The breakage by free impact test with air canon is associated with the breakage probability distribution that is approached by measuring the mass related energy of every granule. In this chapter the breakage probability is connected to the survived granules by pendulum impact test. The survived granules from pretreatment of granules by pendulum impact (see **Chapter 6**) are fired in free impact test. The result proposes the influence of granules pretreatment by double impact pendulum to the breakage probability behaviour.

The testing of pretreated granules by air canon presumably generates another certain result of breakage probability depending on repeated stressing. A correlation between the breakage probability and mass related energy is observed in this chapter. The orientation of granules by double impact by pendulum is in random direction.

7.2 Material test and description of impact test by air canon

Granules of γ-Al_2O_3 with size d = 1.80 mm are used as material test in this experiment. Two equipments are combined in this experiment i.e. pendulum impact and air canon test.

Small scale air cannon test is designed to carry out the impact tests (see **Figure 7.1**). The acceleration of the moving wagon with a granule occurs inside of a 900 mm along hard aluminium tube with core diameter of 12 mm. The driving pressure of compressed air varies from 0.5 to 3 bars. The charge of a granule into the moving piston occurs at the end of the acceleration tube. The permanent magnet allows putting the piston with the granule in the start position.

Figure 7.1 Schema of air canon test

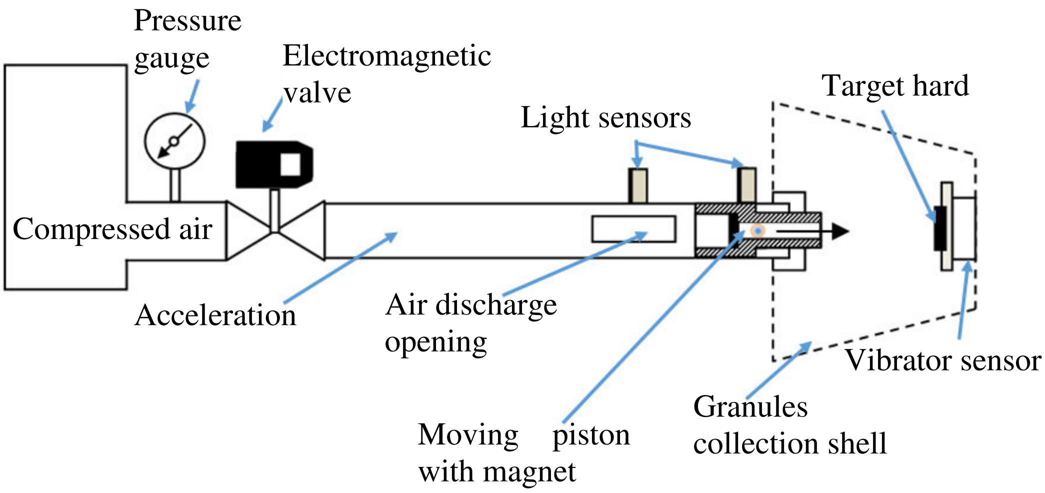

Figure 7.2. The arrangement of measurement system of air canon test.

The type of the equipment and its components are shown in **Figure 7.2**. The component parts of the air canon equipment are acceleration tube, sensors, wagon controller, target, speed measurement displayed by means of the lab view, granule collection shell, valve, moving piston with magnet, vibration sensor, and pressure gauge.

Impact velocity (v_i) related to input energies as large as 1800 J kg^{-1}. In these tests the input energy (E_i) is given by

$$E_i = \frac{1}{2} m_G v_i^2 \tag{7. 1}$$

There is a granule velocity that is defined as the average velocity of individual granules accelerated under a fixed air pressure. The maximum value of the variation coefficient variation of the average velocity is about 3%.

An air cannon is used to investigate the breakage probability distribution depending on mass of granule (m_G) related energy. The specific input energy ($E_{m,i}$) that is related to the granule mass related energy is

$$E_{m,i} = \frac{E_i}{m_G} = \frac{v_i^2}{2} \tag{7. 2}$$

Experiment is divided into two parts: **impact without pretreatment** and **impact with pretreatment** by pendulum impact. Granules are launched one by one with the same air pressure with impact angle of zero degree.

7.2.1 Impact without pretreatment

Amount 200 granules of γ-Al_2O_3 (d =1.8 mm) are weighed one by one by using analytical balance. After that, granules are introduced into air canon. The samples are putted at the wagon that is mounted at the equipment. Regardless to the orientation of the impact contact, each granule is launched one by one with the same air pressure and impact angle. The broken granules are related to the size reduction that is visible observed directly. From these observations, the total number that remained unbroken from each original batch is recorded.

7.2.2 Impact with pretreatment

In this step, granules beforehand are treated by using pendulum double impact. Granules one by one are stressed 10 times at the certain height of striking regardless the specific contact points of stressing (see **Section 6.2.2**). The stressed granules are classified into several percentage of breakage by double impact ($p_{i,d}$) that is defined as breakage probability increments. The survived granules afterward are tested individually by air canon.

7.3 Discussion of test results by air canon

7.3.1 Breakage probability without pretreatment

The breakage probability depends on the input energy and granule properties i.e. individual granule mass. The approach that is commonly applied to obtain the breakage probability is by measuring the percentage of the number of broken granules. The breakage probability of impacted granules γ-Al_2O_3 by air cannon test as a function of breakage energy distribution is shown in **Figure 7.3.** In this way median $E_{m,i,50}$ at every breakage probability distribution is normalized by a value of breakage energy correspondingly. The dimensionless normalized distributions are fitted then with lognormal function. During test, the orientation of granules is not taken into accounted.

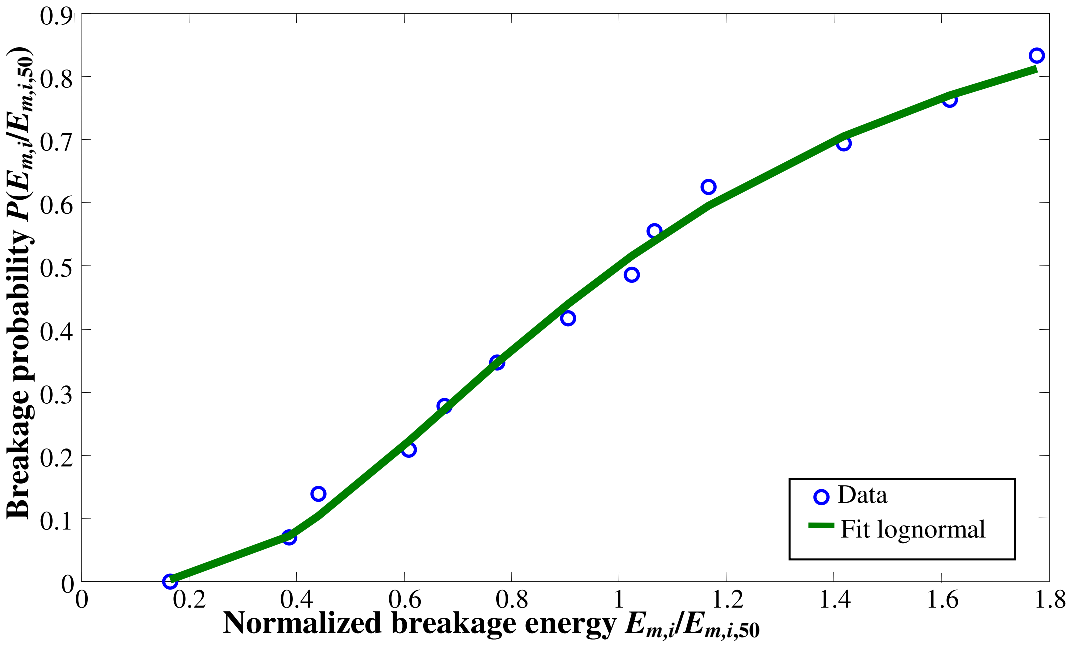

Figure 7.3 Normalized data distribution of γ-Al_2O_3 granules (d =1.8 mm) in air canon test.

Cumulative breakage probability distribution by impact test is associated with mass related energy of granules (E_m). That means the calculation is determined by individual granule mass. In this term, energy refers to input energy at every collision for individual granule with a certain mass m. The input energy is calculated by using Equation (7.2). Experimental distributions of E_m is fitted with log-normal function for impacted granules, see **Figure 7.4**.

The cumulative experimental distribution of breakage probability is obtained by variation of the E_m in the relevant range. The distribution corresponds to the increasing of breakage probability from 0 up to about 1. Small E_m around 75 -175 J/kg generates low brakeage probability. It needs large energy to generate a significant damage at the granules.

Interestingly, E_m at the range 225-470 J/kg exhibits small breakage probability. For small mass or at E_m range between 470-550 J/kg granules tend to have large breakage probability. Generally, the result shows that for the small mass the increasing of mass related energy raises also significantly the breakage probability. In this way, large kinetic energy causes the rapid cracks formation within granules.

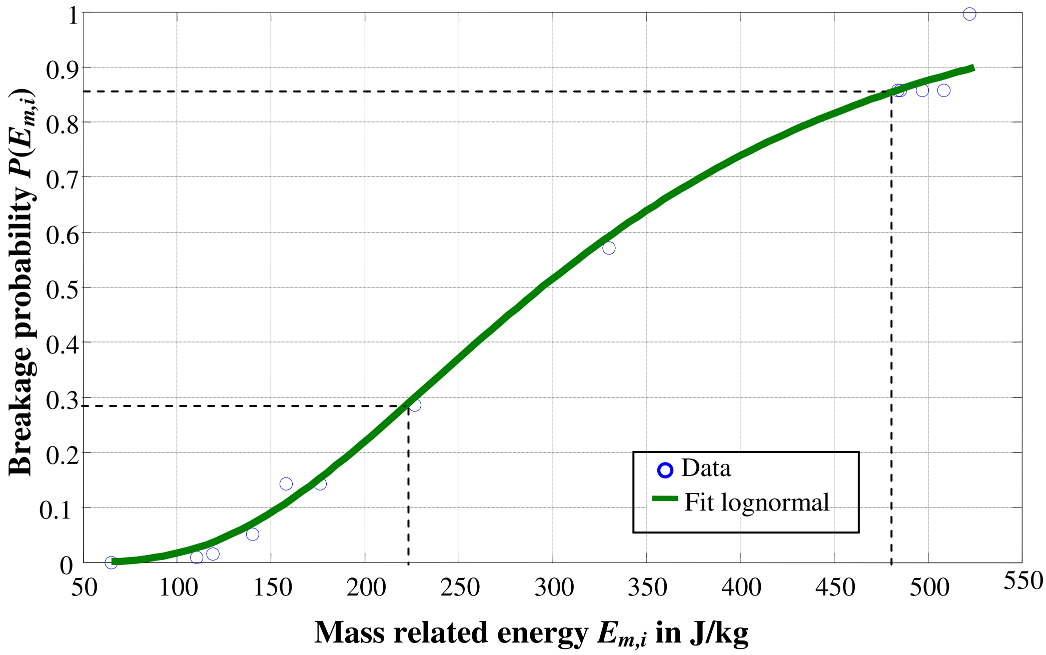

Figure 7.4 Breakage probability of γ-Al_2O_3 granules (d = 1.8 mm) in impact canon test without pretreatment.

7.3.2 Breakage probability with pretreatment

Repeated stressing as a pretreatment for granules refers to the realistic of multiple stressing in industrial situation. By varying the height h_1 of striker in double impact pendulum test (see section **6.2.3.b**), the surviving granules perform a different $p_{i,d}$ that is referring to the breakage probability increment by repeated stressing in double impact by pendulum. The granules then are introduced into the air canon test. The surviving granules are grouped in the classes (quintiles) of $p_{i,d}$ i.e. 8,3; 26,7; 49.8; 50.0; 61.4; and 82.0 percent, see **Table 7.1**.

In this equipment, similar with the impacting of non pretreatment procedure above (see **section 7.3.1**), the treated granules are fired moves through the pneumatic tube and eventually hit the wall target. The cumulative probability of breakage is investigated and compared with the non treated granules.

Table 7.1 Percentage of breakage $p_{i,d}$ by pendulum double impact related to height magnitude of striker h_1.

h_1 in mm	$p_{i,d}$ in %
12.0	8.3
14.0	26.7
15.9	49.8
16.0	50.0
16.3	61.4
16.8	82.0

A typical probability breakage of stressed granules for $p_{i,d}$ 82.0 % is shown in **Figure 7.5.**

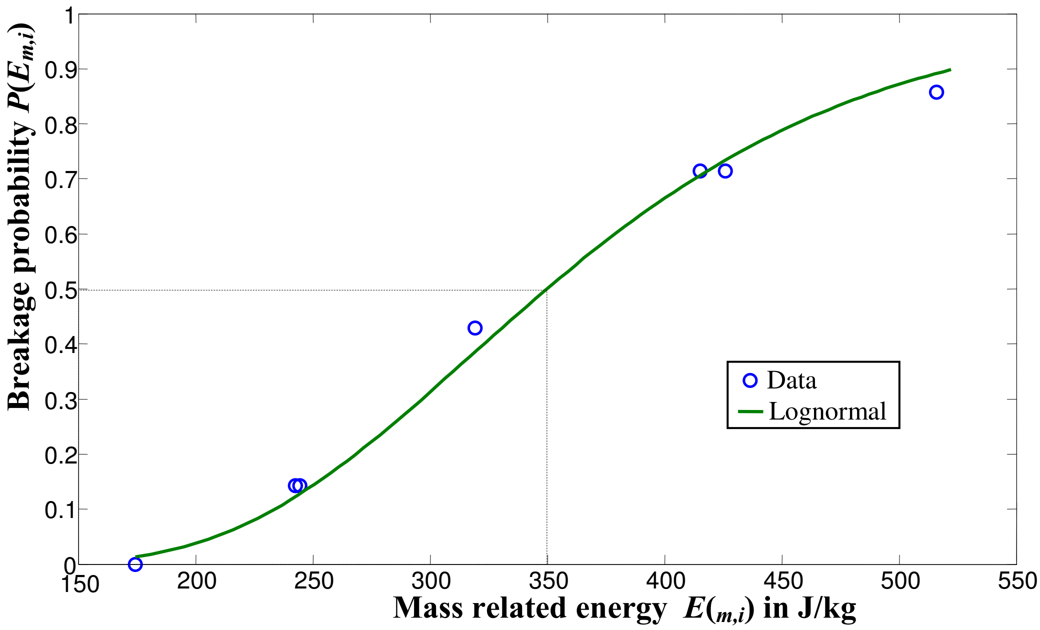

Figure 7.5 The breakage probability fitted with lognormal cumulative distribution function of stressed γ-Al_2O_3 granules (d = 1.80 mm) for $p_{i,d}$ = 82.0% in air canon test.

Different breakage probability characteristic is performed at $p_{i,d}$ = 82.0 %. In this pretreatment the survived granules tend to attain large breakage probability. It is because the dissipated energy as the remaining of the stressing by double impact in $p_{i,d}$ = 82.0% creates more damage accumulation within granules. This investigation is explained in **Chapter 4, 5** and **6.** Definitely, there is no damage accumulation for granules without pretreatment.

In the other hand, the survived or the pretreated granules after stressed by double impact with pendulum have lower breakage probability than these without pretreated granules. The pretreated granules (see **Figure 7.6**) overall require large energy to be broken, at the same energy and same granule size or mass, but granules without pretreatment break easily.

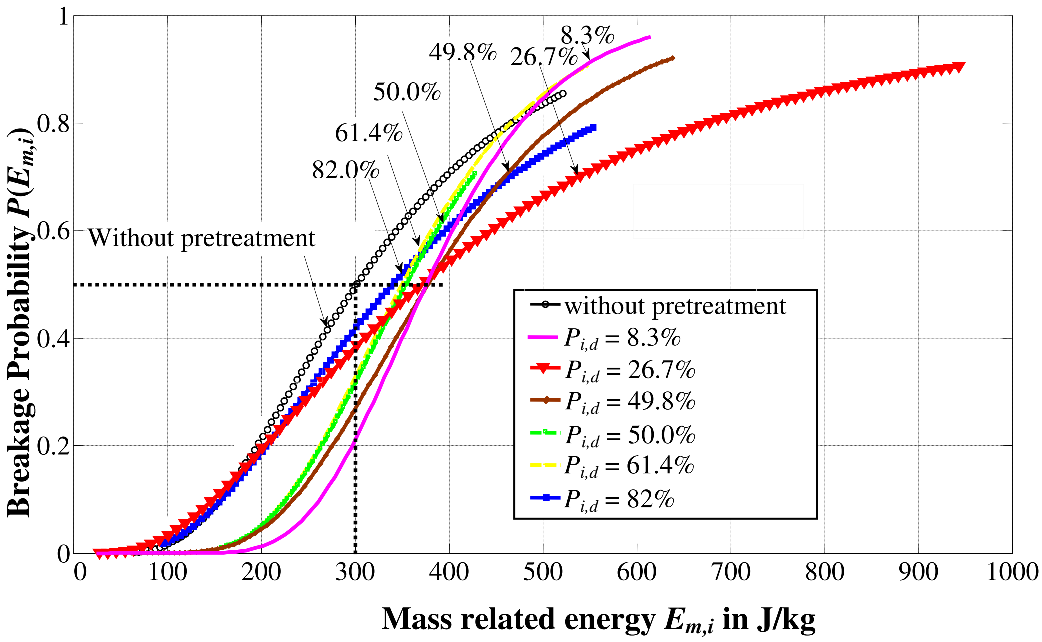

Figure 7.6 The breakage probability distribution and mass related energy of γ-Al_2O_3 granules *d*= 1.80 mm) after pretreatment compared to without pretreatment.

This is confirmed by the median of mass related energy of non pretreatment $E_{m,50}$ (300 J/kg) while for pretreated granules $E_{m,50}$ is 320 - 380 J/kg. In the other word, the energy to break pretreated granules at $E_{m,50}$ is larger than that without pretreated granules. For example, at breakage probability of pretreated granules P_r (50 %) the $E_{m,50}$ is 354.9 J/kg. Overall for varied $p_{i,d}$, the breakage probability of pretreated granules is lower than those without pretreatment.

Table 7.3 The breakage probability *P* of every treated granules at E_m = 300 J/kg

$p_{i,d}$ in %	*P*(i) in %
Without pretreatment	50
82.00	42
61.40	33
50.00	30
49.80	27
26.70	38
8.30	20

From experiment, for the same E_m (300 J/kg) breakage probability of pretreatment $p_{i,d}$ 8.3% is 20%. Meanwhile for granules without pretreatment the breakage probability is 50%. The complete result of breakage probability of granules under varied stressing at the same E_m is shown in **Table 7.3**.

The collision energy by air impact canon also exhibits different results depend on the $p_{i,d}$ The breakage probability value (50% of granules are broken) or $E_{m,50}$ of every stressed granules is shown in **Table 7.4**.

Table 7.4 The mass related energy $E_{m,i}$ at P(i) = 50% of stressed granules by air canon test.

$p_{i,d}$ in %	$E_{m,50}$ in J/kg
Without pretreatment	300.00
82.00	338.10
61.40	350.00
50.00	354.90
49.80	370.00
26.70	370.00
8.30	375.50

Even thought $p_{i,d}$ of each stressing granules for the complete $E_{m,50}$ are obtained in irregular order, however it is definitely clear that the $E_{m,50}$ (300J/kg) of the granules without pretreatment is lower than that of granules with pretreatment. It indicates that the pretreatment by repeated stressing select weak granules and leaves the stronger one. The treated granules by air canon require enhanced energy to generate fracture. The pre-stressed granules are stronger than without pre-stressed granules. In this way there is a selection event as confirmed by Petukov [14]. The lower $p_{i,d}$, the stronger granules and eventually the lower the breakage probability. This is clearly different with damage accumulation results in previous chapter or investigation that is revealed in this thesis. It is because damage accumulation only occurs at low input energy while at large input energy the stressed granules exhibit a selection event.

7.4 Conclusions of breakage probability by impact stressing in air canon test

The breakage probability of pretreated granules by free impact test with air canon apparatus is lower than breakage probability without pretreated granules. Pretreatment selects out weak granules and leaves the stronger one. Impacting the survived granules from pendulum impact by air canon require enhanced energy to generate a fracture.

The treated granules are stronger than those without stressed one. There is a selection event that is different from the damage accumulation. The lower $p_{i,d}$ the stronger granules due to selection events and eventually the lower breakage probability in air canon test.

CHAPTER 8
CONCLUSION AND OUTLOOK

8.1 Conclusion

This thesis focuses on the breakage probability of granules regarding to the fixed and randomly stressing contact points on granule surface. The simulation of deformation and breakage behavior of granules during cyclic stressing was carried out. The breakage behavior of granules regarding to the compression, double impact and single impact test by repeated stressing was examined. The application of stress to fixed and randomly stressing contact points on granules performs a typical breakage behavior.

Simplified one parameter model was developed and verified basing on Monte-Carlo analysis. The analysis determines the breakage probability by means of contact point configuration of granules during stressing. The developed model is examined with considering particle properties, stresses and breakage force distributions.

Only one parameter that is called as degradation parameter q model is introduced to describe the breakage behavior by means of repeated stressing. Parameter q refers to the change of particles properties due to cyclic stressing. The fitting of Monte-Carlo data that was obtained by normal, lognormal, random and Weibull distribution of particle strength and applied forces was carried out by use of this developed model. There is a good correlation between Monte-Carlo data and developed model.

The developed model includes two opposed tendencies in breakage behavior. The first tendency is the increasing of breakage probability due to damage accumulation. In this case the damage accumulation is modeled by means of the reduction of parameter q.

The second tendency is the decreasing of breakage probability with stressing number due to the breakage of weak granules at the earlier tests. The remaining granules for the advanced test exhibit an increased strength. That both tendencies can be described with the degradation parameter. Consequently, this parameter changes depending on granules properties and dominate tendency that takes place by conceding stress conditions. By this model, the breakage probability of particles with normal distributed strength is larger compared to the random and Weibull distributed strength.

The model is validated experimentally by double impact − drop and pendulum weight. The used material tests are Gamma Aluminum Oxide (γ-Al_2O_3), Zeolite 4AK, and Zirconium (ZrO_2) granules.

By using degradation parameter q as a fitted model, breakage probability by repeated stressing in particularly by double impact is revealed. The model denotes the change of granules strength by repeated stressing.

The degradation parameter q shows the tendency to increase proportionally with the mass related stressing energy $E_{m,G}$. The values of q consistently changes from q<1 by low stressing energy to q>1 by high stressing energy. It implies the damage accumulation is generated by successive stressing.

On the other hand, with the increasing of stressing number, the breakage probability increments decrease consecutively. This behaviour represents the hardening effect by cyclic stressing

The configuration of stressing contact point by fixed and randomly stressing contact points of granules testing diminishes the damage accumulation events. It creates the selection events as resulted in double impact test. The stressing either may find the stronger or the weaker point of the surface contact.

The weakening effect is exhibited as well by compression test with very low stressing rate. The stiffness increases at the fixed granules. At the first stressing, γ-Al_2O_3 and Zeolite 4A of different size granules perform large elastic-plastic deformation. The reduction of deformation shows a stiffening effect with the increasing of stressing. It is because the intensive cyclic stressing consolidates the solid bridge bonds that propagate within the specimen and the structure in the contact zone. The elastic-plastic deformation behavior depends on the contact zone and it is not strongly affected by the number of stressing event (see **Chapter 4**). The strength of particle i.e. breakage force at given location is reduced by force application. This result confirms the damage accumulation due to repeated stressing events that is proposed theoretically by using Monte-Carlo analysis as modeled in **Chapter 3**.

However, for randomly stressing contact points of granules in compression test, the stiffness tends to be distributed randomly, and only weak points are affected by the stressing. The deformation behavior is more or less similar at all stressing events. It is because the stiffness does not significantly vary depending on the force. After a single stressing with different forces, stiffness is considered to be nearly constant.

Furthermore, by contact area or image view, the contact or deformation radius r_k of the contact area of γ-Al_2O_3 surface after some stressings, increases proportionally with stressing number. In the other side, at randomly stressing contact points of granules, r_k is considered constant.
For another test by single impact, damage accumulation by repeated stressing does not occur in single impact test but rather the selection effect. The repeated stressing by single impact test selects the surviving or stronger granules depending on breakage probability increments $P_{i,d}$. The stressed granules that are survived from pendulum impact are stronger than that the non-stressed granules. In this context there is a selection phenomenon. The lower breakage probability increment the stronger granules and eventually the lower cumulative breakage probability.

8.2. Outlook

This work studies the influence of location of stressing points of dry granules. Therefore in the future it is recommended to investigate the stressing of granules or particles by taking into account the moisture content with respecting to the contact point of stressing. The breakage mechanism needs also to be identified by observing microscopically the mechanisms that occurs during stressing. This investigation will help to understand the liberation of solid bridge bonds either in fixed or randomly or selected contact points.
It is important to simulate the orientation of contact point of stressing as well by using Discrete Element simulations. In the next test it is recommended to integrate experiments with industry systems. This integrating will help to obtain the other parameters that are possibly involved in repeated stressing.

REFERENCES

[1] Antonyuk, S, Tomas, J., Heinrich, S. and Mörl, L. (2005). "Breakage behaviour of spherical granulates by compression." Chem. Eng. Technol. , 28 (5), 623-629.

[2] Russell, A, Müller, P and Tomas, T. (2014), "Quasi-static diametrical compression of characteristic elastic-plastic granules: Energetic aspects at contact", Chem. Eng. Sci. 114, 70-84. DOI: 10.1016/j.ces.2014.04.016.

[3] Tomas, J. (2001). "Assessment of mechanical properties of cohesive particulate solids—part 1 particle contact constitutive model." s.l. Part. Sci. Technol. 19(2), 95–110.

[4] Agniel, Y. (1992). "Bedeutung der Einzelgranalieneigenschaften zur Defektvermeidung." Doctoral dissertation, University of Karlsruhe.

[5] Goder, D., Kalman, H. and Ullmann, A. (2002). "Fatigue characteristics of granular materials. " Powder Technology, Vol. 122 (1), 19-25.

[6] Tavares, L.M. and King, R.P. (1998). "Single-particle fracture under impact loading." Int. J. Miner. Process, 54, 1-28.

[7] Rozenblat,Y., Kalman, H., (2011). "Strength distribution of particles under compression." Powder Technology 208, 215–224.

[8] Kalman, H., Rodnianski, V., Haim, M. (2009). "A new method to implement comminution functions into DEM simulation of a size reduction system due to particle–wall collisions." Granular Matter 11 253–266.

[9] Pitchumany, R., Strien, S.A., Meesters, G.M.H., Schaafsma, S.H., Scarlett, B., (2004). "Breakage of sodium benzoate granules under repeated impact conditions." Powder Technology 140, 240–247.

[10] Beekman, W.J., Meesters, G.M.H., Becker, T., Gaertner, A., Gebert, M., Scarlett, B. (2003). "Failure mechanism determination for industrial Granules using a repeated compression test." Powder Technol. 130, 367–376.

[11] King, R.P., Tavares, L.M. (1997). "Middlemiss, Establishing the energy efficiency of a ball mill. " in S.K. Kawatra (Ed.), Comminution Practices, Society of Mining Engineers, Littleton, 311 – 316.

[12] Tavares, L.M., King, R.P., (2002). "Modeling of particle fracture by repeated impacts using continuum damage mechanics." Powder Technology 123, 138–146. .

[13] Tavares, L.M., Carvalho, R.M. (2007). "Impact work index prediction from continuum damage model of particle fracture.“ Miner. Eng. 20 1368–1375.

[14] Petukhov, Yevgeny., Kalman, Haim (2004). "Empirical breakage ratio of particles due to impact.” Powder Technology 143– 144, 160– 169.

[15] Kalman, H.. (2000). "Particle breakage and attrition.” Kona 18, 108–120.

[16] Peukert, W.,Vogel, L. (2001). "Comminution of polymers—an example of product engineering.” Chemical Engineering & Technology 24, 945–950.

[17] Weibull, W. (1939). "A statistical theory of the strength of materials.” Ingeniörsvetens-kakademiens Handlingar 151, Generalstabens Litografiska Anstalts Förlag, Stockholm.

[18] Morrison, R. F., Shi., Whyte, R. (2007). "Modelling of incremental rock breakage by impact;for use in DEM models, Mineral Engineering 20, 303–309. s.l. Powder Technology, 2002, Vols. 129, p.101– 110.

[19] Rumpf, H. (1973). "Physical aspects of comminution and new formation of law of communition, Powder Technology, Vol. 7, 145-159.

[20] Weichert, R. (1991). "Theoretical Prediction of Energy Consumption and Particle Size Distribution in Grinding and Drilling of Brittle Materials.” Part. Part. Syst. Charact., 8, 55-62.

[21] Salman, A.D., Fu, J., Gorham, D. A. and Hounslow, M. J. (2003). "Impact breakage of fertiliser granules.” Powder Technology, Volume 130, Issues 1-3, 359-366.

[22] Aman,S., Tomas, J. and Kalman, H. (2010). "Breakage probability of irregularly shaped particles, Chem. Eng. Sci., 65, 1503-1512.

[23] Aman, S, Tomas, J, Kalman, H, (2011). ”Breakage Probability of Irregularly Shaped Particles by Impact Stressing.” Chemie Ingenieur Technik, Volume 83, issue 5 p. 704-709. ISSN: 0009-286X DOI: 10.1002/cite.201000152 WILEY-VCH Verlag.

[24] Tomas, J. (2007). "Adhesion of ultra fine particles a micromechanical approach.” Chem. Eng. Sci., 62, 1997-2010.

[25] Schreier, M., Tomas, J., Gröger, T., Ehlers, S. (1999). ”Impact crushing of concrete for liberation and recycling.” s.l. Powder Technology, Vol. 105, 39–51.

[26] Schubert, W., Khanal, M., Tomas, J. (2005). "Impact crushing of particleParticle compounds – experiment and simulation.” Int. J. Mineral Processing, 75(1–2), 41–52

[27] Salman, A.D., D.A. Gorham, A. Verba, (1995). "A study of solid particle failure under normal and oblique impact, Wear.” 186– 187, 92–98.

[28] Khanal, M., Schubert, W., Tomas, J. (2004). "Ball impact and crack propagation – simulations of particle compound material.” Granular Matter, 5 (4), 177-184.

[29] Antonyuk, S., Khanal, M.,Tomas, J., Heinrich, S. and Mörl, L. (2006). "Impact breakage of spherical granules: experimental study and DEM simulation.” Chem. Eng. Sci., Vol. 45, 838-856.

[30] Simmchen, E., Riehle, M., (2000). "Grundlagen der Werkstofftechnik.“ Dt.Verl. fuer Grundstoffindustrie, Stuttgart.

[31] Müller, P., Antonyuk, S., Tomas, J. (2011). "Investigation on the influence of moisture content on the compression behavior of granules.” Chem. Eng. Technol. 34 (9), 1543-1550.

[32] Russell, A., Tomas, J., "Multiple Compression of Moist Spherical Elastic-Plastic Zeolite 4A Granules.” Chemical Engineering Technology, 2013, 36, No. 7, 1240–1248.

[33] Han, T., Kalman H. and Levy, A., (2003). "Theoretical and experimental study of multi-compression particle breakage.” Advanced Powder Technology, Vol. 14, No. 5, 605-620,

[34] Carey, W.F., Bosanquet, C.H., (1933). "A study of crushing brittle solids.”Journal of the Soc. Glass Technology 17, 348.

[35] Gabrie M.H. Meesters, Elsevier, “Strength in an Industrial Environment”, Particle Breakage, p.917-925, Chapter 21, 2007

[36] Antonyuk, S. (2006). "Deformations- und Bruchverhalten von kugelförmigen.“ Doctoral Dissertation, University of Magdeburg, Docupoint Publishers

[37] Ghadiri, M. D.G. (1994). "Influence of material properties on attrition and comminution of particulate solids.” In: Proc. IFPRI Annual Meeting, Goslar.

[38] Vogel, L., Peukert, W. (2005). "From single impact behaviour to modelling of impact mills.” Chemical Engineering Science 60, 5164–5176.

[39] Athanasios Papoulis, S. Unnikrishna Pillai, (2002). "Probability, random variables, and stochastic processes with Errata Sheet.” McGraw-Hill, 4 edition.

[40] Agresti A, Coull BA (1998) "Approximate is better than 'exact' for interval estimation of binomial proportions". The American Statistician 52,119–126

[41] Salman, D., Reynolds, G. K., Fu, J. S., Cheong, Y. S., Biggs, C. A., Adams, M.J. Gorham, D. A., Lukenics, J. and Hounslow, M. J. (2004). "Descriptive classification of the impact failure modes of spherical particles.” Powder Technology, vol. 25, 143-144.

[42] Vogel, L., Peukert, W. (2003). "Breakage behaviour of different materials construction of a mastercurve for the breakage probability," Powder Technology 129, 101–110.

[43] Kalman, H., Hubert, M., Grant, E., Petukhov., Y. M. Haim, (2004). "Fatigue behavior of impact comminution and attrition units." Powder Technology 146, 1–9.

[44] Tavares, L. M. (2007). "Breakage of Single Particles Quasi-Static." Handbook of Powder Technology, Vol. 12, Particle Breakage, ed. by Salman A. D., Ghadiri M. and Hounslow M.J., 3-68.

[45] Austin, L.G. (2002). "A treatment of impact breakage of particles." Powder Technol. 126, 85–90.

[46] Khanal, Manoj., Schubert, Wolfgang., Tomas, Jürgen., (2005), "DEM simulation of diametrical compression test on particle compounds, Granular Matter." vol. 7, no. 2, 83-90

[47] Mac Kay, David (2003). "Information theory, inference and learning algorithms". Cambridge University Press, First Edition

[48] Cool, Mc, John I., (2012), "Using the Weibull distribution: reliability, modeling and inference," Wiley, New York. 23.

[49] Schubert, W., Jeschke, H. (2005). "DEM-Simulation of the breakage process in an impact crusher, new orders of the comminution." WISSENSPORTAL baumaschine.de 4, 34-37.

[50] Haibo, Zhao., Chuguang, Zheng., Minghou, Xu (2005). "Multi-Monte Carlo approach for general dynamic equation considering simultaneous particle coagulation and breakage." Powder Technology 154, 164-178.

[51] O.G. Pauw, (1988). "The minimization of overbreakage during repetitive impact breakage of single ore particles." Powder Technology 56, 251–257.

[52] Chen, W., Cheng, F., Lu, M., (2002). "Tension and compression tests of two polymers under quasi-static and dynamic loading". Polym. Test 21, 113–121.

[53] Gildmeister, H., Schonert, K., (1972). „Berechnung zur Wellenausbreitung in Kugeln und Bruchphanomene in Kreisscheiben bei Prallbeanspruchung". Dechema Bd. 69, Nr. 17, 1–35.

[54] Agresti A, Coull BA (1998) "Approximate is better than 'exact' for interval estimation of binomial proportions". The American Statistician 52,119–126

[55] Draper, N.R.; Smith, H. (1998). "Applied Regression Analysis (3rd ed.)." John Wiley, New York.

[56] Hamza, K. (1995). "The smallest uniform upper bound on the distance between the mean and the median of the binomial and Poisson distributions." Statistics & Probability Letters 23: 21–25.

[57] Kaas, R., Buhrman, J.M. (1980). "Mean, median and mode in binomial distributions." Statistica Neerlandica 34 (1): 13–18

[58] Feller, William (1950). "Introduction to Probability Theory and its Applications." Vol I. Wiley. p. 221

[59] Hogg, R.V., Ledolter, J. (1987). „Engineering statistics." MacMillan Publisher, Toronto.

[60] Kolmogorov, A.N. (1941). "On the logarithmic normal size distribution of particles by grinding." Dokl. Akad.

[61] Wefers, K., Misra, C. (1987). "Oxides and Hydroxides of Aluminum." Alcoa Technical Paper No. 19, Alcoa Laboratories.

[62] Petzold, A., Ulbricht, J. (1991). "Aluminiumoxid Rohstoff, Werkstoff, Werkstoffkomponente." Dt. Verl. Für Grundstoffind. Leipzig.

[63] Sivaraj, Ch., Contescu1, Cr., Schwarz, J.A. (1991). "Effect of calcination temperature of alumina on the adsorption/impregnation of Pd(II) compounds." Journal of Catalysis, Volume 132, Issue 2, December, Pages 422–431.

[64] Herausgeber F. Falbe, M. Regnitz, Georg Thieme, (1995). "Römpp Chemielexikon. 9. Auflage", Verlag Stuttgart, New York.

[65] Philip, M. Parker (2010). "The world market for alumina (aluminum oxide) excluding corundum", A 2011 Global Trade Perspective.

[66] Auerbach, Scott M., Carrado, Kathleen A., Dutta , Prabir K., (2004), "Handbook of zeolite science and technology", Edition: 1, Publisher: CRC Press; 1 edition New York.

[67] Kamarudin., Khairul, Mat, Hanapi., Hamdan, Halimaton., (2007), "Zeolite as natural gas adsorbents", Diplome Dissertation, Universiti Teknologi Malaysia Universiti Teknologi Malaysia.

[68] Roy, Priscille., Bertrand, Ghislaine., Coddet, Christian., (2005). "Spray drying and sintering of zirconia based hollow powders." Powder Technology, Volume 157, Issues 1–3, 29 September Pages 20–26.

[69] Bastow, T. J.; Smith, M. E., Stuart, S. N. (1993). "A novel characterisation of phases in zirconia-based ceramics." In Science and Technology of Zirconia V." Technomic Publishing Co. Lancaster, PA, pp 1.

[70] Bastow, T. J.; Smith, M. E.; Stuart, S. N. (1992). "Observation of Zr-91 Nmr in Zirconium-Based Metals and Oxides", Chem. Phys. Lett. 191, 125– 129.

[71] Heinrich, S., Peglow, M., Ihlow, M., Henneberg, M., Mörl, L., (2002). "Analysis of the start-up process in continuous fluidized bed spraygranulation by population balance modeling". Chemical Engineering Science 57 (20), 4369–4390.

[72] W.J. Beekman, (2000).“Measurement of the mechanical strength of granules and agglomerates.”PhD thesis, Delft University of Technology, Delft, Netherlands.

[73] Aman, S., Tomas, J., Kalman, H. (2011), "Monte-Carlo-Simulation der Bruchwahrscheinlichkeit bei der Prallbeanspruchung irregulär geformter Partikel." Chemie Ingenieur Technik, Volume 83, Issue 5, pages 704–709.

[74] Hertz, H., 1882. Über die Berührung fester elastischer Körper. Journal fur die Reine und Angewandte Mathematik 92, 156–171.

[75] Stieß, M., (1976), "Die Druckbeanspruchung von elastischen und inelastischen Kugeln bis zum Bruch. Dissertation.“ Universität Karlsruhe (TH).

[76] Pisarenko, G.S., Agarev, V.A., Kvitka, A.L., Popkov, V.G., Umanskii, E.S., (1986) Festigkeitslehre 5. Aufgabe. Vischa schkola, Kiev.

[77] Huber, M.T., (1904). "Zur Theorie der Berührung fester elastischer Körper", Annalen der Physik14, 153–163.

[78] Gross, D., Seeling, Th., (2001). "Bruchmechanikmit einer Einführung in die Mikromechanik 3", Aufgabe. Springer, Berlin, Heidelberg, New York.

[79] Fischer-Cripps, A.C., (2000). "Introduction to Contact Mechanics", Springer, Berlin, Heidelberg, New York.

[80] Lurje, A.I., (1963), "Räumliche Probleme der Elastizitätstheorie.“ Akademie Verlag, Berlin.

[81] O. Molerus, (1975). “Theory of yield of cohesive powders”, Powder Technology Volume 12 (3), 259–275.

CURRICULUM VITAE

Personal data

Name	:	Salman
Birth Date	:	11th October 1973
Nationalist	:	Indonesian
Marital status	:	Married
Recent occupation	:	Lecturer in Mechanical Engineering Dept., University of Mataram, Indonesia

Educational background

Junior High School	:	SMP N 3 Watansoppeng, Indonesia (1986-1989)
Senior High School	:	SMA N 1 Watansoppeng, Indonesia (1989-1992)
Bachelor program	:	Dept. of Mechanical Engineering, Fact. of Engineering, University of Hasanuddin, Makassar, Indonesia (1992-1997)
Master program	:	Quality-Safety and Environment, Otto-von-Guericke University of Magdeburg, Germany, (2002-2003)
PhD program	:	Institut für Mechanische Verfahrenstechnik, Otto-von-Guericke University of Magdeburg, Germany, (2009-2014)

Magdeburg, 5th June 2014 Salman